

A072444

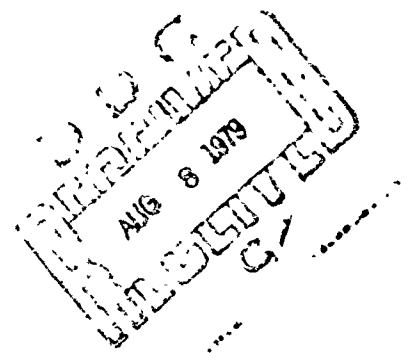
LEVEL

2

Report AFFDL-TR-79-3044

## EJECTION SEAT FOR HIGH-G ESCAPE

Douglas Aircraft Company  
McDonnell Douglas Corporation  
Long Beach, California 90846



April 1979

DDC FILE COPY

Final Report for Period June 1978-April 1979

Approved for Public Release; Distribution Unlimited

Prepared for  
AIR FORCE FLIGHT DYNAMICS LABORATORY  
Air Force Systems Command  
United States Air Force  
Wright-Patterson AFB, Ohio 45433

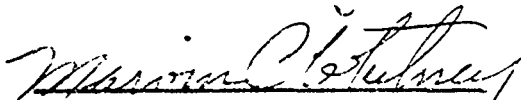
79 08 06 077

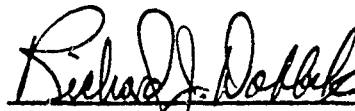
# NOTICE

When Government drawings, specifications, or other data are used for any purpose other than in connection with a definitely related Government procurement operation, the United States Government thereby incurs no responsibility nor any obligation whatsoever; and the fact that the government may have formulated, furnished, or in any way supplied the said drawings, specifications, or other data, is not to be regarded by implication or otherwise as in any manner licensing the holder or any other person or corporation, or conveying any rights or permission to manufacture, use, or sell any patented invention that may in any way be related thereto.

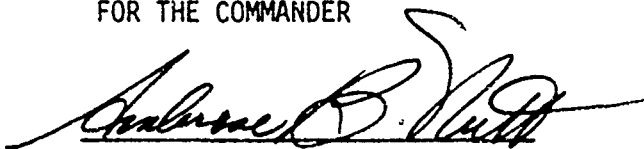
This report has been reviewed by the Information Office (OI) and is releasable to the National Technical Information Service (NTIS). At NTIS, it will be available to the general public, including foreign nations.

This technical report has been reviewed and is approved for publication.

  
MARVIN C. WHITNEY  
Project Engineer  
Crew Escape & Subsystems Branch  
Vehicle Equipment Division

  
RICHARD J. DOBBEK  
Crew Escape & Subsystems Branch  
Vehicle Equipment Division

FOR THE COMMANDER



If your address has changed, if you wish to be removed from our mailing list, or if the addressee is no longer employed by your organization please notify AFFDL/FER, W-PAFB, OH 45433 to help us maintain a current mailing list.

Copies of this report should not be returned unless return is required by security considerations, contractual obligations, or notice on a specific document.

UNCLASSIFIED

SECURITY CLASSIFICATION OF THIS PAGE (When Data Entered)

REPORT DOCUMENTATION PAGE		READ INSTRUCTIONS BEFORE COMPLETING FORM
1. REPORT NUMBER AFFDL TR-79-3044	2. GOVT ACCESSION NO.	3. RECIPIENT'S CATALOG NUMBER
4. TITLE (and Subtitle) EJECTION SEAT FOR HIGH G ESCAPE	5. TYPE OF REPORT & PERIOD COVERED Final Technical Report June 1978-April 1979	6. PERFORMING ORG. REPORT NUMBER MDC-J8434
7. AUTHOR(s) E. E. Howland	8. CONTRACT OR GRANT NUMBER(s) F33615-78-C-3416	
9. PERFORMING ORGANIZATION NAME AND ADDRESS McDonnell Douglas Corporation Douglas Aircraft Company 3855 Lakewood Blvd. Long Beach, California 90846	10. PROGRAM ELEMENT, PROJECT, TASK AREA & WORK UNIT NUMBERS 2402-03-22	
11. CONTROLLING OFFICE NAME AND ADDRESS Air Force Flight Dynamics Laboratory Wright-Patterson Air Force Base, Ohio 45433	12. REPORT DATE April 1979	
13. MONITORING AGENCY NAME & ADDRESS (if different from Controlling Office)	14. NUMBER OF PAGES 183	
	15. SECURITY CLASS. (of this report) Unclassified	
16. DISTRIBUTION STATEMENT (of this Report) Approved for public release, distribution unlimited.		
17. DISTRIBUTION STATEMENT (of the abstract entered in Block 20, if different from Report)		
18. SUPPLEMENTARY NOTES		
19. KEY WORDS (Continue on reverse side if necessary and identify by block number) Seats Escape Systems Ejection Seats Aircraft Systems Aircraft Equipment		
20. ABSTRACT (Continue on reverse side if necessary and identify by block number) Advanced flight vehicles operating at acceleration loads beyond human functional capabilities require a new reclining seat design. An ejection seat compatible with this requirement must provide safe ejection and aircraft clearances under high-G conditions as well as the requirements associated with high dynamic pressures and low altitudes.		

DD FORM 1 JAN 73 1473

EDITION OF 1 NOV 65 IS OBSOLETE  
S/N 0102-014-6601UNCLASSIFIED  
SECURITY CLASSIFICATION OF THIS PAGE (When Data Entered)

116400

Glu

UNCLASSIFIED

SECURITY CLASSIFICATION OF THIS PAGE(When Data Entered)

20. ABSTRACT (Continued)

Design criteria and interface requirements have been established. Ejection seat subsystems have been developed and seat design concepts generated to meet criteria and interface requirements.

Candidate seat concepts have been analyzed to determine cockpit integration effects, accelerations, ejection clearances, escape performance, structural requirements and weights.

A final design concept has been selected to meet all requirements of an ejection seat for high-G escape. The final report includes a parametric study of tail clearances and discusses technical design details and conclusions of the work performed.

UNCLASSIFIED

SECURITY CLASSIFICATION OF THIS PAGE(When Data Entered)



## FOREWORD

This report describes the work performed by the Douglas Aircraft Company, McDonnell Douglas Corporation, Long Beach, CA under the Ejection Seat for High-G Escape Program. This work was sponsored by the Air Force Flight Dynamics Laboratory, Air Force Wright Aeronautical Laboratories, Air Force Systems Command, Wright-Patterson Air Force Base, Ohio. Work was authorized under Contract F33615-78-C-3416, Project No. 2402, Task No. 240203. This research work is part of an effort to obtain new crew escape concepts for providing safe survivable high G escape. The period covered is from 1 June 1978 to 1 March 1979 and the report was submitted on 15 March 1979.

This report consists of one volume titled, "Ejection Seat for High G Escape." The principal investigator and author was Orville E. Howland.

Marvin C. Whitney of the Crew Escape and Subsystems Branch (AFFDL/FER) was the Air Force Project Engineer during this program.

Accession For	
NTIS	<input checked="checked" type="checkbox"/>
DDC TAB	<input type="checkbox"/>
Unannounced	<input type="checkbox"/>
Justification	
By _____	
Distribution/	
Availability Codes	
Dist	Available and/or special

## TABLE OF CONTENTS

SECTION	PAGE
I. INTRODUCTION AND SUMMARY	1
II. STINFO LITERATURE SEARCH	3
III. INTERFACE REQUIREMENTS	5
IV. DESIGN CRITERIA	9
V. SEAT SUBSYSTEMS	11
5.1 SUPPORT/RESTRAINT	11
5.2 SEAT POSITIONING	21
5.3 EJECTION INITIATION	31
5.4 EJECTION PROPULSION	34
5.5 SEAT STABILIZATION	38
5.6 CANOPY JETTISON	43
VI. HIGH G EJECTION SEAT CONCEPTS	47
VII. SEAT/COCKPIT INTEGRATION	53
VIII. SEAT CONCEPT ANALYSIS	55
8.1 ACCELERATION/DRI EFFECTS	55
8.2 EJECTION CLEARANCES	65
8.3 ESCAPE PERFORMANCE	71
8.4 STRUCTURAL ANALYSIS	72
8.5 WEIGHT ANALYSIS	73
IX. CONCEPT SELECTION CRITERIA	75
9.1 SYSTEM WEIGHTING RATIONALE	75
9.2 RATING RANGE	76
9.3 HIGH-G SEAT CONCEPT EVALUATION	77
9.4 SELECTION CRITERIA EVALUATION	84

# TABLE OF CONTENTS (CONCLUDED)

SECTION	PAGE	
X	SELECTED CONCEPT FOR HIGH-G ESCAPE	93
	10.1 SELECTED CONCEPT DEFINITION	93
	10.2 SELECTED CONCEPT ANALYSIS	100
XI	CONCLUSIONS AND RECOMMENDATIONS	104
	APPENDIX - REPORT MDC J7976 - PARAMETRIC STUDY OF TAIL CLEARANCE TRAJECTORIES FOR HIGH-G CONDITIONS	105
	LIST OF REFERENCES	179

# LIST OF ILLUSTRATIONS

FIGURE		PAGE
1.	F-15 HAC CREW STATION ARRANGEMENT	6
2.	RECLINED PILOT INTERNAL VISION	7
3.	INSTRUMENT PANEL KNEE CLEARANCE	7
4.	INTEGRATED TORSO HARNESS RESTRAINT SYSTEM	12
5.	CHEST STRAP REEL	12
6.	INTEGRATED TORSO HARNESS LAP BELT	14
7.	CONTOUR AND INFLATION BLADDER	15
8.	CONTOUR BLADDER ARM RESTRAINT	15
9.	POWERED TORSO/HEAD SUPPORT-UPRIGHT	17
10.	POWERED TORSO/HEAD SUPPORT RECLINED	18
11.	TORSO/HEAD SUPPORT-ROTATED	18
12.	EJECTION LIMB RESTRAINT SYSTEM	20
13.	SEAT POSITIONING SYSTEM	22
14.	GEAR MOTOR TORQUE/ROTOR SPEED	24
15.	AIRCRAFT FLOOR MOUNTED POSITIONING GEAR MOTOR	24
16.	GUIDE RAIL AND SEAT REPOSITIONING CONFIGURATION	25
17.	SCHEMATIC-GUIDE RAIL AND SEAT REPOSITIONING SYSTEM	27
18.	RETRACTION REEL FORCE - VS. - TIME	28
19.	SEAT RETRACTION TIME - VS. - G LOAD FACTOR	28
20.	SEAT RETRACTION VERTICAL ACCELERATION	29
21.	SEAT RETRACTION HORIZONTAL ACCELERATION	29
22.	INITIATION SYSTEM SCHEMATIC	33
23.	CATAPULT IMPRESSED G EFFECTS	35

# LIST OF ILLUSTRATIONS (CONTINUED)

FIGURE		PAGE
24.	FLUIDIC THRUST VECTOR CONTROL (REF. 16)	41
25.	TVC ROCKET NOZZLE (REF. 16)	41
26.	VERTICAL SEEKING SEAT GIMBALLED ROCKET	42
27.	VERTICAL SEEKING SEAT-INVERTED TRAJECTORY	42
28.	SMDC CANOPY FRACTURING SYSTEM	45
29.	HIGH-G SEAT CONCEPT B	50
30.	HIGH-G SEAT CONCEPT D <sub>1</sub>	51
31.	HIGH-G SEAT CONCEPT E <sub>1</sub>	52
32.	CATAPULT THRUST -VS. - TIME	58
33.	CATAPULT DRI PARAMETER $\delta$ - VS - TIME	59
34.	CATAPULT DRI - VS - PEAK G	60
35.	CATAPULT $\delta$ AND DRI - VS - TIME, 150% THRUST	61
36.	CATAPULT THRUST DURATION DRI - VS - PEAK G	62
37.	ACCELERATION VECTOR DIAGRAM - SEAT CONCEPTS D <sub>1</sub> AND E <sub>1</sub>	63
38.	SPINAL COMPONENTS/DRI/CATAPULT PEAK G	64
39.	TAIL CLEARANCE EFFECT OF + G <sub>z</sub>	67
40.	RAIL ANGLE/ROCKET THRUST VECTOR/SPINAL G- VS - AIRCRAFT TAIL CLEARANCE	68
41.	TAIL CLEARANCE HEIGHT - VS - RAIL ANGLE, -4 G <sub>x</sub> /+10 G <sub>z</sub>	69
42.	TAIL CLEARANCE HEIGHT - VS - RAIL ANGLE, +2 G <sub>x</sub> /+10 G <sub>z</sub>	70
43.	HIGH-G SEAT CONCEPTS SELECTION CRITERIA EVALUATION	85
44.	SUPPORT/RESTRAINT SUBSYSTEMS - SELECTION CRITERIA EVALUATION	86
45.	SEAT POSITIONING SUBSYSTEMS - SELECTION CRITERIA EVALUATION	87

# LIST OF ILLUSTRATIONS (CONTINUED)

FIGURE		PAGE
46.	EJECTION INITIATION SUBSYSTEMS - SELECTION CRITERIA EVALUATION	88
47.	SEAT STABILIZATION SUBSYSTEMS - SELECTION CRITERIA EVALUATION	89
48.	EJECTION PROPULSION SUBSYSTEMS - SELECTION CRITERIA EVALUATION	90
49.	CANOPY JETTISON SUBSYSTEMS - SELECTION CRITERIA EVALUATION	91
50.	HIGH-G EJECTION SEAT SELECTED CONCEPT CONFIGURATION	94
51.	HIGH-G EJECTION SEAT INITIATION SYSTEM SCHEMATIC	97
52.	SELECTED CONCEPT TAIL CLEARANCE TRAJECTORIES, HIGH-G SPEED MODE	101
53.	SELECTED CONCEPT TAIL CLEARANCE TRAJECTORIES, LOW-SPEED MODE	102
54.	TYPICAL EFFECT OF IMPRESSED G ON CATAPULT THRUST	113
55.	CATAPULT IMPRESSED G EFFECTS	114
56.	ROCKET THRUST VARIATIONS	116
57.	LIFT AND DRAG COEFFICIENTS, $M = 0.6$	117
58.	LIFT AND DRAG COEFFICIENTS, $M = 0.9$	118
59.	ACES/B1 SEAT TEST DATA	120
60-A.	SEAT ATTITUDE ANGLES, $30^{\circ}$ RAIL, 150% ROCKET THRUST	123
60-B.	SEAT ATTITUDE ANGLES, $30^{\circ}$ RAIL, 150% ROCKET THRUST	124
61-A.	SEAT ATTITUDE ANGLES, $30^{\circ}$ RAIL, 200% ROCKET THRUST	126
61-B.	SEAT ATTITUDE ANGLES, $30^{\circ}$ RAIL, 200% ROCKET THRUST	127
62.	PITCH VARIATIONS, $30^{\circ}$ RAIL, 200% ROCKET THRUST	129
63.	EFFECT OF PITCH VARIATION ON TAIL CLEARANCE - 200 % ROCKET THRUST	130

# LIST OF ILLUSTRATIONS (CONTINUED)

FIGURE		PAGE
64.	PARAMETRIC TRAJECTORIES, $30^{\circ}$ RAIL ANGLE, 200% ROCKET THRUST, EFFECT OF AIRCRAFT $G_x$	132
65-A.	PARAMETRIC TRAJECTORIES, $15^{\circ}$ RAIL ANGLE, 200% ROCKET THRUST	134
65-B.	PARAMETRIC TRAJECTORIES, $15^{\circ}$ RAIL ANGLE, 200% ROCKET THRUST	135
66.	ACCELERATION VECTORS, $30^{\circ}$ RAIL ANGLE, 150% ROCKET THRUST	138
67.	ACCELERATION VECTORS, $30^{\circ}$ RAIL ANGLE, 200% ROCKET THRUST	139
68-A.	PARAMETRIC TRAJECTORIES, $30^{\circ}$ RAIL ANGLE, 150% ROCKET THRUST	140
68-B.	PARAMETRIC TRAJECTORIES, $30^{\circ}$ RAIL ANGLE, 150% ROCKET THRUST	141
69-A.	PARAMETRIC TRAJECTORIES, $30^{\circ}$ RAIL ANGLE, 200% ROCKET THRUST	143
69 B.	PARAMETRIC TRAJECTORIES, $30^{\circ}$ RAIL ANGLE, 200% ROCKET THRUST	144
70.	TAIL CLEARANCE AND SPINAL $G_z$ , $30^{\circ}$ RAIL ANGLE, 150% ROCKET THRUST	145
71.	TAIL CLEARANCE AND SPINAL $G_z$ , $30^{\circ}$ RAIL ANGLE, 200% ROCKET THRUST	147
72.	PARAMETRIC TRAJECTORIES, $30^{\circ}$ RAIL ANGLE, 150% ROCKET THRUST, 34.0 G CATAPULT	148
73.	ACCELERATION VECTORS, $45^{\circ}$ RAIL ANGLE, 200% ROCKET THRUST	150
74-A.	PARAMETRIC TRAJECTORIES, $45^{\circ}$ RAIL ANGLE, 200% ROCKET THRUST	151
74-B.	PARAMETRIC TRAJECTORIES, $45^{\circ}$ RAIL ANGLE, 200% ROCKET THRUST	152
75.	TAIL CLEARANCE AND SPINAL $G_z$ , $45^{\circ}$ RAIL ANGLE, 200% ROCKET THRUST	153

# LIST OF ILLUSTRATIONS (CONCLUDED)

FIGURE		PAGE
76.	ACCELERATION VECTORS, $60^{\circ}$ RAIL. 200% ROCKET THRUST	156
77-A.	PARAMETRIC TRAJECTORIES $60^{\circ}$ RAIL ANGLE, 200% ROCKET THRUST	157
77-B.	PARAMETRIC TRAJECTORIES $60^{\circ}$ RAIL ANGLE, 200% ROCKET THRUST	158
78.	TAIL CLEARANCE AND SPINAL $G_z$ , $60^{\circ}$ RAIL ANGLE, 200% ROCKET THRUST	159
79.	TAIL CLEARANCE HEIGHT VERSUS RAIL ANGLE, $-4 G_x/+10 G_z$	162
80.	TAIL CLEARANCE HEIGHT VERSUS RAIL ANGLE, $+2 G_x/+10 G_z$	163
81.	PARAMETRIC TRAJECTORIES, 450 KEAS, $30^{\circ}$ RAIL ANGLE, 200% ROCKET THRUST	166
82.	PARAMETRIC TRAJECTORIES, 450 KEAS, $45^{\circ}$ RAIL ANGLE, 200% ROCKET THRUST	167
83.	PARAMETRIC TRAJECTORIES, 450 KEAS, $45^{\circ}$ RAIL ANGLE, 150% ROCKET THRUST	169
84.	PARAMETRIC TRAJECTORIES, 450 KEAS, $60^{\circ}$ RAIL ANGLE, 200% ROCKET THRUST	170



## SECTION I

### INTRODUCTION AND SUMMARY

This report presents the results of the Phase I and Phase II design study and analysis of an ejection seat for high-G escape under Air Force Contract F33615-78-C-3416.

Phase I is an investigative phase for the definition and establishment of Concept Criteria and Interface Requirements leading to the Phase II Design Synthesis phase for the definition, analysis and integration of a selected seat concept for the high acceleration cockpits generated under the F-15/F-16 HAC studies.

Existing sources of literature having application to high G escape have been searched and reviewed and a list of references included in this report. Design criteria and interface requirements have been established. Seat subsystems have been developed and candidate seat design concepts, incorporating the various subsystems, generated to meet the design criteria and interface requirements.

Each of eight candidate seat concepts have been analyzed to determine cockpit integration effects, accelerations, ejection clearances and performance, structural requirements and weights. From this analysis a final design concept has been selected to meet all requirements for an ejection seat for high-G escape.

## SECTION II

### STINFO LITERATURE SEARCH

Existing sources of literature having application to the high G escape program have been searched and reviewed. Areas relevant to the objectives of this study have included high-speed, high-G escape, wind-blast protection, crew support and restraint, ejection propulsion, thrust vector control, biodynamic response to high G and computer analysis of ejection systems.

The literature search covered a relatively wide range of subjects due to the large number of interfaces involved. On some subjects there is little information readily available while on other subjects there is a great deal of information available; although it is not all directly applicable or relevant.

The design data contained in the Air Force design handbooks and specifications is considered to be applicable where directly relevant.

A summary of the design data situation is contained in the following paragraphs:

#### High G Protection/Posture:

Present design trends indicate a 65 degree back angle (Ref. 1, 2, 3, 4, 10). One study (Ref. 5) suggests a 50-degree optimum angle, and one study (Ref. 8) indicates that raised legs are beneficial. Chest side supports aid breathing (Ref. 6,7). Fatigue, comfort and heart-rate benefits are shown at 40-degree back angle (Ref. 9).

#### Escape Under High G and Maneuver Conditions:

There is some data available relative to escape under high acceleration conditions. This data indicates that current propulsion systems will be unsatisfactory under the specified +G conditions. Work has been done which indicates that current rocket catapults will impose ejection forces which are likely to cause injury under high +Gz conditions. (Ref 11 through 17 and 26, 27). There is no data available on systems which will perform under all the conditions required.

#### High Acceleration Cockpit (HAC):

Information generated by McDonnell Douglas with regard to HAC, AFTI and other advanced design programs provides the primary source of data relative to the design of articulating seats, cockpit configurations, displays and controls and combat operations. (Ref. 18 through 25). This data is directly usable for cockpit/seat integration and interface requirements.

#### Restraints:

Due to the novel requirements of this study, the majority of restraint data available is not relevant (Ref. 28 through 35). The most pertinent data is that associated with the HAC-AFTI programs.

With regard to protection against windblast, the data generated by Payne for AMRL provides basic aerodynamic information while a recent study by Grumman for the Navy, although directed at the near-term improvement of an existing seat, examines several approaches for restraint and protection for high speed conditions.

In terms of current limb flail protection systems, there is considerable design experience within Douglas as a result of the development of limb restraint systems for the ACES seat for the B-1 Aircraft.

#### Disorientation and Vision Under High G:

Pressures applied to the crewman, externally and internally, are important factors in acceleration protection. Experiments have shown that loss of vision was related to the effective systolic arterial pressure to the eye. This was demonstrated by showing that the application of external suction to the eye restored vision under high acceleration conditions. Anti-G suits have been in use since WW II and recent experiments have indicated that design changes can improve their effectiveness. (Ref 36 through 40). It appears that there is a need for a comprehensive review of the design parameters to establish comparative effectiveness of methods to improve vision and reduce disorientation under high G conditions.

### SECTION III

#### INTERFACE REQUIREMENTS

Interface requirements provide for positioning the crewman from a 13-degree normal upright position to a 65-degree reclined position within the constraints of the F-15/F-16 HAC cockpit designs. The relationship of the crewman to the instrument panel, consoles and controls in the F-15 HAC cockpit is shown in Figure 1.

The interfaces which are most influenced by seat articulation are external and internal vision, rudder pedal and leg position, and functional reach. Primary variables in HAC seat geometry are pan angle, back angle, headrest angle and headrest/shoulder offset. Pilot shoulder and head/eye position has a first-order influence on pilot reach, vision and the utility of the crew station. Internal cockpit vision is affected in the reclined eye position. In this position the pilot's lower torso and legs block vision to the lower portion of the main instrument panel. All primary controls and displays, HUD, engine and fuel instruments must be visible from this position as shown in Figure 2. Only the standby instruments, located on the center console, may be obstructed when reclined.

Constraints on the main instrument panel control and display arrangement are the pilot's knee position, the 30-inch ejection clearance line, the windshield contour and the sill structure. Pilot leg position influences HAC integration because of the interaction of the seat pan for thigh support, rudder pedal location, instrument panel depth and reduction of the panel area to provide adequate knee clearance in the reclined position as shown in Figure 3. A limited displacement pedal is integrated to provide a common pedal location.

The articulating seat configuration must be compatible with 5th-through 95th-percentile USAF pilot population and the location and vision of all critical controls and displays consistent with the crew member reach envelopes in all seat positions. Design concepts for high G escape will maintain all noted cockpit interface requirements.

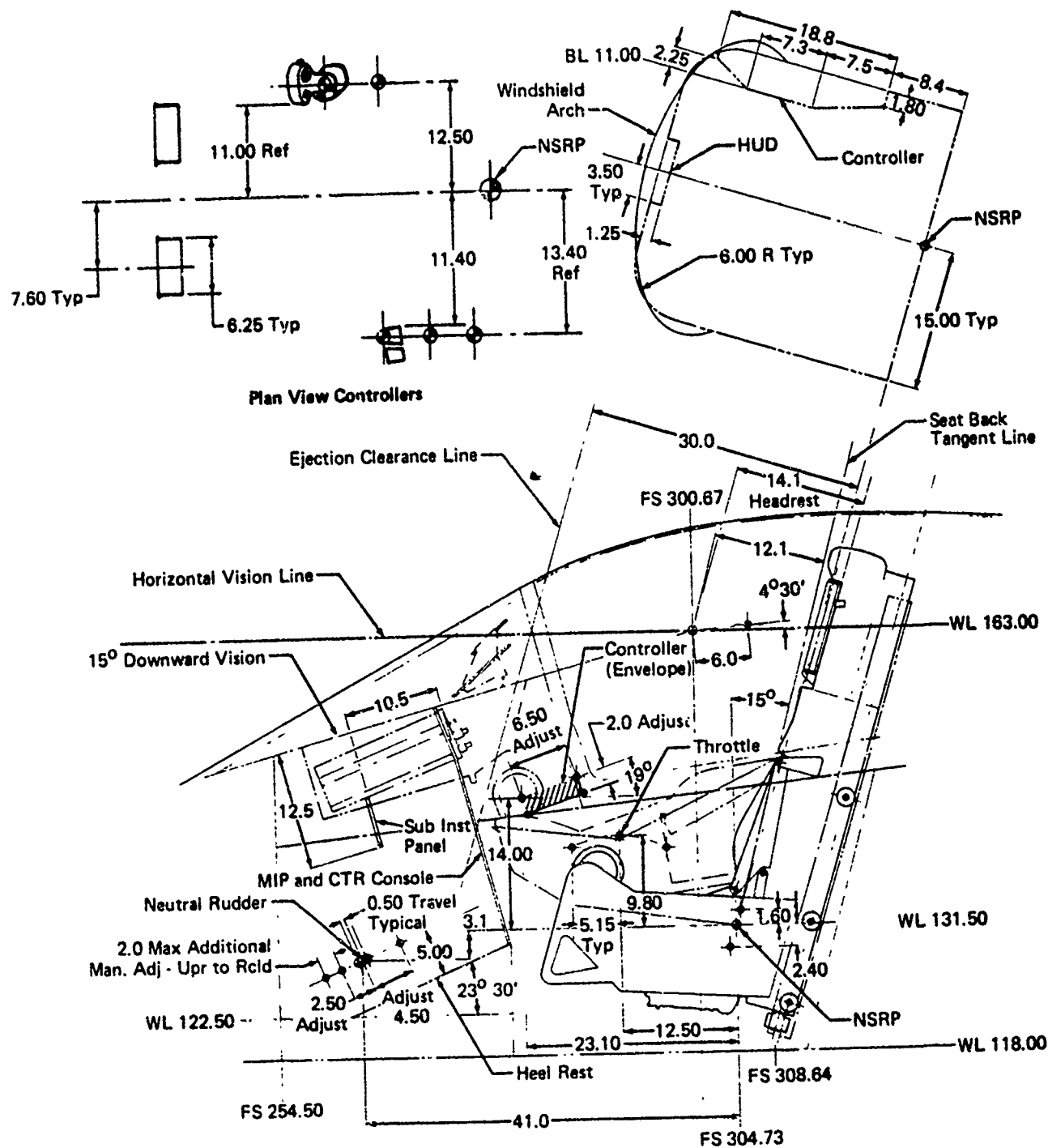


Figure 1. F-15 HAC Crew Station Arrangement

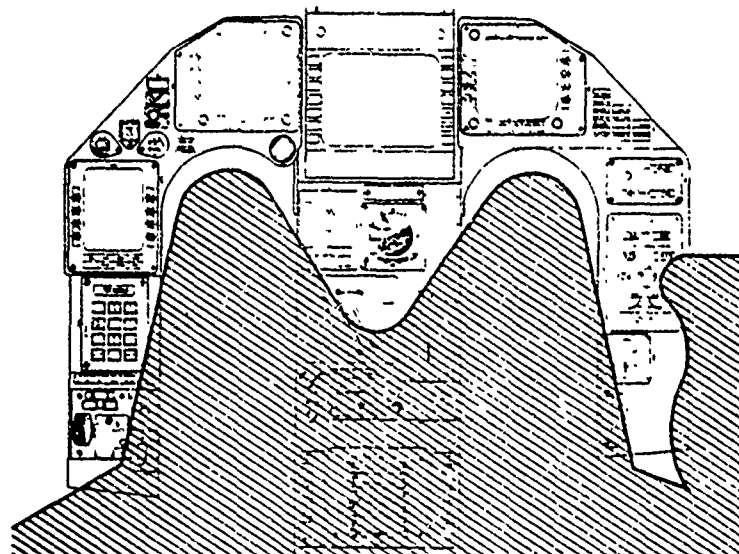


Figure 2. Reclined Pilot Internal Vision

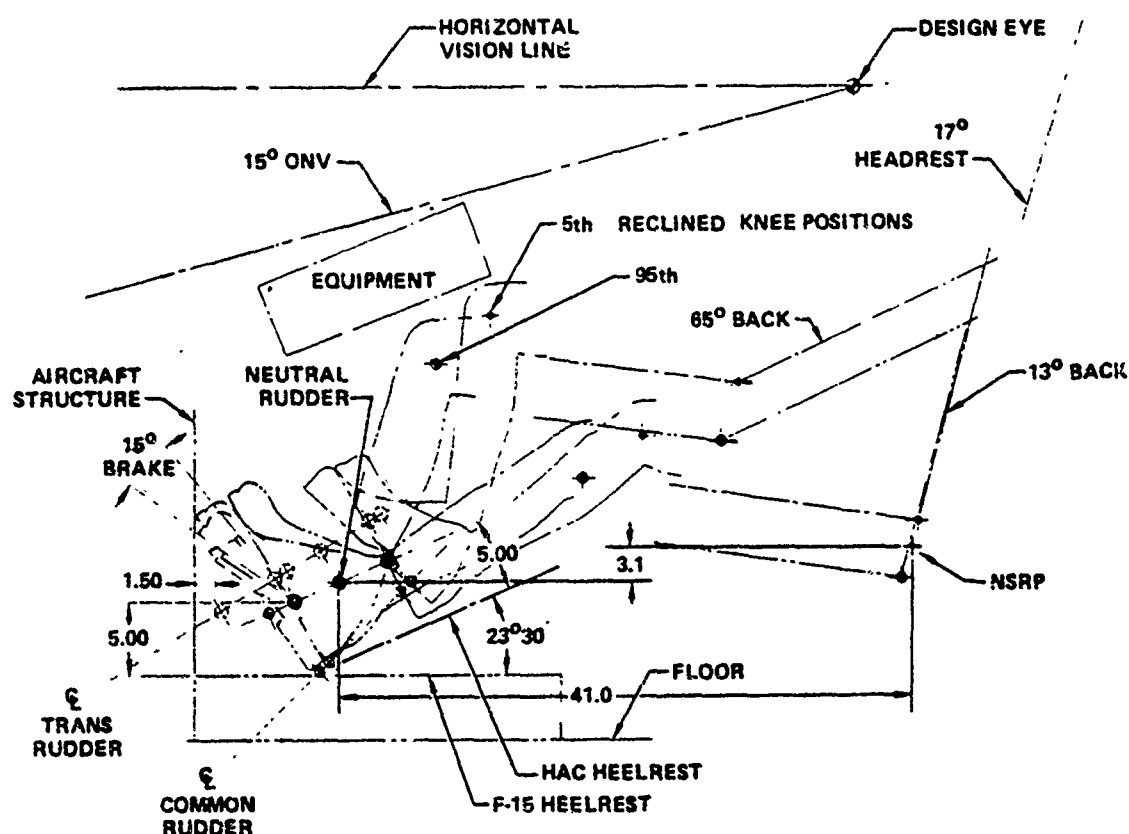


Figure 3. Instrument Panel Knee Clearance

SECTION IV  
DESIGN CRITERIA

Design criteria elements are defined from the established interface requirements. The following design criteria has been identified and will remain within the requirements of USAF Specification MIL-S-9479B.

1 COCKPIT/SEAT/MAN INTERFACE

Side stick controllers.

Common rudder pedal position.

Instrument panel and HUD functional reach and vision.

Crew motions possible at maximum aircraft G loads:

- |                                  |    |
|----------------------------------|----|
| • raising the arm above the head | 6G |
| • moving the head                | 4G |
| • raising the arm from armrest   | 8G |
| • raising the knee               | 3G |
| • moving the foot fore and aft   | 5G |
| • raising the foot               | 3G |

2 SEAT POSITIONING

Seat articulation - 13 degrees to 65 degrees.

Manual actuation to recline or Automatic-pilot select actuation.

Shoulder pivot backrest.

Seat pan angle - 8 degrees to 7 degrees.

3 CREW SUPPORT/RESTRAINT

Maximum crew mobility.

Minimum preflight hookups.

Compatible with preflight procedures.

Minimum time to emergency egress.

Windblast protection during and after canopy jettison.

Restraint under all flight and ejection conditions.

4 EJECTION INITIATION

Functional reach in all seat positions.

Operation under all combined flight loads.

5 EJECTION PROPULSION

Ejection envelope - 0 to 50,000 ft. altitude and 0 to 600 KEAS.

Any combined design G limits of +2, -4  $G_x$      $\pm 2 G_y$     +10, -3  $G_z$

6 EJECTION CLEARANCES

Tail clearance under all combined flight loads.

Automatic retraction to upright seat position or Pre-ejection rail repositioning in any seat position.

Retraction or repositioning within ejection G limits.

7 SEAT STABILIZATION

Damped oscillation of  $\pm 5$  degrees.

Operation under all combined flight loads.

8 CANOPY JETTISON

Windblast protection.

Operation under all combined flight loads.



## SECTION V

### SEAT SUBSYSTEMS

To meet the requirements for high G escape the following major subsystems have been identified:

- Support/restraint system
- Seat positioning system
- Ejection initiation system
- Ejection propulsion system
- Seat stabilization system
- Canopy jettison system

#### 5.1 SUPPORT/RESTRAINT

High G, multi-axis, aircraft acceleration forces require crew restraint and support under all flight conditions and positive positioning during emergency retraction and ejection. The restraint systems presently employed in conventional ejection seats will not hold the crewman in the position necessary for aircraft operation when the specified high acceleration forces are applied. The crewman's lower legs are held in place by the seat and console side panels but his upper body is free to move in response to side forces. Forces above 0.7 g become very fatiguing and lateral restraint is necessary. The restraint system must afford crew mobility for efficient operation of the aircraft. The restraint system must be compatible with the seat and crewman in both the upright and reclined positions and must provide sufficient structural integrity to withstand ditching and crash loads.

##### 5.1.1 Basic Restraint Harness

The combination of shoulder harness straps, torso harness and chest straps are considered as a total integrated restraint system. The integrated torso harness system shown in Figure 4, consists of restraint straps that snap to rings on the PCU 15/P torso harness adjacent to the harness chest strap. This concept uses a chest strap reel, shown in Figure 5, to permit pilot mobility in the unlocked condition. The reel is locked or unlocked in conjunction with the shoulder harness inertia reel. This permits freedom of movement in the unlocked condition and interacts with the torso harness to prevent submarining in the locked condition. The reel straps are released automatically with the existing lap belt and shoulder harness release system for seat/man separation after ejection.

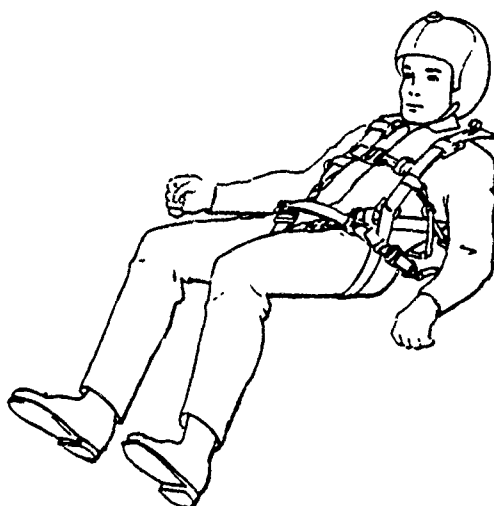


Figure 4. Integrated Torso Harness Restraint System

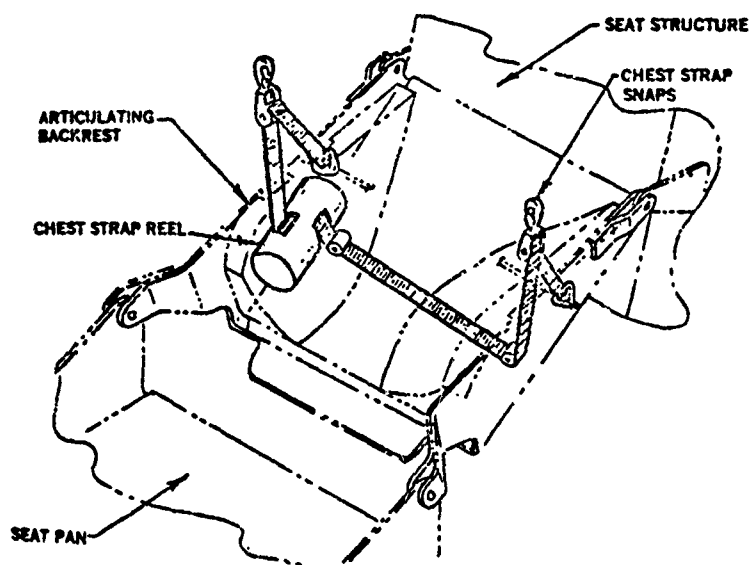


Figure 5. Chest Strap Reel

Combinations of integrated harness, crotch strap and lap belt are required to provide adequate pelvic restraint in all seat positions. The integrated harness lap belt consists of a cross strap on the PCU 15/P restraint harness shown in Figure 6. This arrangement prevents submarining without the addition of a separate crotch strap arrangement. An automatic lap belt take-up system compensates for the loosening of the lap belt that occurs as the body moves from the upright to the reclined position. A lap belt end fitting link is depressed by a striker arm on the lower articulating back rest as the seat reclines. This motion maintains the belt adjustment and prevents the belt from riding up and over the hips in the reclined position.

#### 5.1.2 Contour Bladder Restraint

This concept consists of the addition of an inflatable torso and limb fixation system as shown in Figures 7 and 8. The articulating backrest consists of three segments which have projections to retain and support the body. One segment encloses the shoulders while the two lower segments enclose the upper and lower torso. The projecting portions are fitted with a contour and inflation bladder system. The contour bladder system assembly consists of three elements: A contour bladder, an inflation cell and the supporting structure. The contour bladder assumes the contour of whatever shape with which it is in contact. When suction is applied the bladder retains the formed shape and becomes rigid. The bladder is constructed of frothed neoprene and is filled with "microbearings" of expanded polystyrene. The microbearings move to assume the shape being imposed on the bladder but lock together under vacuum forming a rigid shape.

The contour bladder is attached to an inflation cell which, in turn, is secured to the support structure. For normal conditions, when the "body fixation" support is not required, the contour cushion is flaccid and the inflation cell is evacuated. In this condition there is sufficient space between the bladder assembly and the surface of the crewman to permit freedom of movement. When the "body fixation" is required, the inflation cell is pressurized causing the contour bladder to press against the crewman. The contour bladder is then evacuated and the rigid surface provides a support restraint evenly distributed over the portion of the crewman with which it is in contact.

The bladder system is also used to provide restraint for the thighs and for the forearms. In the case of the forearms, the bladder system is contained in a trough which forms the arm support for operation of the side-stick controllers. When the system is activated, the bladder system holds the forearm firmly in place and also prevents motion of the elbows.

The system may be actuated in any of three modes:

- a. Automatically upon ejection.
- b. Manual pilot selection.
- c. Automatic sensing of aircraft G loads.

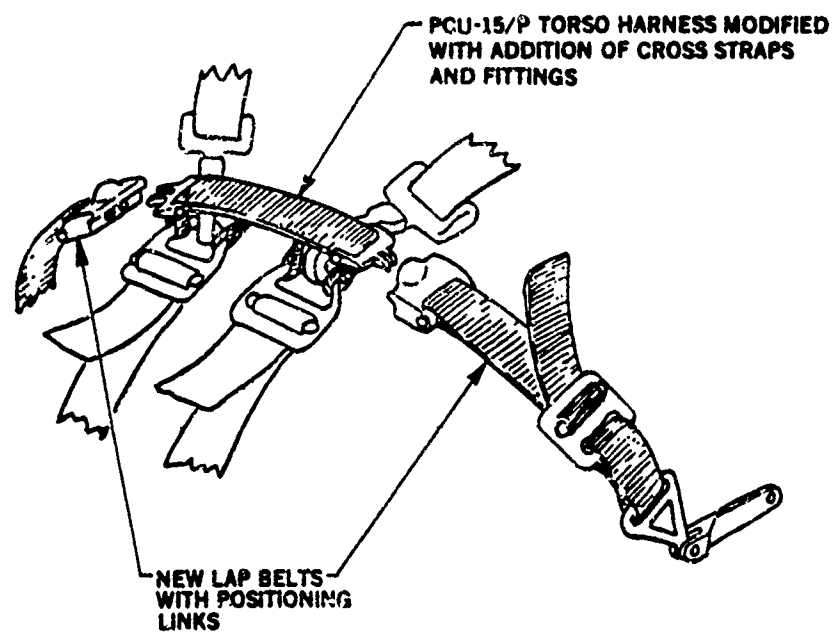


Figure 6. Integrated Torso Harness Lap Belt

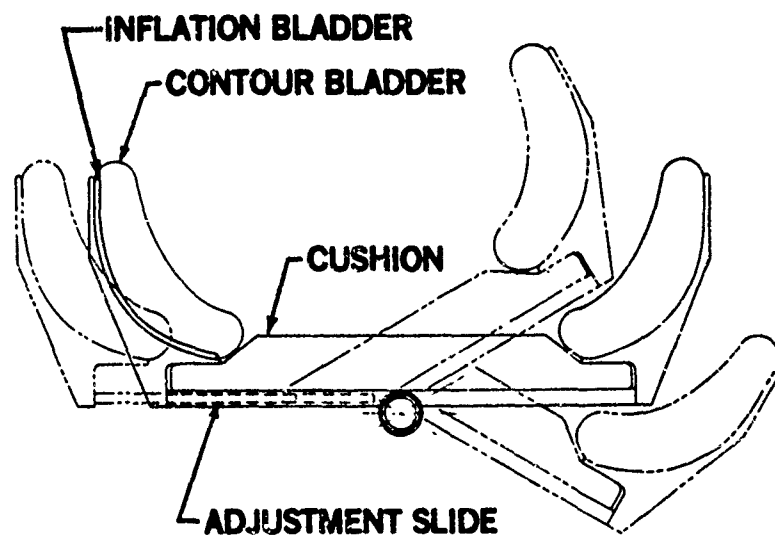


Figure 7. Contour and Inflation Bladder

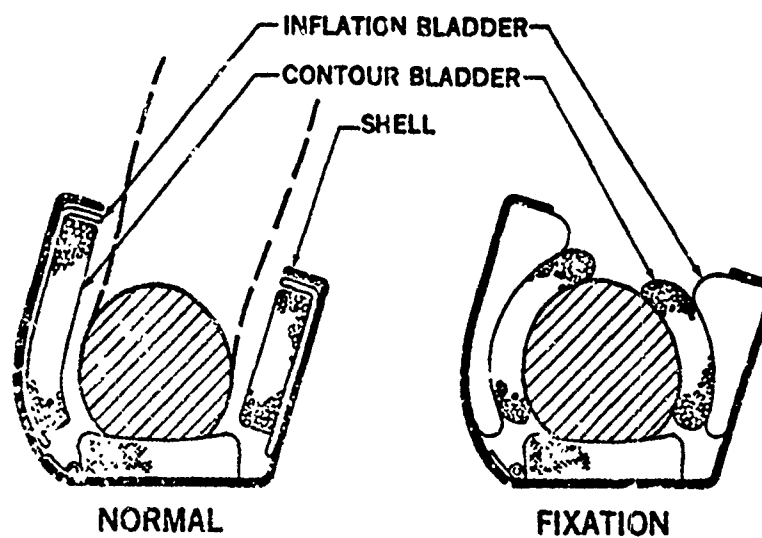


Figure 8. Contour Bladder Arm Restraint

### 5.1.3 Head/Torso Support

Primary design considerations require provisions for lateral head support without compromising head mobility and aft and overhead pilot vision. A concept has been developed incorporating rubber rollers to facilitate head rotation for side vision. This concept does not restrict aft and overhead visibility beyond the available in current ejection seats. These rollers have been positioned to contact the pilot's helmet at points further forward than conventional "V" block supports and so provide added side support to the head and helmet.

Lateral support is provided without the constraints of added harness strap arrangements by a new design concept providing support in the shoulder area. Fixed shoulder supports are mounted on the aircraft ejection guide rail structure and do not eject with the seat. This fixed location maintains a constant relationship to the pilot's shoulder throughout the 5th through 95th percentile range of sizes as the seat is adjusted vertically to the desired design-eye position.

### 5.1.4 Powered Twist Torso/Head Support

A powered restraint/support concept consists of a basic approach to provide the body with an external shell into which  $G_y$  loads are distributed. The support shell takes the form of padded, load-carrying segments which are installed on the seat, as shown in Figure 9. During seat articulation the segments automatically reposition to provide maximum comfort in either the upright or reclined positions, as in Figure 10.

The head and helmet are supported by an adjustable headrest to permit conventional head freedom-of-movement. When restraint is required, the headrest pads move forward, either at pilot discretion or at the onset of a lateral acceleration force, and a pair of padded arms move in to support the helmet in the occupant's preselected comfort position.

A feature of this concept is a system which allows the crewmember to rotate the upper torso and head by means of powered assist system, as shown in Figure 11. To facilitate visibility when the crewman is subjected to high  $G$  forces the backrest segments are mounted on a spine so that the segments can be rotated in the lateral direction. The articulating spine has adjustable spline portions so that as the backrest articulates between the upright and recline positions the length of the spine adjusts so that scrubbing of the crewman's back will be minimized.

When a twisting motion of the upper torso is desired for additional external visibility the crewman can actuate the electrically driven backrest system. The powered drive rotates the upper backrest segment, at the shoulders, until the desired angle of twist is reached.

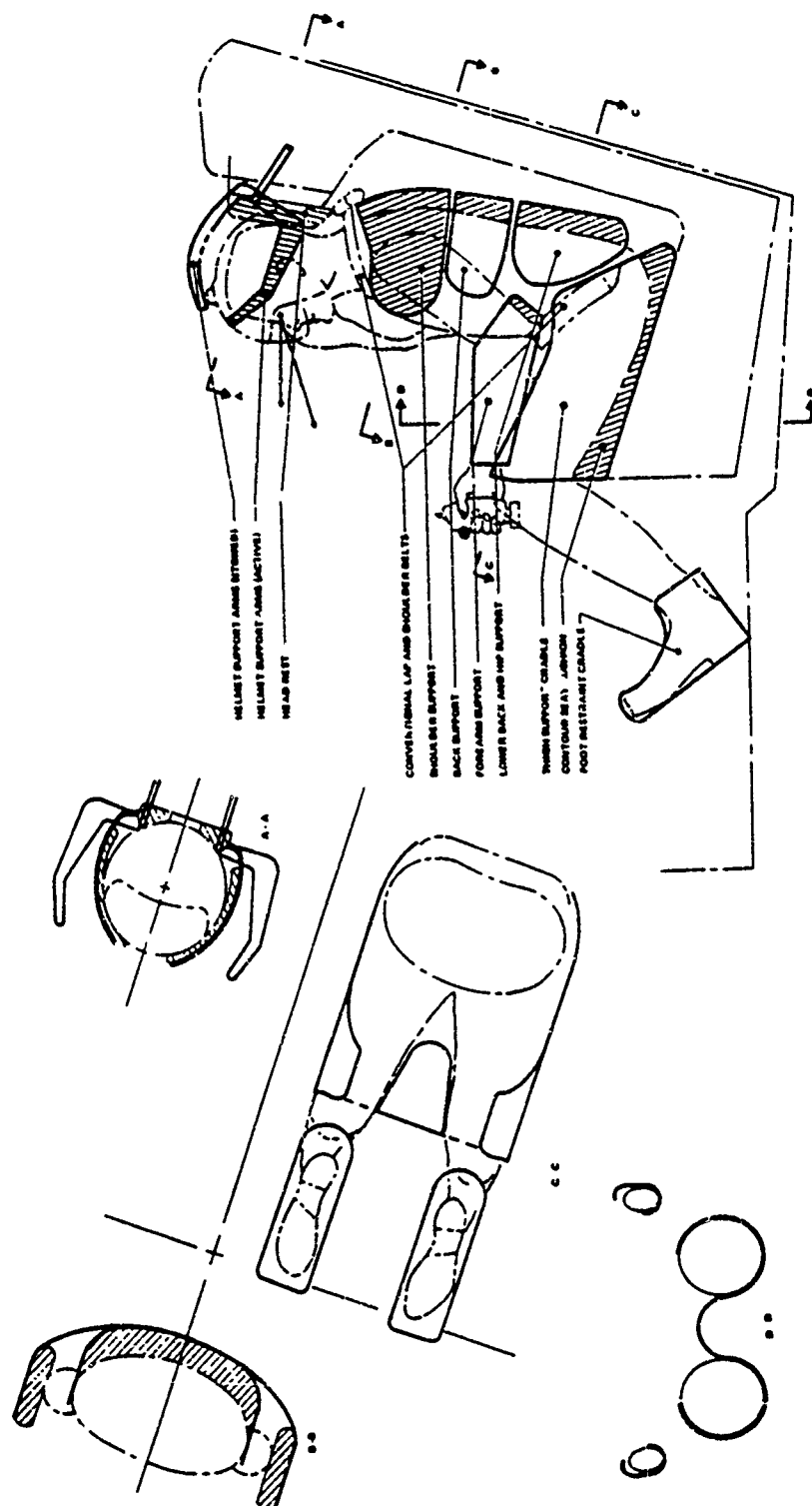


Figure 9. Powered Torso/Head Support-Upright

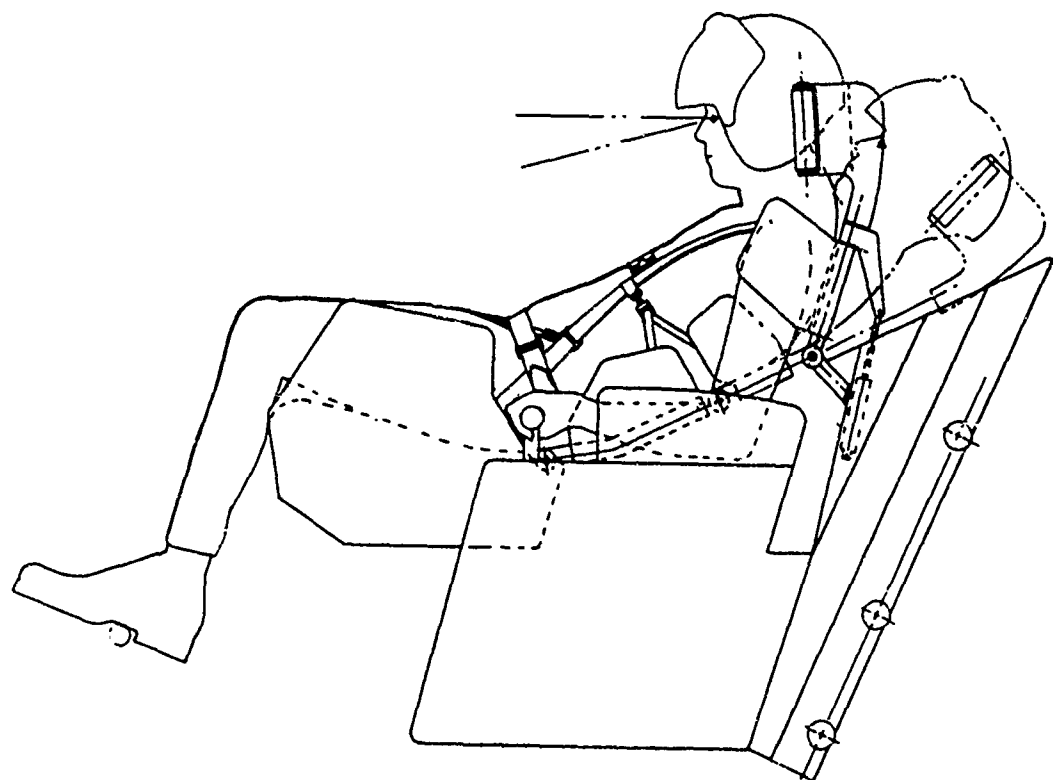


Figure 10. Powered Torso/Head Support Reclined

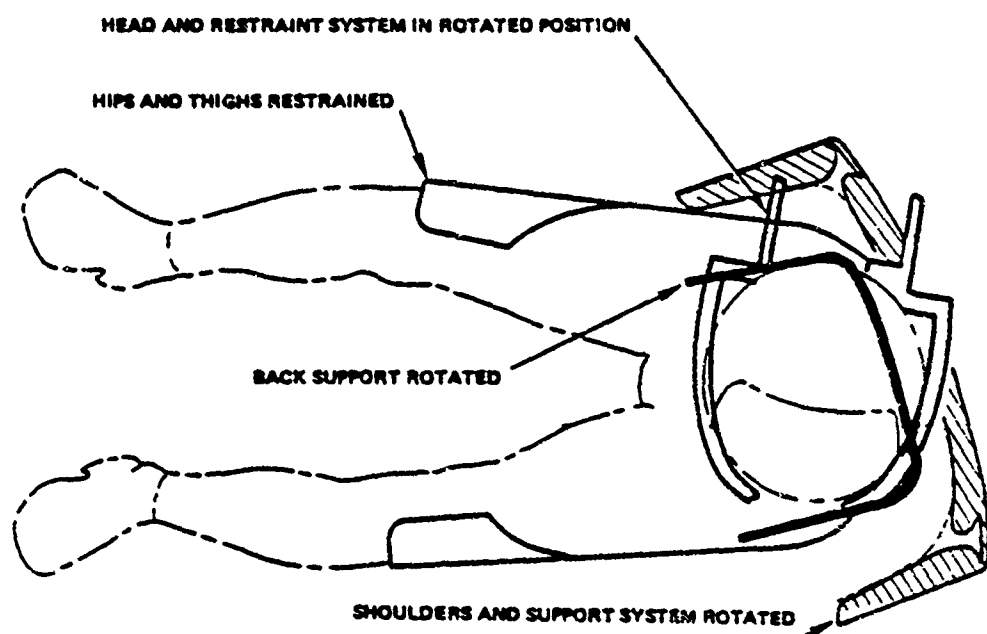


Figure 11. Torso/Head Support-Rotated



### 5.1.5 Ejection Limb Restraint

Candidate concepts to solve the recurring problem of limb restraint injuries during high speed, high g ejections, consist of a restraint strap system used in ACES B-1 ejection seat, the contour bladder restraint system and an advanced technology system employing inflatable restraint.

The restraint strap system, shown in Figure 12, minimizes preflight connections and the possibility of misrigging upon entering the aircraft. It also eliminates the necessity for any secondary release operation for ground emergency or normal egress.

Two restraint straps, normally stowed on the ejection seat, are donned by the seated crewmember when connecting the torso harness and lap belt fittings. No pre-flight adjustments are required. When donned, the restraint straps permit unrestricted arm movement in the cockpit. Leg restraint is provided by straps that require pre-flight connections with leg garters worn by the crewman before entering the aircraft.

Restraint occurs only upon seat motion during ejection. In the fully restrained position the crewmembers arms are held firmly against his sides by strap loops above and below the elbow. Hands and wrists are not restrained. The legs are held in position at the front beam of the seat bucket. All straps are automatically released at seat/man separation by the existing harness release subsystem after ejection. For normal or emergency ground egress the restraint straps are released by disconnection of the lap belt fittings or by actuation of the harness release handle.

The contour bladder restraint system concept provides protection against windblast by the body fixation and leg-restraint system. Neck protection is provided by an inflatable collar. The body fixation system and the neck collar are activated during the pre-ejection sequence. The forearm fixation system is released at seat man separation by automatic release of the outboard bladder supports.

The advanced technology concept involves the use of inflatables to shield the crewman from windblast as he enters the airstream. This concept uses rigid inflatable structures to shield, support and restrain the crewman. This concept is based on the use of fast-acting inflatables to provide a predetermined shape having suitable structural and aerodynamic characteristics.

Side panels are normally stowed at the rear of the escape system with the inflatable structures. Upon initiation of the escape system, the shoulder harness is retracted and the side panels are forced forward, pushing the arms inward in front of the body. When movement of the side panels is complete, the shield structure is inflated in front of the crewman. As the seat leaves the cockpit, the leg restraints and shields are activated and inflated. The shield system is designed to remain rigidly inflated only long enough to protect the crewman from the high-speed windblast.

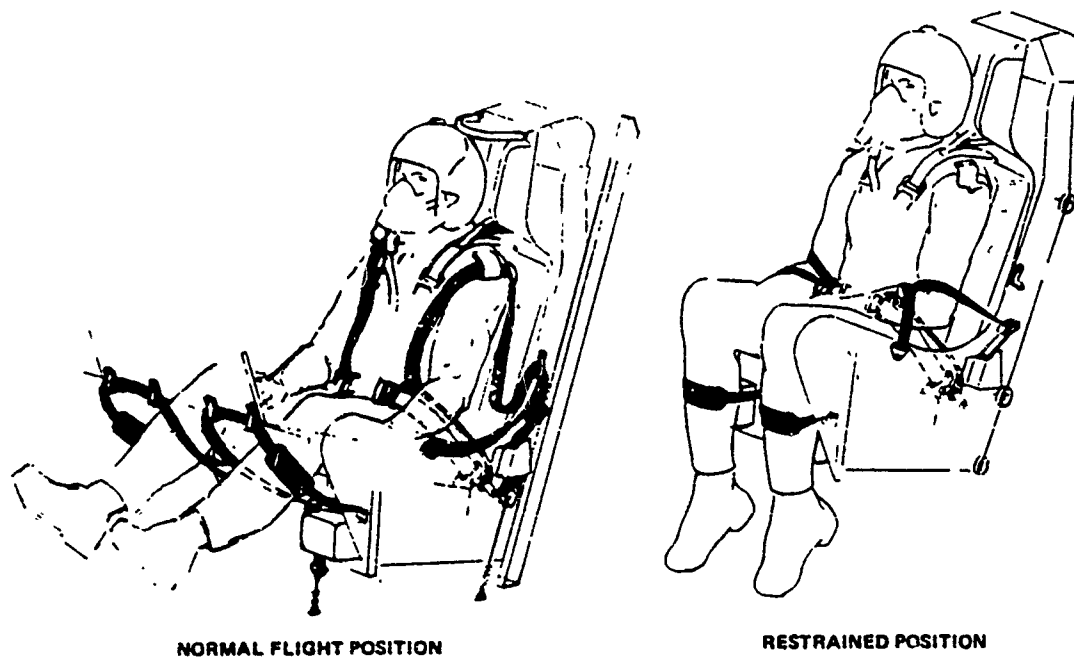


Figure 12. Ejection Limb Restraint System

## 5.2 SEAT POSITIONING

Integration of a pilot positioning system into a high G ejection seat may be accomplished by the addition of articulating segments to a basic seat structure providing a multi-position range of seat back angles from a 130° normal upright position to a reclined back angle position of 65°.

Design criteria has been established to determine articulation rates under the following design considerations:

- Operation under G fields from  $-3 G_z$  to  $+10 G_z$ .
- Acceptable acceleration on the pilot during repositioning.
- Rapid repositioning effect on pilot disorientation with cockpit displays and controls under flight conditions.
- Pilot response in positioning the seat at intermediate back angles.
- Effect of articulating mechanism requirements on seat/cockpit envelope, survival kit volume, power requirements, seat weight and escape performance.

Design concepts will position to any pre-selected intermediate back angle with a minimum of coast, over-travel and braking action. Automatic shut-off and braking at the extremes of travel with mechanical stops to prevent over-travel will be provided. Normal articulation rate of the seat positioning system will not be more than 30 msec/degree seat back angle (1.5 seconds upright to reclined, or reverse).

A design concept consists of the integration of the seat positioning system into the ejection seat. This concept is shown in Figure 13. The positioning system consists of the addition of the articulating backrest and shoulder support, the seat pan and bucket, and the gear motor assembly unit. Positioning motion of the seat pan is controlled by a four-bar linkage consisting of the seat back, bucket, primary seat structure and lower links. The lower links are integral with gear sectors driven by a pinion gear and cross shaft assembly that is part of an integral gear motor unit. This arrangement provides lateral stability of the articulating components and maintains the structural integrity of the basic seat.

Normal articulation rates of 1.5 seconds, operating under 10 G conditions requires a gear motor rated at approximately 2 HP. In this analysis motor acceleration and braking times are significant factors. A motor weight of 12 lbs. and a total volume of 80 cu. in. meets these requirements.

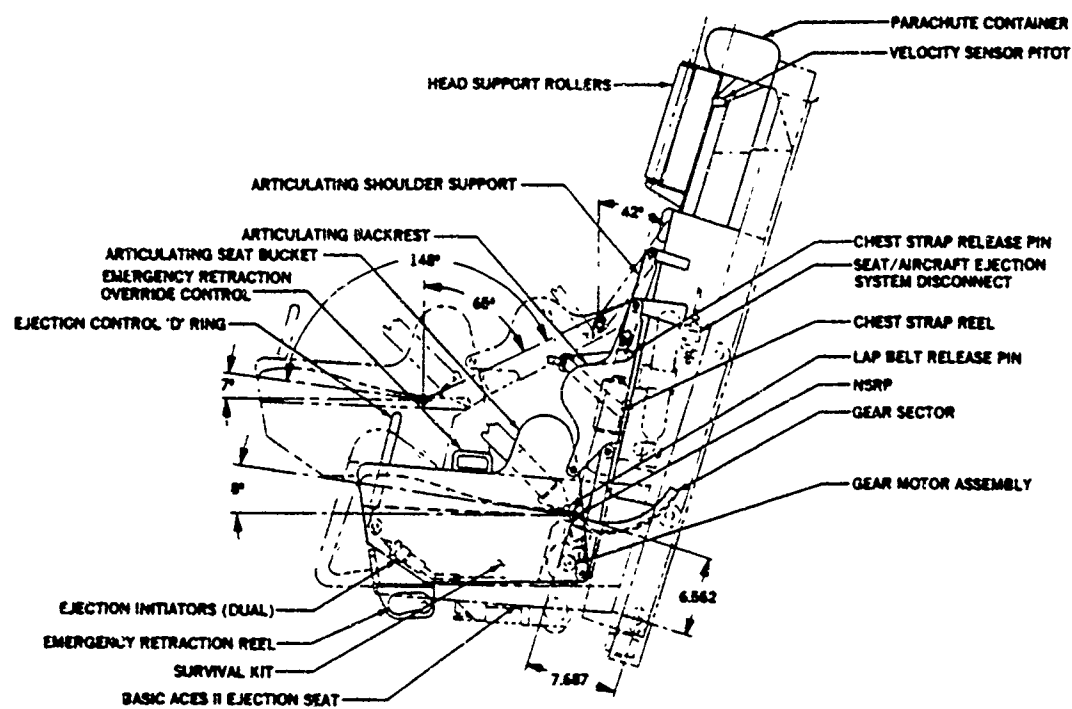


Figure 13. Seat Positioning System

Acceleration and deceleration loads on the seat occupant during normal articulation are minimal. For zero G flight conditions acceleration on the pilot will be 0.12 G and deceleration/braking loads will be In 10 G flight conditions acceleration is 0.05 G and deceleration is 0.29 G, with a maximum rate of onset of 3.24 G/second. Deceleration under varying conditions of motor brake design, vertical and horizontal G loads, and occupant weight show minor variations from those noted, with negligible effect on the seat occupant.

These calculations are based on a maximum efficiency gear motor with a rated HP at a rotor RPM at which the motor torque equals one half the starting torque. As shown in Figure 14, a rotor speed of 9200 RPM provides these rated load and torque requirements. The average accelerating torque will be 83.2% of the starting torque when acceleration and deceleration are linear. Braking torque is established at 1.44 times the starting torque.

An alternate design concept has been developed for the high G ejection seat to minimize the weight and volume effect on escape performance. The seat will be driven by an electromechanical gear motor mounted on the aircraft cockpit floor, as shown in Figure 15. This concept consists of floor mounted bevel gear boxes and torque shaft and a seat-mounted bevel gear box and spline shaft. This arrangement permits normal vertical seat adjustment and automatic disengagement for ejection. A weight reduction of the ejected mass of 10.5 pounds from an integral seat-mounted gear motor has been estimated for this system.

#### 5.2.1 Guide Rail and Seat Repositioning System

A concept to position the seat from the 15 degree upright position to the 65 degree reclined position by pivoting the seat and guide rails as a unit is shown in Figure 16. The pivot point for rotation is located at the same shoulder pivot location as the articulating seat concept to maintain shoulder, design eye and knee positions. This pivot is mounted on a guided structure to permit normal vertical adjustment independent of any reclined seat position.

A pyro-mechanical seat/rail thruster is mounted on the vertically adjustable structure. Normal electro-mechanical operation of this thruster rotates the seat/rail unit into any reclined position. Pyro operation occurs only upon ejection to eject the seat from the fully reclined position.

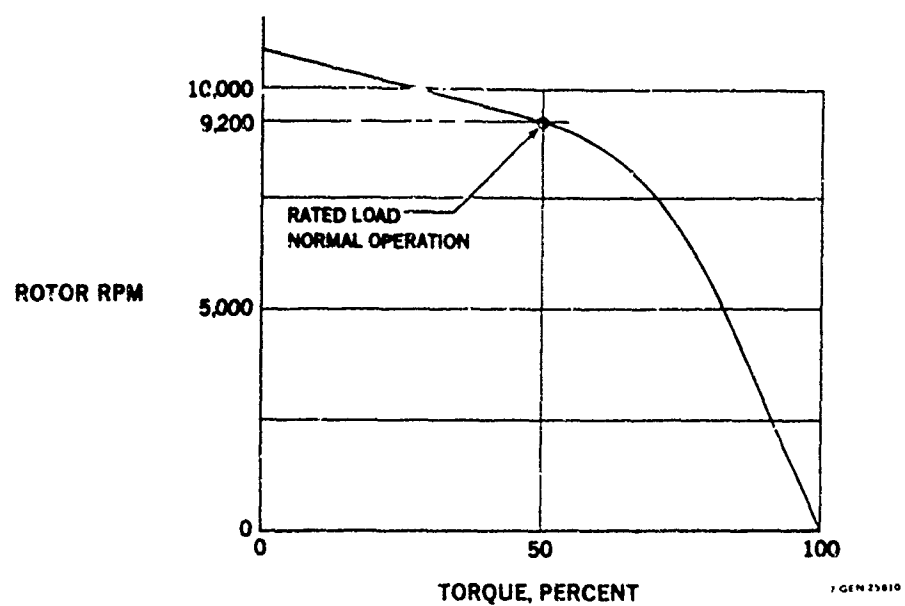


Figure 14. Gear Motor Torque/Rotor Speed

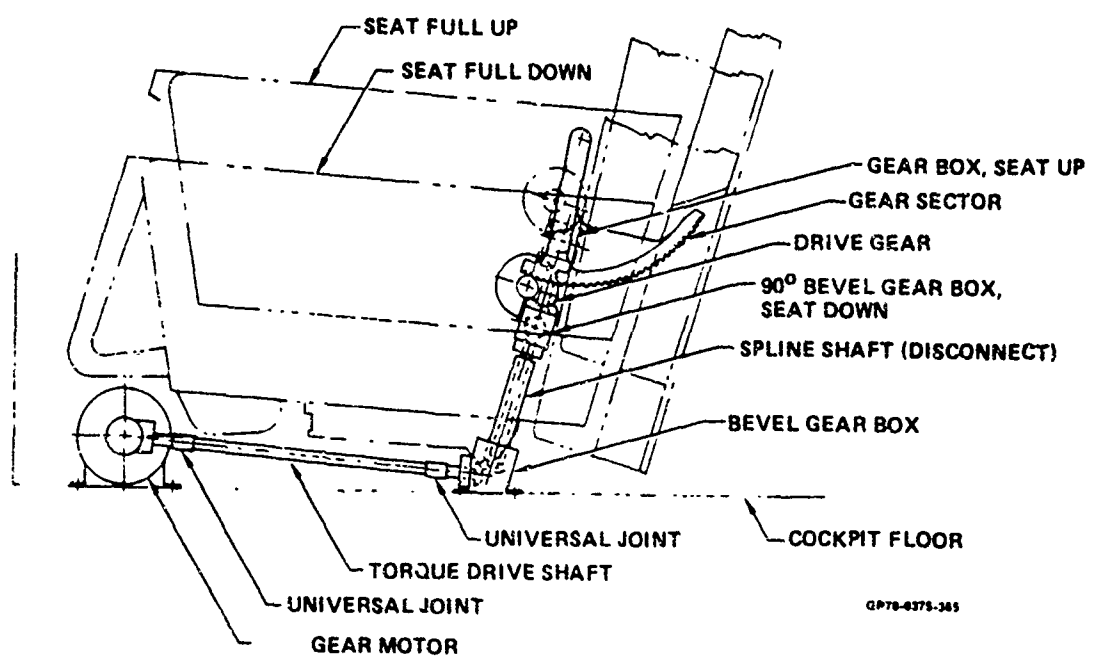


Figure 15. Aircraft Floor Mounted Positioning Gear Motor

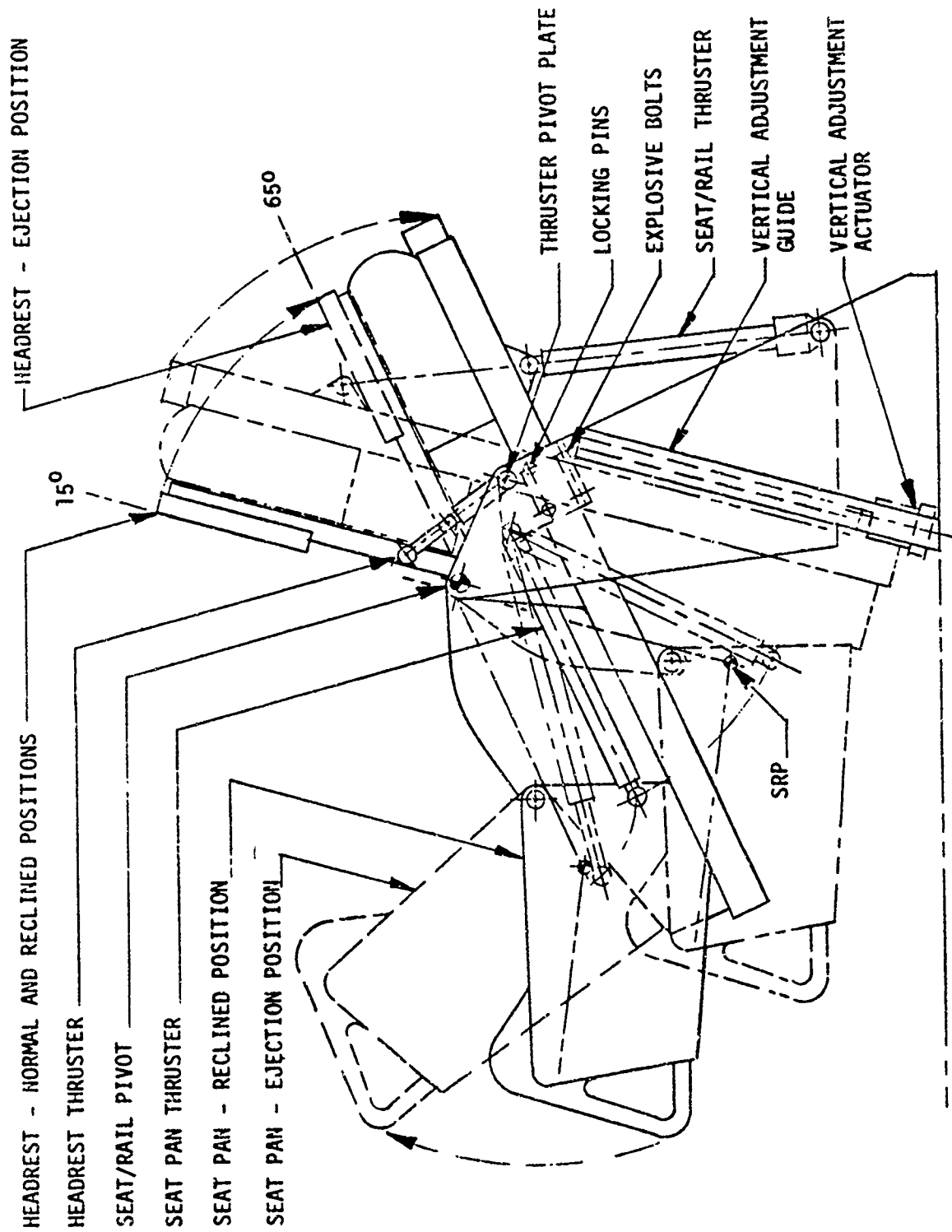


Figure 16. Guide Rail and Seat Repositioning Configuration

The seat pan and the headrest are articulating segments with positioning controlled by fixed thruster/links. These thruster/links remain fixed during normal seat positioning rotation. Thruster actuation occurs only at ejection to recline the headrest and raise the seat pan to their ejection positions. Both thrusters are mounted on a pivot support plate that is attached to the guide structure by explosive bolts. Seat-mounted locking pins engage the pivot plate and the explosive bolts are simultaneously released upon ejection. Thruster/links and support plate are ejected with the seat, maintaining headrest and seat pan in the ejection position. The seat/rail positioning thruster operates to rotate the seat/rail unit to the 65 degree ejection position as part of these pre-ejection functions. These operations are shown schematically in Figure 17.

#### 5.2.2 Emergency Retraction

For high G ejection seat concepts that include retraction to the upright position prior to ejection, an automatic emergency retraction system is required. The retraction system will operate within the required pre-ejection time delays for canopy removal, shoulder harness power retraction and other pre-ejection functions of the escape system. Emergency retraction will be initiated and be automatic with actuation of the primary ejection control. Operation, functioning and sequencing of all ejection subsystems will not be affected by the emergency retraction system, except that an interlock may be provided to prevent seat catapult ignition unless positive indication is received that the articulating components are down and locked in the upright ejection position.

Emergency retraction system design will ensure that the pilot's injury threshold will not be exceeded under all retraction/ejection conditions. Retraction forces, velocities, accelerations, rates of onset, damping and stopping forces will remain within physiologically acceptable limits.

Emergency retraction in 0.3 seconds has been established as a design requirement. This retraction rate will be provided by a pyro reel with a constant retraction force of 715 pounds as shown in Figure 18. This provides a maximum retraction time of 0.3 seconds in a -3 G field condition and a minimum retraction time of .06 seconds when operating in a +10 G condition as shown in Figure 19. These retraction rates result in vertical and longitudinal accelerations as shown in Figures 20 and 21.



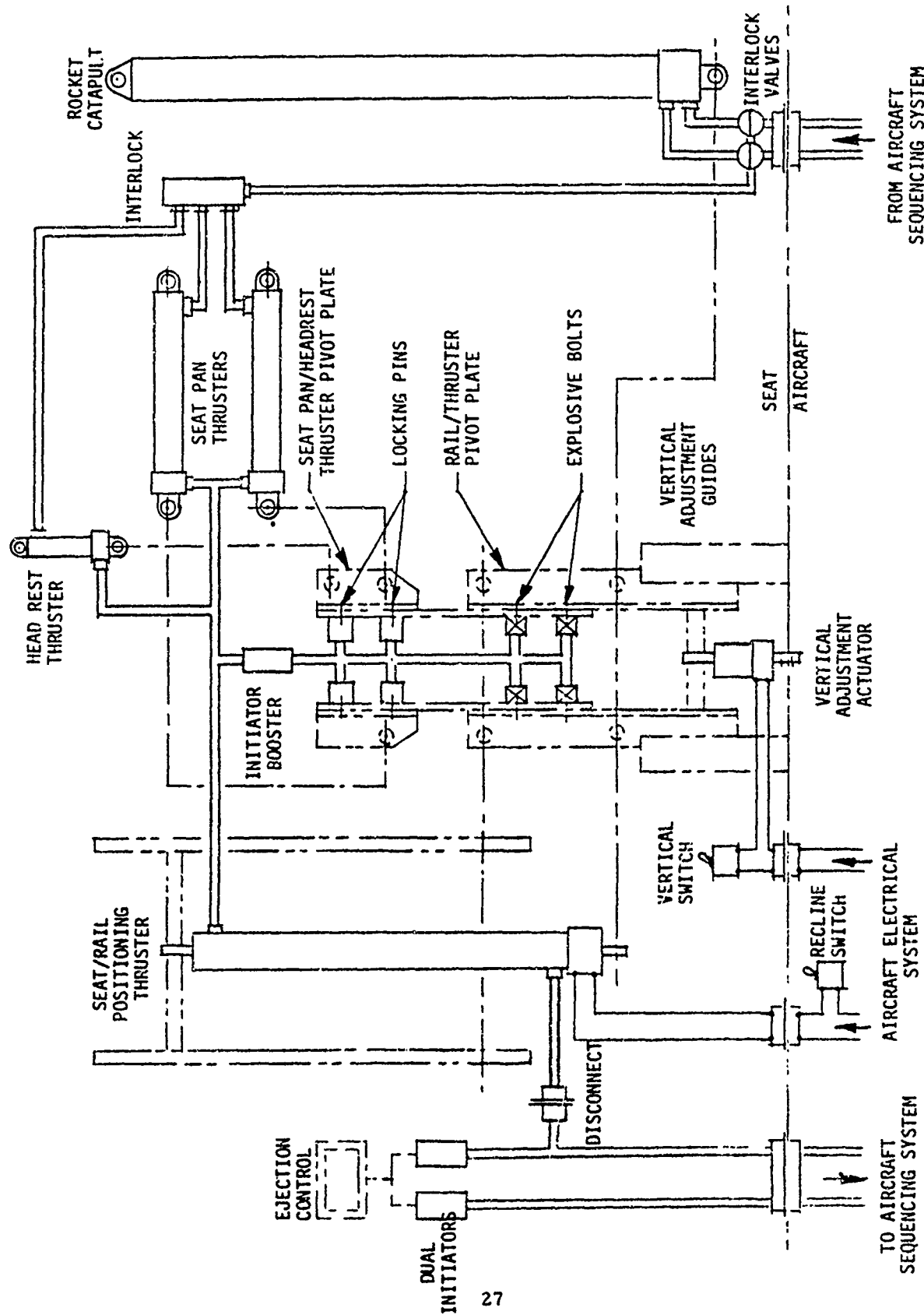


Figure 17. Schematic-Guide Rail and Seat Repositioning System

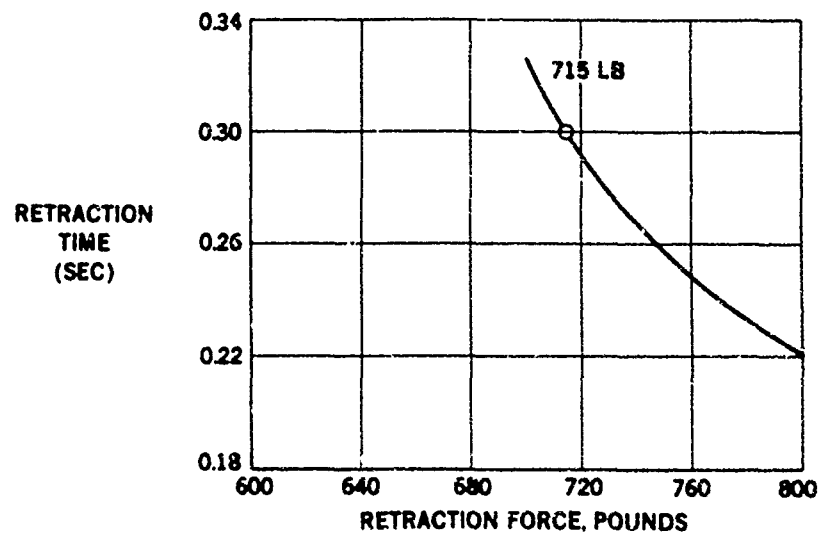


Figure 18. Retraction Reel Force — Versus — Time

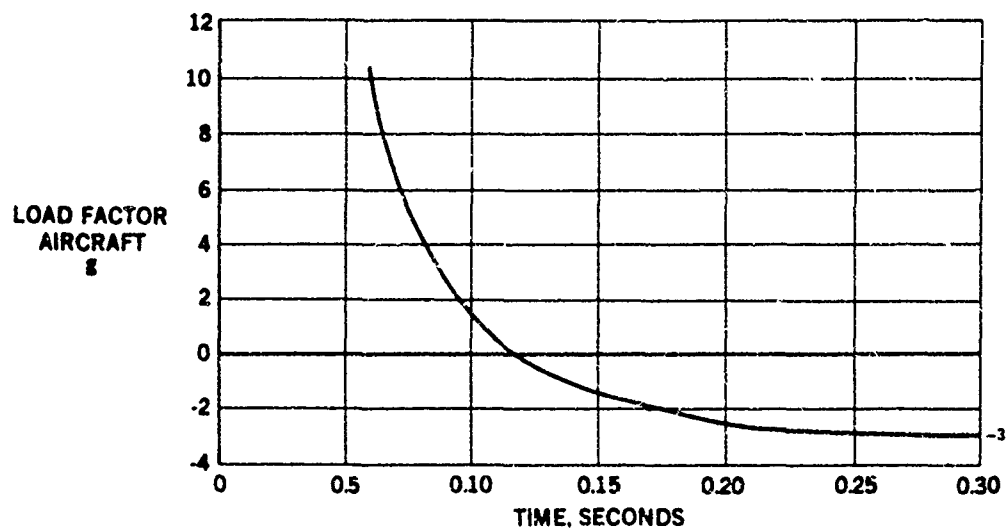


Figure 19. Seat Retraction Time — Versus — G Load Factor

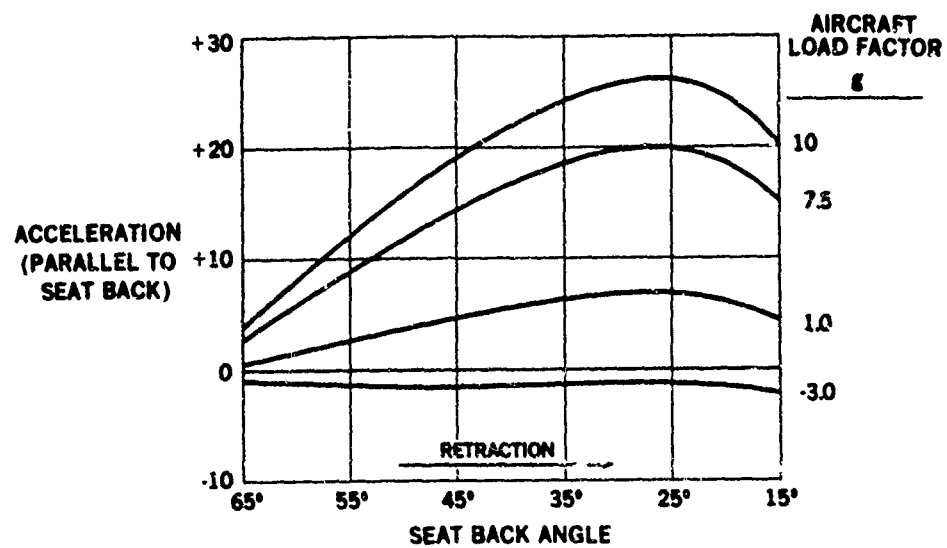


Figure 20. Seat Retraction Vertical Acceleration

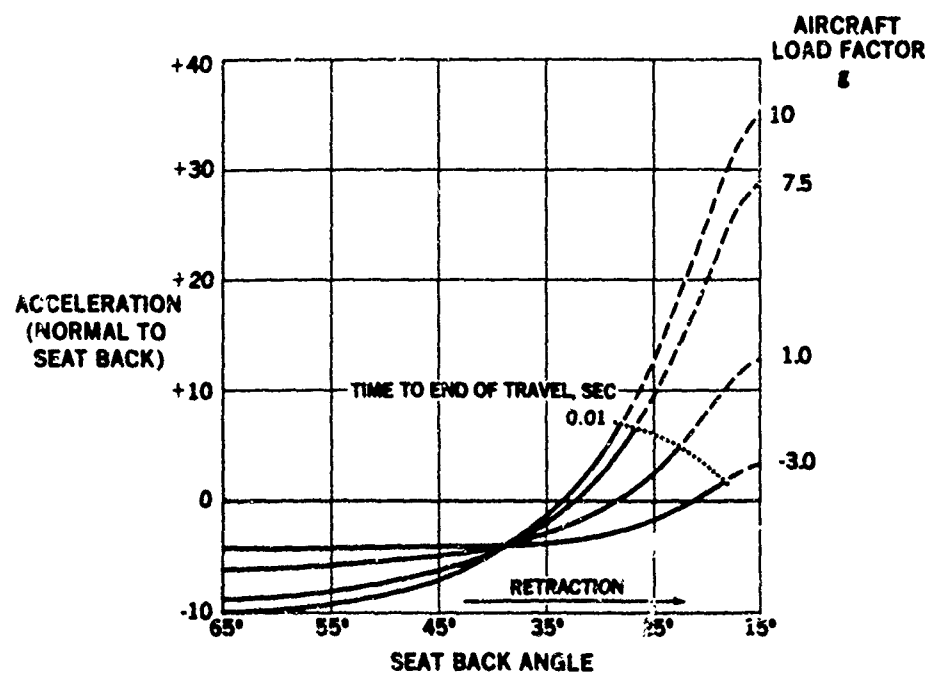


Figure 21. Seat Retraction Horizontal Acceleration

To reduce acceleration forces on the crewman during emergency retraction a rate-sensitive snubbing device will be introduced to limit retraction times to a minimum of 0.2 seconds under all G field conditions and to absorb the energy of the seat/man mass at the lower end of emergency retraction travel. This snubbing action is accomplished by mechanical, inertial-spring struts between the articulating seat bucket and the fixed seat structure. An internal inertial spring mass in the struts will limit acceleration rates to the predetermined value independent of the amount of force applied. Accelerations below the threshold value will not result in snubbing action so that torque requirements of the normal articulating gear motor and retraction reel force will not be affected.

### 5.3 EJECTION INITIATION

Initiation of the ejection control for the high G articulating seat involves considerations of pilot reach capability from any seat position, ease of operation, safety and impact on the cockpit configuration. In the reclined 65° position the control must be accessible to the 5th through 95th percentile range of pilot population and operable under all multi-axis G conditions.

Four methods of ejection initiation have been considered. These alternative methods may be required for actuation under 10 G<sub>z</sub> conditions when arm movement and operation of conventional systems would be extremely difficult:

- Seat side handles.
- Center D-ring - upward motion.
- Center D-ring - downward motion
- Electrical initiation.

#### 5.3.1 Seat Side Handles

A major consideration in the use of side handle controls involves the location of the HAC cockpit side-stick controller on the right hand sill. This projection into the ejection envelope is a potential source of pilot injury if conventionally located side handle ejection controls are used.

In order to maintain side handle ejection controls, alternate methods of integration are required. The integration of side handles requires that they be located aft and higher than currently acceptable positions to ensure access from all seat positions for the full range of pilot size. They would have to be mounted inboard, possibly over the pilot's leg, to preclude any chance of injury during seat ejection due to interference between the hands and the side-stick or throttles.

#### 5.3.2 Center D-Ring - Upward Motion

A center-mounted ejection control handle on the forward beam of the articulating seat pan is used to ensure safe actuation and access from any seat position. This concept permits ejection from any reclined seat position with minimum impact on cockpit ejection clearance considerations. Commonality of ejection control type and location with other high performance aircraft are other advantages of this concept. Currently, USAF aircraft such as the F-15, F-16, F-4 and A-10 are equipped with D-ring ejection controls.

### 5.3.3 Center D-Ring - Downward Motion

An alternative method of initiation is by use of a center firing control which would be actuated by applying the operating force in the downward direction. This control will be guarded or require two-motion operation (squeeze and push) to prevent inadvertent actuation. Ease of operation may be expected under +10 G<sub>z</sub> conditions.

### 5.3.4 Electrical Initiation

This system consists of guarded, two-motion, electrical switches on or under the forward seat sides. Both right and left switches will initiate ejection by a self-contained seat electrical power source. This power source may be supplied by a thermal, high-rise, battery similar to that currently in use on the ACES II ejection seat ejection sequencer.

### 5.3.5 Initiation System

Pre-ejection and ejection sequence functions will be actuated in a similar manner by any of the initiation concepts discussed. Initiation of the system retracts the shoulder harness inertia reel and actuates the canopy jettison system. In aircraft which have a separate windshield and canopy, the windshield may be hinged at the front and, on ejection or loss of canopy, the aft end of the windshield raised by thrusters. This will provide additional windblast protection for the crewman. In aircraft which have a single piece canopy and windshield, an inflatable bladder, located in the upper surface of the glareshield, may be inflated to afford similar protection.

For high G ejection seat concepts that require automatic return to the upright back position prior to ejection an emergency retraction system may be used. For emergency retraction an initiator supplies pre-ejection pressure to disengage the pinion gear, actuate a seat retraction reel and simultaneously initiate the aircraft canopy jettison and seat ejection sequence system, as shown schematically in Figure 22. This emergency retraction system illustrates the center D-ring concept of initiation and includes a manual override control to return the seat to the upright position in the event of malfunction to the normal seat articulation system. This override control will not effect the emergency ejection system or prevent its subsequent operation.

For seat ejection concepts requiring guide rail repositioning for cockpit ejection clearances repositioning thrusters will be actuated simultaneously with canopy removal as part of the pre-ejection functions.

Guide rail and seat positioning system schematic has been shown in Figure 17. The same ejection initiation considerations apply to all seat concepts.

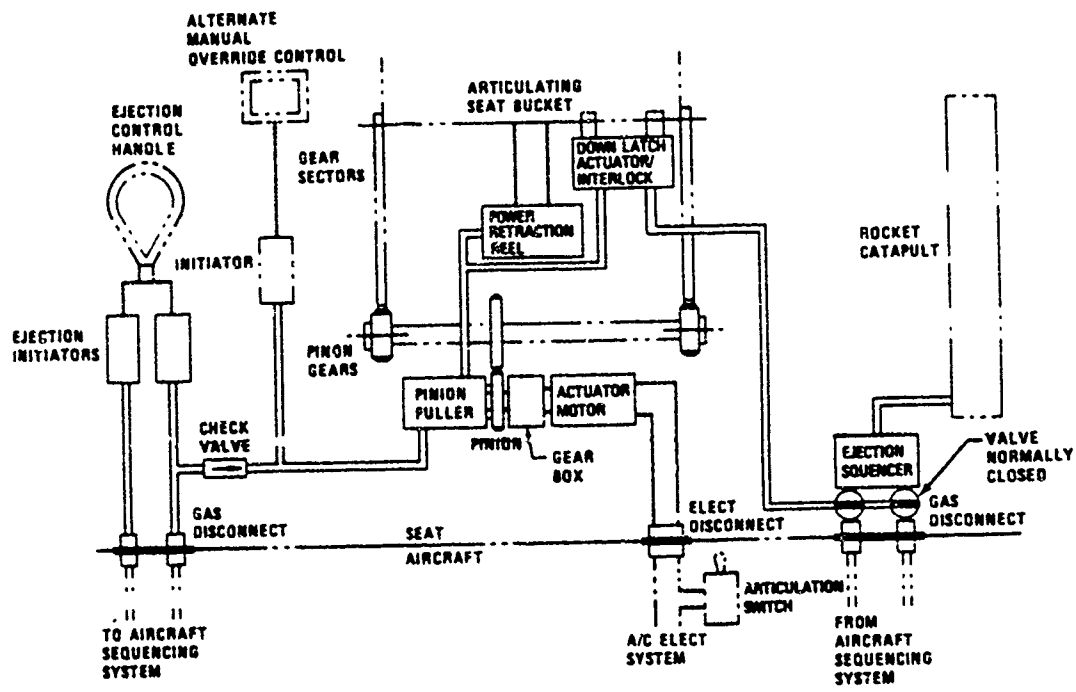


Figure 22. Initiation System Schematic

## 5.4 EJECTION PROPULSION

Ejection during 10 G aircraft load factor conditions requires lower catapult velocities and/or varied ejection rail angles to meet the dynamic response index, DRI, limits of MIL-S-9478B. Maximum catapult acceleration, must be reduced to meet the acceptable DRI limit of 18. As the ejection rails are inclined aft of the vertical, catapult forces may be increased, but added rocket thrust is required to provide adequate tail clearance. This increase in rocket thrust may result in degraded escape performance in adverse attitude and inverted ejection conditions. Increased rocket thrust is also critical in low speed, low drag conditions where accelerations may exceed human tolerance limits.

Ejection propulsion systems, in combination with varying ejection and seat back angles, required to meet all conditions of high G escape consist of the following candidate concepts:

- Low boost phase/high thrust rocket
- Twin sustainer rocket motors
- Two-stage rocket motor
- Twin low-boost catapults
- Catapult pressure limiting valve

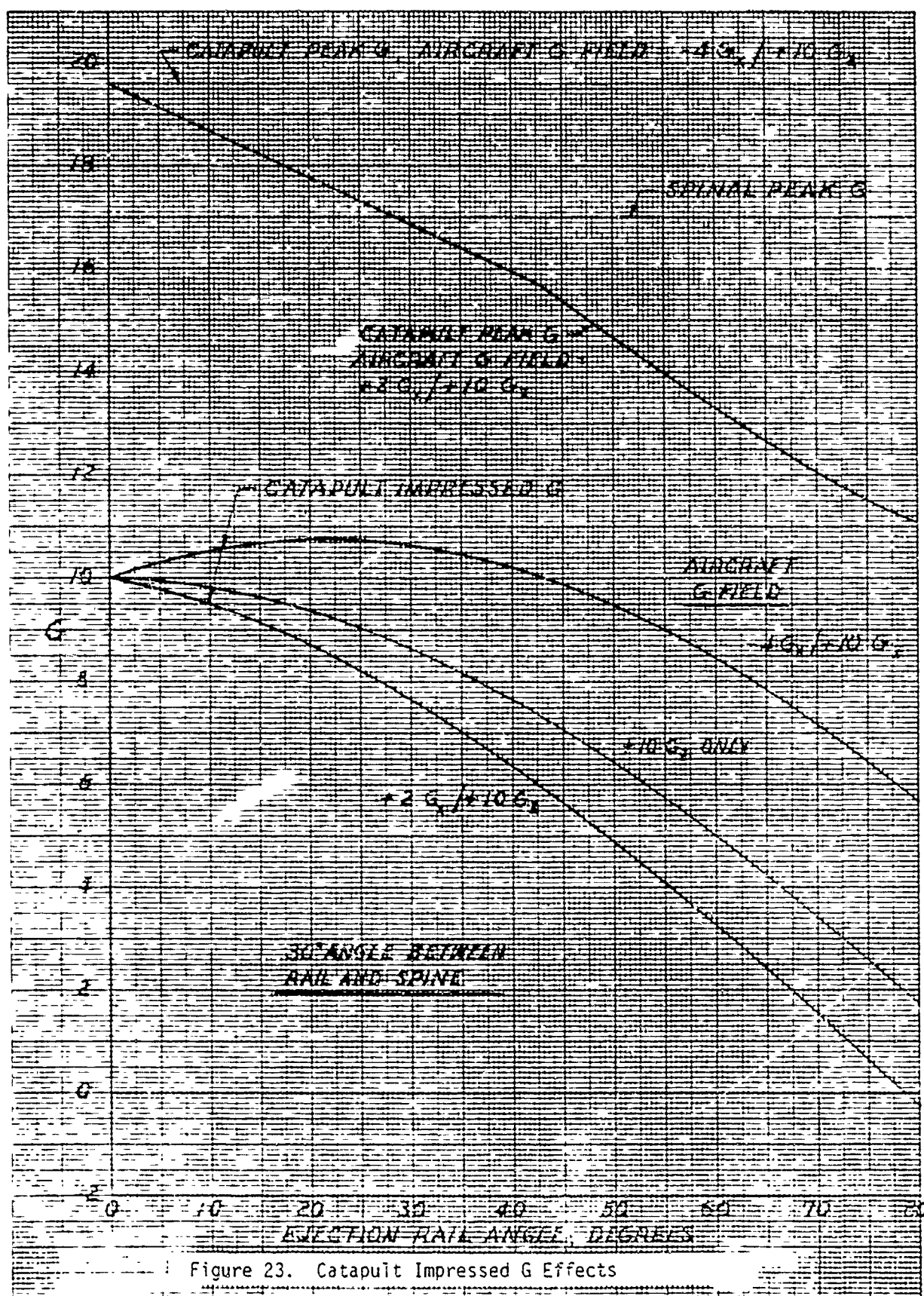
### 5.4.1 Low Boost Phase/High Thrust Rocket

Reduction of catapult boost phase thrust is governed by DRI limits and by the angles of the various acceleration vectors. These total DRI effects are determined by using the acceleration-time curve generated by catapult action and adding the constant preload component on the spine due to the impressed g field prior to ejection.

Reclining the crewman with respect to the rails permits increasing catapult thrust. These levels are eventually limited by the +30  $G_x$  acceleration limit of MIL-S-9479B. Figure 23 shows the variation of catapult impressed G field with rail angle. A constant spinal angle of 30 degrees aft of the rail is used for all rail angles. A peak spinal  $G_z$  of 17.0 permits a catapult peak G of 19.6 for the -4  $G_x$ /+10  $G_z$  aircraft load condition at all rail angles. Impressed G fields for 0.0, +2 and -4  $G_x$  conditions are shown in the lower curves of Figure 23.

Although peak G for the +2  $G_x$  condition is reduced with increasing rail angle, the differential between peak and impressed G curves remains fairly constant at 9 to 10 G. A similar situation prevails for the -4  $G_x$  case. Catapult performance is therefore not strongly affected by rail angle.





EJECTION RATE ANGLE, DEGREES

Figure 23. Catapult Impressed G Effects

The catapult cartridge will be sized so that under the most adverse combination of  $G_z$  and  $G_x$  the spinal acceleration force does not exceed specified limits for any ejection seat concept with varying back angle and ejection angle combinations. The resulting performance loss at low speeds will be compensated for by the increased rocket thrust required for tail clearance at high speeds.

The rocket motor may be sized so that tail clearance is assured under all conditions. The rocket contribution to ejection velocity at low aircraft speeds is approximately twice that of the catapult. For the candidate ejection seat concepts under consideration rocket thrust levels of 4950 to 6600 pounds of thrust are estimated. These thrust levels are 150 to 200 percent greater respectively than the CKU-5/A rocket catapult of the ACES II ejection seat. Upright ejection performance will be improved with these higher thrust levels but adverse attitude and inverted performance will be degraded. Other candidate propulsion system concepts to maintain performance in all attitudes are discussed in the following paragraphs.

#### 5.4.2 Twin Sustainer Rocket Motors

Two rocket motors may be used to improve adverse attitude performance at low ejection speeds when high G conditions are not present. For this concept ignition of one rocket motor will always occur. Ignition of the second motor will be prevented in low G conditions by a G-sensing microprocessor. Thrust levels of each motor will be proportioned to accommodate high G requirements and maximize performance in low-speed, adverse attitude conditions.

The rocket motors may be mounted in tandem on the longitudinal seat centerline, with the aft rocket nozzle above the forward nozzle. The thrust vector of each motor will pass through the ejected mass C. G. with the thrust of the second (aft) motor more perpendicular to the spinal axis to reduce accelerations in the spinal direction.

#### 5.4.3 Two-Stage Rocket Motor

A single-nozzle rocket motor may provide thrust variation by controlled, two-stage, burning of the motor grain. Ignition of the second stage will be controlled by a G sensor similar to the twin rocket motor concept. The two-stage rocket motor grain may be separated by an interposed inhibitor either axially or longitudinally in a single motor case. Required increase in nozzle area to accommodate second stage burn may be accomplished by shaped charge blow-out of a nozzle diaphragm or by mechanical opening to a larger nozzle throat.

#### 5.4.4 Twin Low-Boost Catapults

Twin catapults will be used for initial, low-boost, phase thrust when a separate main rocket STAPAC stabilization concept is employed. These twin catapults may be integrated with the seat structure along each aft edge of the seat back. An upper, overhead manifold will connect the twin launch cylinders for ignition and equalized thrust.

#### 5.4.5 Catapult Pressure Limiting Valve

Spinal loading may also be reduced by employing a valve to limit catapult pressure. The valve will bleed combustion gases from the catapult and provide automatic reduction of pressure and thrust increases due to high impressed G field conditions.

Total DRI effect on the crewman will be maintained within acceptable limits with this concept and catapult failure due to over-pressure prevented. Normal catapult performance will also be maintained for low-speed, low-G conditions.

## 5.5 SEAT STABILIZATION

Current ejection seats are inherently unstable in pitch and yaw. They require immediate stabilization as they leave the aircraft guide rails and become free bodies. When ejection occurs under high impressed g field conditions this instability may be aggravated due to the effects upon the forces involved as the seat leaves the guide rails. This may cause the aerodynamic forces imposed on the crewman to exceed the allowable human acceleration limits of MIL-S-9479B. Design criteria has established a damped oscillation limit of  $\pm 5$  degrees.

Ejection tail clearance is also affected by the motion of the seat after separation from the aircraft guide rails. The relation between lift, drag and thrust components is governed by pitching moment trends initiated by aero pitching moments and tip-off forces at the start of the seat/man trajectory. Control of these motions may be achieved by the following candidate concepts for seat stabilization:

- Inflatable stabilizer/decelerator
- Two-axis main rocket STAPAC
- Thrust vector control (TVC)
- Gimballed rocket

### 5.5.1 Inflatable Stabilizer/Decelerator

The current ACES II seat system is stabilized in pitch by the gyro-controlled STAPAC rocket stabilizer and in yaw by a drogue parachute. The current drogue system requires between .21 and .29 seconds after seat/rail separation to become fully effective. These times vary with airspeed and are required for drogue chute deployment and inflation. In this time interval seat rotation of up to 15 degrees in yaw may be experienced, approaching the limits of human tolerance to acceleration. Ejection under high g conditions may also present problems of tail clearance with the early deployment of a drogue parachute.

A concept to solve the noted problems replaces the present drogue system with an inflatable stabilizing structure that is stowed in a container on the seat back. During ejection a pyrotechnic gas generator is initiated just prior to seat/rail separation. The gas generator inflates the structure to approximately 12 psi in 30 milliseconds at any air speed. The required stabilizing forces are applied to the seat before the degree of seat rotation becomes a problem. Analysis has shown that such an inflatable can be provided by existing technology and within the current state-of-the-art.

Additional design analysis will be required to select final configuration providing the best aerodynamic shape compatible with internal gas shaping forces and stowage considerations.

#### 5.5.2 Two-Axis Main Rocket STAPAC

Trajectory studies indicate that pitch attitude control stabilization may improve tail clearance and reduce DRI effects. Aft seat pitch attitude imposes large  $G_z$  forces on the spine due to aerodynamic drag on the seat bottom. These forces in combination with the upward component of rocket thrust may result in excessive DRI values. This suggests the possibility of reducing thrust required at high  $G$  levels by pitch attitude control. This may be accomplished by providing STAPAC-type pitch control for the main rocket. Although yaw moments are essentially zero for zero yaw angle, aircraft yaw or rail-induced disturbance may result in a yaw rate early in the trajectory. A main rocket STAPAC-type attitude control in the yaw direction will counteract these yaw rates.

Use of the above techniques indicate a main rocket with a two-axis, ball-and-socket nozzle. Initial pitch rate of the seat will be aft at high speeds, due to tipoff, causing a nozzle-down initial travel and resulting in an upward thrust vector. Separate twin-catapults, providing initial boost-phase propulsion, would be used with this concept and will not cause DRI problems as long as aft seat pitch is not excessive.

#### 5.5.3 Thrust Vector Control (TVC)

Thrust vector control of the main rocket indicates advantages in seat stabilization. A two-axis, hydrofluidic TVC system is described in References 15 and 16.

The results of these studies show that the two-axis system reduces unsafe  $g$  loads by 30 percent compared to STAPAC and 60 percent compared to a seat with no TVC. This reduction is the result of reducing maximum yaw angles by a factor of 10. Maximum pitch rates are also reduced by 30 and 60 percent at high speed. In all cases, the pitch and yaw rates are reduced to near zero at the onset of parachute line stretch.

The primary benefit of two-axis TVC is reduction of unsafe  $g$  loads due to yaw instability during high speed deceleration. Stabilizing seat attitude also increases recovery altitude. TVC is more stable in yaw than STAPAC and has more than twice the control authority because the sustainer rocket is used to produce control moments instead of a vernier rocket. The TVC system gains height over the uncontrolled seat by keeping the thrust vector in a vertical attitude by maintaining a positive pitch angle during rocket burn.

This TVC concept consists of attitude stabilization controllers and an internally actuated nozzle. The controllers have no moving parts and obtain their power from the main rocket. The controller also contains a four-stage position servovalve which has no moving parts and no linkages connecting it to the nozzle. The nozzle provides 20 degrees of deflection with less than 150 in-lb actuation torque. The integrated fluidic circuit contains a rate sensor, integrator and a position control valve. The control valve drives the nozzle with hydraulic pressure fed into piston-like bladders around the nozzle. Position transducers on the nozzle feed back pressure signals proportional to nozzle angle. Figures 24 and 25 are shown from the referenced reports.

#### 5.5.4 Gimballed Rocket

The gimbal rocket motor concept provides the greatest deflection angle and stabilization capability of all the TVC moment producers. Its travel is limited only by the gimbal stops. This system concept can recover from adverse attitudes with less altitude if a vertical seeking sensor and a longer burn time are used. The vertical sensor would simply interface with the pitch and yaw attitude references. An autopilot may sense direction cosines and get its initial airspeed, altitude and attitude inputs from the airplane's systems. If no signal is available it will command a normal straight up ejection. If inverted or banked it will command the seat to fly vertically.

A vertical seeking ejection seat, using a gimbal rocket motor is being developed and tested by the U. S. Navy. The rocket motor is 8.12 inches in diameter and is gimballed to permit rotation  $\pm 16$  degrees in pitch and roll. This is powered by a pressurized hydraulic power unit and a battery. The rocket thrusts for 1.8 seconds with a gradual increase to 3500 lbs. and a smooth tail off. The total impulse of 3500 lb. seconds is obtained from HTPB propellant. A micro-processor guidance system is being studied as a possible replacement of the gyro guidance system. The MICRAD system uses 3 horizontal and one vertical antenna to sense the earth's natural radiometric temperature. The sky is approximately  $20^{\circ}$  K while the earth is  $150^{\circ}$  K, ocean  $130^{\circ}$  K and horizon  $90^{\circ}$  K. Thus the system can select and command the rocket to aim the seat at the relatively cold sky.

In the most recent test of this system a seat was ejected suspended inverted 100 ft. above the ground. The rocket turned the seat upward in the planned trajectory. The drogue and main recovery parachute deployed and inflated prior to ground impact. Telemetered data indicated a 10 g initial spike with 5 g acceleration up the rails. The maximum accelerations just off the rails were 13.5 g vertical in foot, 12.5 g vertical in chest and 10.5 g vertical in the head. The turn up was at 370 degrees per second with maximum accelerations of 2.5 g lateral in chest, 5 g lateral in foot, and 2 g lateral in the head. Chute opening occurred at 4.5 sec. with 450 degrees per second yaw and 550 degrees per second pitch. Figures 26 and 27 show details of this system.

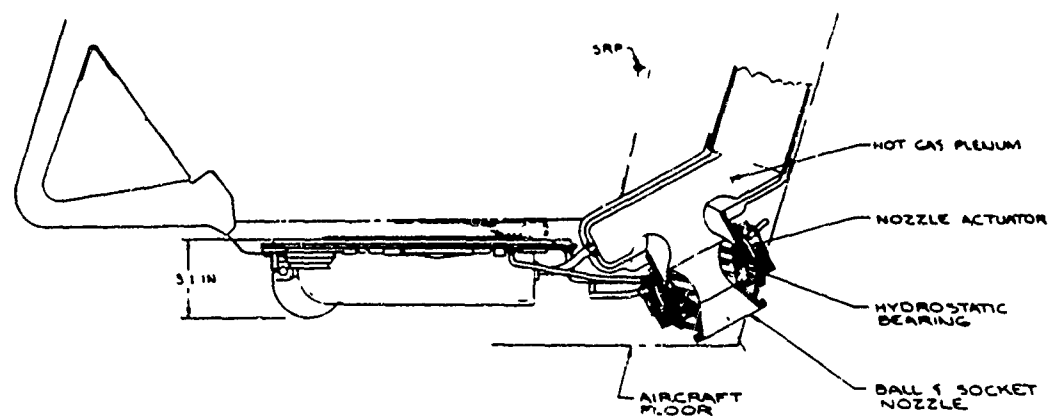


Figure 24. Fluidic Thrust Vector Control (Reference 16)

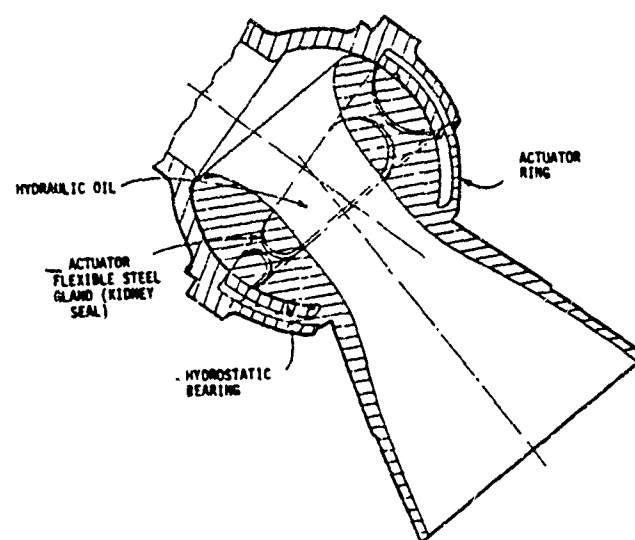


Figure 25. TVC Rocket Nozzle (Reference 16)



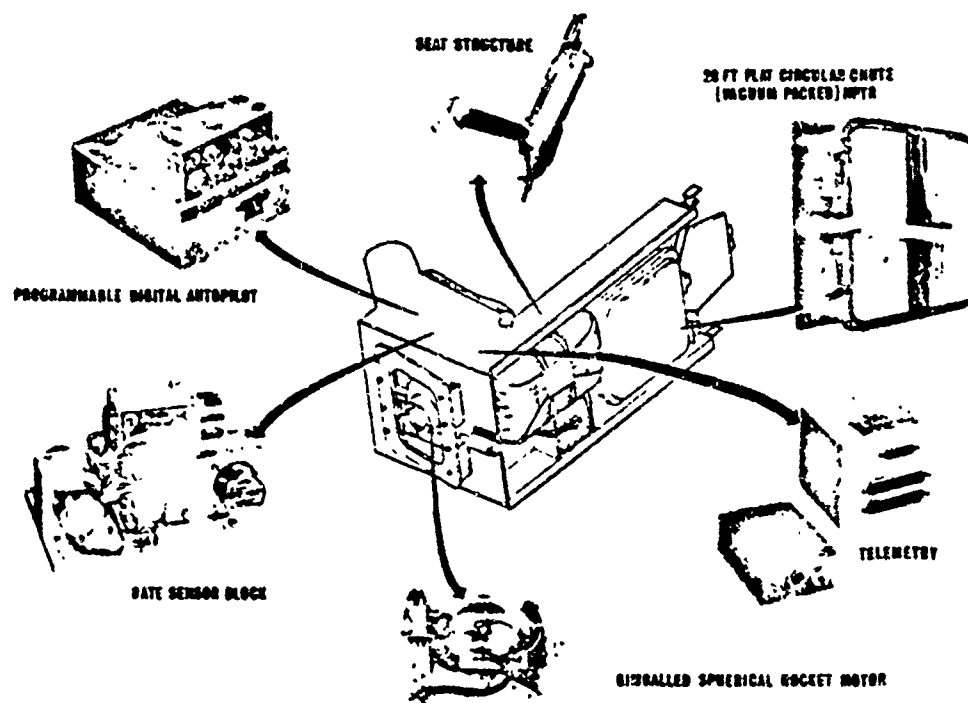


Figure 26. Vertical Seeking Seat Gimballing Rocket

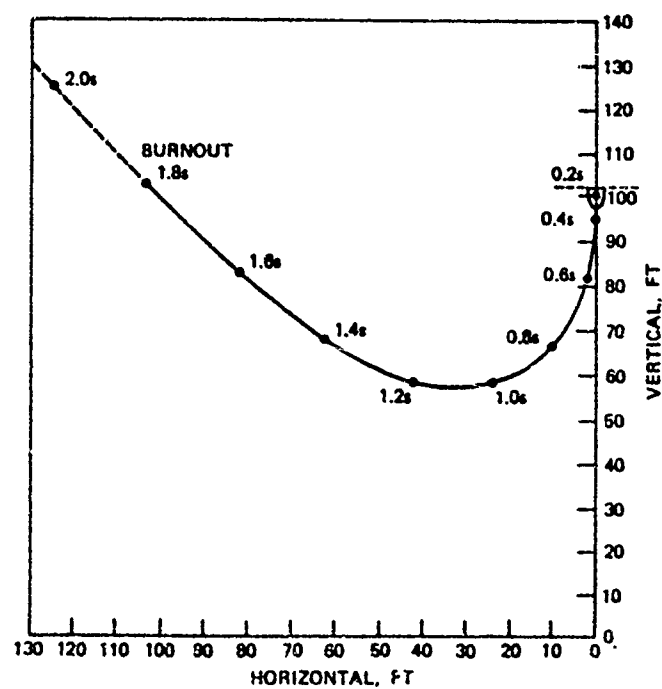


Figure 27. Vertical Seeking Seat-Inverted Trajectory



## 5.6 CANOPY JETTISON

Canopy jettison is accomplished on F-15 aircraft by a pyrotechnic thruster unit and on F-16 aircraft by a rocket motor. The required thruster or rocket force is determined by considerations of canopy weight, aircraft  $g$  loads and aerodynamic forces acting on the canopy. Increased aircraft acceleration loads of  $10 G_z$  at initiation of the escape system requires increased remover forces and possible structural modifications.

Seat ejection from F-15/F-16 aircraft is initiated by an actuation lanyard from the canopy as the canopy clears the seat ejection path. The time delay for seat ejection decreases as airspeed increases and aerodynamic forces assist canopy jettison. In the F-15 this time delay varies from 520 milliseconds at zero speed to 140 milliseconds at 600 knots. Under  $+10 G_z$  conditions at time of escape system initiation, canopy jettison may be delayed or the canopy prevented from clearing the seat ejection path. Degraded or unsuccessful escape system performance may result.

Alternate candidate concepts for canopy jettison/removal under high  $G$  conditions consist of increased thrust canopy removers, auxiliary rocket thrust motors and a canopy fracturing system employing Shielded Mild Detonating Cord (SMDC) to permit ejection through the canopy.

### 5.6.1 Increased Remover Force

Analysis of increased remover forces has established the following performance requirements:

Operating environment:	0 to 600 KEAS	-3 to $+10 G_z$
Resistive force:	7000 lbs. (Max.)	
Operating time:	1500 milliseconds (Max.)	
Stroke:	29 + inches (approx.)	
Canopy weight:	220 lbs.	
Canopy moment of inertia:	239 slug-ft <sup>2</sup>	
Pressure load:	8640 lbs.	
Remover thrust:	10,000 lbs.	

These calculations result in a remover having the following characteristics:

Initial volume ..... 57.4 in.<sup>3</sup>  
Final volume ..... 107.8 in.<sup>3</sup>  
Expansion ratio ..... 1.88  
Ballistic stroke ..... 29.1 in.  
Piston area ..... 1.76 in<sup>2</sup>  
Remover weight ..... 25.0 lbs.

The analysis shows that the canopy remover develops adequate thrust to open the canopy through the full ballistic stroke of the piston. Piston separation occurs at 181 milliseconds and at a canopy angle of 23.5 degrees.

#### 5.6.2 Canopy Fracturing System

This concept involves modifying escape system sequencing to eliminate canopy jettison by the addition of an SMDC cutting charge on the transparency. This method improves escape performance by permitting ejection through the canopy without seat/canopy time delays. This system has been used successfully on the TA-7C.

This alternate system to canopy jettison will produce an overhead fracture (severance) in the canopy acrylic to facilitate a "thru-the-canopy" ejection of seat and pilot for either in-flight or on-ground emergencies. Upon actuation of the ejection handles on the seat, the gas pressure developed in the aircraft escape system hoses will be employed at a cartridge actuated initiator which will convert this pressure into detonation energy. This energy is then transferred, by means of a shielded detonating cord, to an unshielded detonating cord secured to the acrylic in a centerline pattern directly over the seat and the pilot's head, Figure 23. When activated, the resultant output shock wave from this overhead cord assembly will produce, coincident with seat ejection, a centerline fracture in the canopy acrylic.

The Mild Detonating Cord Assembly (MDC) transitions from the SMDC/Union to an unshielded MDC mounted on the acrylic with a silicone rubber back-up retainer for the purpose of fracturing the acrylic. This assembly is bonded/taped to the acrylic directly using special non-crazing pressure sensitive adhesive. Flexible Contained Detonating Cord (FCDC) is a flexible explosive transfer line contained in successive braidings of plastic, Kevlar cord and stainless steel wire for complete containment of products of combustion.

The explosive material used in these components regardless of charge weight or core load is Hexanitrostilbene (HNS). Core loads of transfer lines is expected to be  $2.5 \pm 0.25$  grains per foot. The detonation velocity of the detonating cord used will be more than 6000 meters per second.

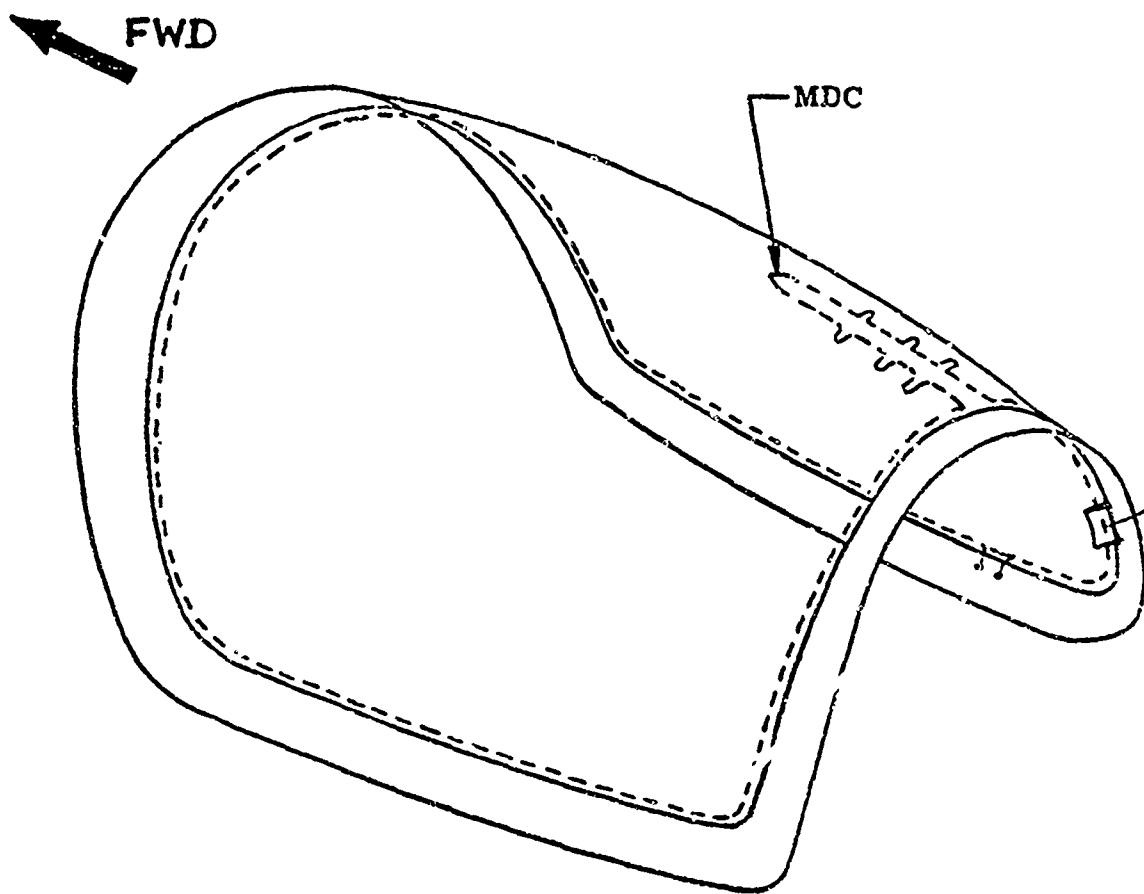


Figure 28. SMDC Canopy Fracturing System

## SECTION VI

### HIGH-G EJECTION SEAT CONCEPTS

Eight candidate ejection seat design concepts have been developed to meet the requirements of high-G escape. These basic concepts are:

- Concept A - Ejection From any seat position.  
Fixed guide rails at 30°.
- Concept B - Ejection from any seat position.  
Guide rails repositioned from 15° to 30°.
- Concept C - Seat retraction to upright position.  
Fixed guide rails at 17°.
- Concept D1- Seat retraction to upright position  
Rail repositioned from 17° forward to 30° aft (high pivot).
- Concept D2- Seat retraction to upright position.  
Rail repositioned from 17° forward to 45° aft (high pivot).
- Concept E1- Seat retraction to upright position.  
Rail repositioned from 17° forward to 30° aft (low pivot).
- Concept E2- Seat retraction to upright position.  
Rail repositioned from 17° forward to 45° aft (low pivot)
- Concept F - Seat and rail repositioned from 15° to 65° aft.

#### 6.1 CONCEPT A

This concept permits ejection in any seat position from the 13° upright back angle to the fully reclined 65° back position. Fixed ejection guide rail angle is 30°. This configuration results in a varying ejection back angles between 13° and 65°, and requires a fixed rocket thrust vector angle of 47 degrees to maintain thrust/CG alignment in both upright and reclined seat positions. Aircraft structural revision is required to main instrument panel mounting and rotation of the panel and heads up display (HUD) to clear the ejection path

A pyrotechnic thruster rotates these cockpit components clear of the ejection path prior to ejection. Rotation of the aircraft windscreen in a similar manner is required only for the F-15 HAC and provides additional windblast protection after canopy jettison. In the F-16 HAC configuration the one-piece canopy-windscreen combination does not require separate windscreen repositioning.

## 6.2 CONCEPT B

This concept also permits ejection in any seat back angle and is similar to Concept A except that the rails are repositioned from the normal flight position of  $15^{\circ}$  to an ejection angle of  $30^{\circ}$ , Figure 29. The rails pivot about a point at the same height as the NSRP. This provides an effective ejection back angle of  $28^{\circ}$  in the upright position and  $80^{\circ}$  in the reclined position. A rocket thrust vector angle of 31 degrees is required for CG alignment in any seat position. Rail repositioning is accomplished at the start of the ejection sequence by a pyrotechnic retractor unit. Forward clearance is provided by pivotal mounting of the instrument panel and HUD unit and the aircraft windscreen in a manner similar to Concept A.

## 6.3 CONCEPT C

Automatic return to the upright,  $13^{\circ}$  back angle from any reclined position is provided in this concept. Fixed ejection guide rail angle is  $17^{\circ}$ . This concept may be considered as a baseline configuration since it is similar to the HAC/ACES II seat as installed in the proposed AFTI-15 cockpit. Ejection clearances are provided by the existing cockpit configuration.

No provisions have been made in this concept to alter ejection angle or seat back to reduce spinal accelerations and DRI effect under  $10 G_z$  conditions.

## 6.4 CONCEPT D<sub>1</sub>

Design Concepts D<sub>1</sub> and E<sub>1</sub>, Figures 30 and 31 respectively, provide automatic return to the upright back position from any reclined angle simultaneous with repositioning on the ejection guide rails. Normal flight rail angle is  $17^{\circ}$  forward of vertical and repositioned ejection angle is  $30^{\circ}$  aft of vertical. This repositioning results in an effective ejection back angle of  $60^{\circ}$  to minimize DRI effect. These two concepts differ primarily in the manner in which cockpit ejection clearances are achieved.

Concept D<sub>1</sub> provides a rail pivot point 21.0 inches above the NSRP to minimize the effect on cockpit/aircraft volumes. This rail position requires pivoting and thruster rotation of the instrument panel, HUD, and windscreen similar to that of Concepts A and B.

## 6.5 CONCEPT D<sub>2</sub>

Concept D<sub>2</sub> is similar to Concept D<sub>1</sub>, except that ejection rail angle is repositioned to 45 degrees resulting in an ejection seat back angle of 75 degrees. Cockpit clearance considerations are the same as those for Concept D<sub>1</sub>.

#### 6.6 CONCEPT E<sub>1</sub>

The rail pivot point of Concept E<sub>1</sub> is located 2.0 inches above the NSRP. This location eliminates the requirement for panel/windscreen repositioning. However, a greater swept volume is required aft of the normal flight position to permit rail repositioning. This trade-off of system complexity versus reduced cockpit/aircraft volumes will influence concept selection criteria. Ejection rail angle is 30° and seat back angle is 60°.

#### 6.7 CONCEPT E<sub>2</sub>

This concept is similar to Concept E<sub>1</sub> except that ejection rail is repositioned to 45 degrees resulting in a seat back angle of 75°. Cockpit volume requirements are the maximum of all candidate configurations.

#### 6.8 CONCEPT F

This concept repositions ejection rail and seat together as a unit as shown previously in Figure 16. Ejection rail and seat back angles are parallel at 65° aft of the vertical. Cockpit volume requirements are approximately the same as those for Concepts A and B. Panel and windscreen repositioning for cockpit clearances are required for this concept.

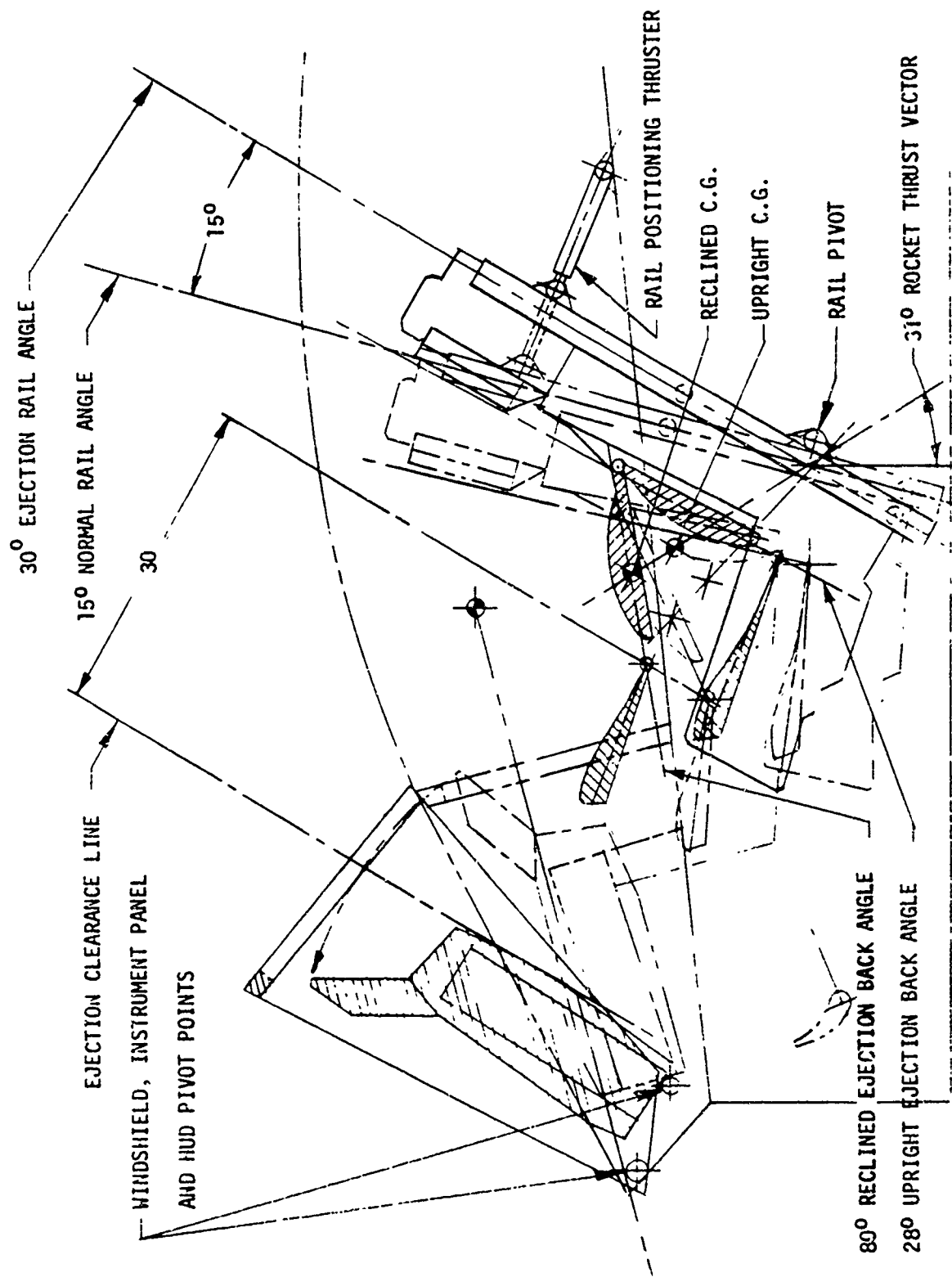


Figure 29. High-G Seat Concept B

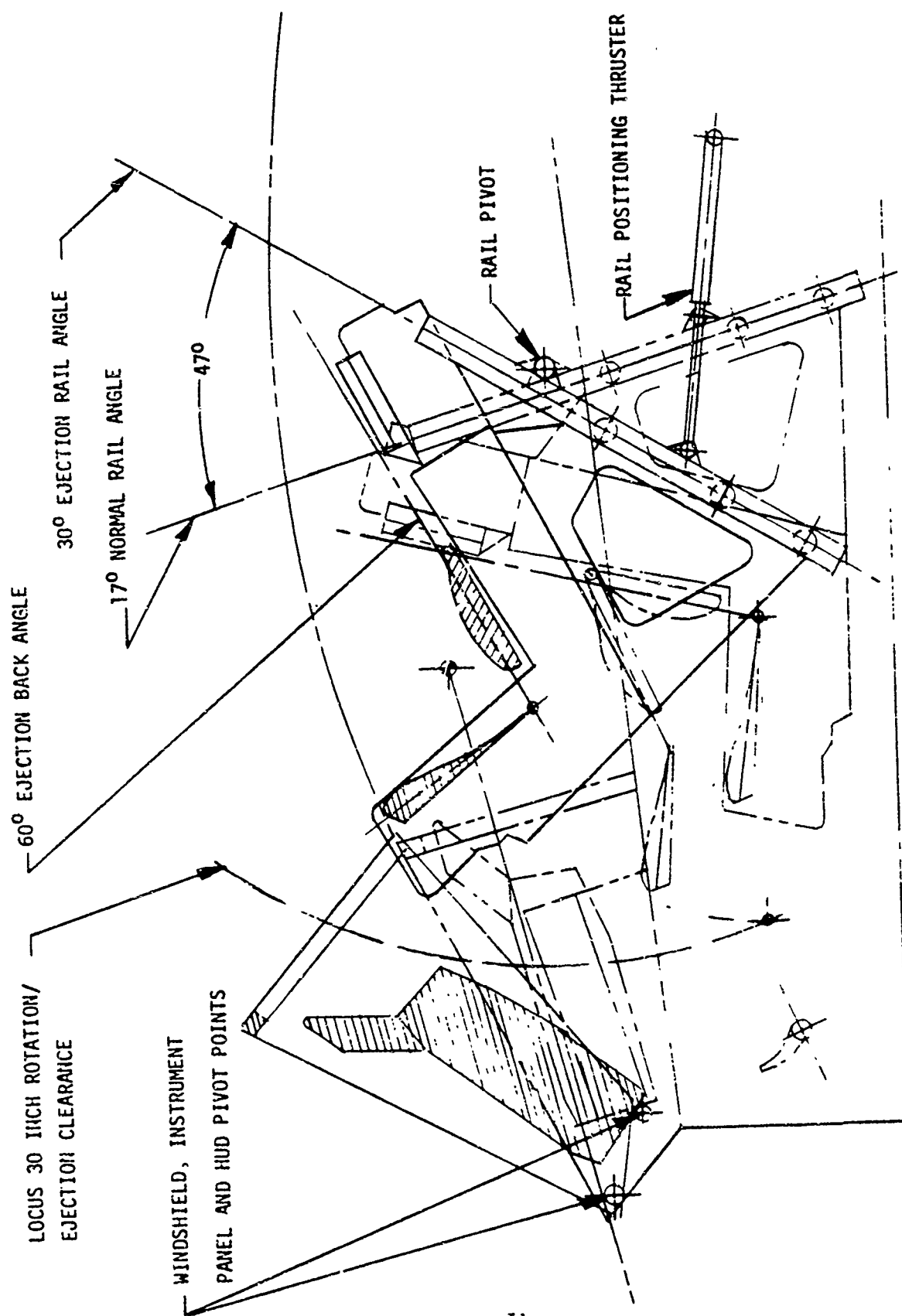


Figure 30. High-G Seat Concept D1



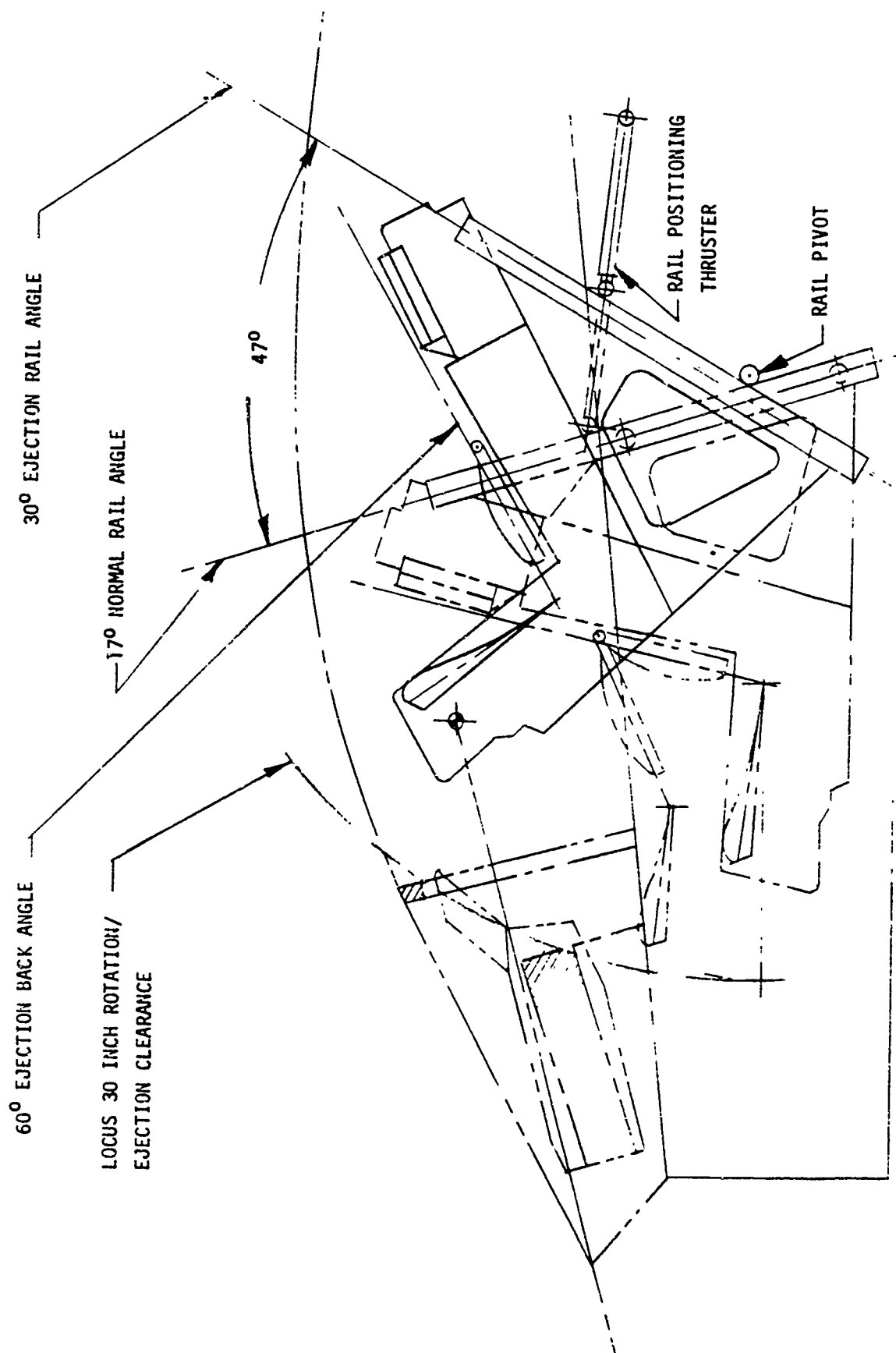


Figure 31. High-G Seat Concept E<sub>1</sub>

## SECTION VII

### SEAT/COCKPIT INTEGRATION

Integration of the high G ejection seat into the F-15/F-16 high acceleration cockpits involves considerations of functional compatibility with the cockpit arrangement for all flight conditions and ejection clearances and safety under emergency conditions.

All candidate seat design concepts maintain cockpit controls and displays within functional reach and vision envelopes. Each seat design concept maintains the pilots shoulder in a near constant position. The seat pan angle selected for both the upright and reclined positions maintains pilot function and comfort and instrument panel depth to accommodate displays when the seat is reclined.

In terms of internal cockpit/aircraft volume requirements, the baseline concept (C), with a fixed ejection guide rail angle of 170°, requires approximately 4.8 cu. ft of cockpit volume aft of the 130° seat back reference plane. Design Concepts A and B each require a volume of 6.8 cu. ft., Concept F requires 7.2 cu. ft., Concepts D<sub>1</sub> and D<sub>2</sub> require 10.5 and 12.5 cu. ft. respectively, and Concepts E<sub>1</sub> and E<sub>2</sub> require 15.8 and 17.8 cu. ft. of cockpit volume respectively.

Detail design of the pivoting rail support structure of Concepts D and E may accommodate a small volume of isolated aircraft electronic components between the rail structural support members provided that ejection clearances are not affected.

Integration of the seat positioning system in to the HAC cockpit requires the addition of an electrical interface between aircraft and seat. Power for the articulating system gear motor, whether seat or floor mounted, may be obtained by the addition of power cables and circuit breakers to the aircraft electrical system. Maximum electrical power demand will be approximately 0.3 KVA for normal seat articulation to the reclined position. The F-15 carries two 115 volt, 400 Hz AC generators, each with an output of 40 KVA, and each sufficient to maintain essential and intermittent power output capabilities.

All other high G seat components are self-contained pyrotechnic units and do not require aircraft/seat integration other than mounting provisions.

Cockpit integration effects required for ejection clearances are discussed in the seat concept section of this report. Minimum effect is noted for design Concepts C, E<sub>1</sub> and E<sub>2</sub> which are the only concepts that do not require instrument panel and windscreen repositioning to maintain the 30-inch ejection clearance line forward of the seat reference point.

## SECTION VIII

### SEAT CONCEPT ANALYSIS

Analysis of each of the eight basic candidate seat design concepts includes:

- Acceleration/DRI effects
- Ejection clearance
- Escape performance
- Structural analysis
- Weight analysis

These analyses are directed toward the establishment of selection criteria and final concept selection to be accomplished under the Phase II Design Synthesis phase of this study.

#### 8.1 ACCELERATION/DRI EFFECTS

Acceleration/DRI limits are established by MIL-S-9479B. Varying DRI limits apply to the candidate seat concepts under consideration. Ejection catapult acceleration, per Paragraph 3.4.11.1 of the MIL-S-9479B, establishes a DRI limit of 18 for acceleration vectors within  $\pm 5^\circ$  of the spinal column Z axis. When the acceleration vector is more than  $5^\circ$  off the Z axis and aft of the plane of the seat back the maximum DRI value is 16.

For seat Concept A ejection may occur at any seat back position. This results in an acceleration vector from  $35^\circ$  forward to  $17^\circ$  aft of the seat back angle. A DRI limit of 16 is thus established as a worst-case requirement for Concept A where aft thrust vectors may exceed  $5^\circ$ .

Seat Concept B also permits ejection from any seat back position but repositioning of the ejection guide rails results in thrust vectors from  $50^\circ$  forward to  $2^\circ$  aft of the seat back plane. In this case a DRI limit of 18 applies since the maximum aft thrust vector does not exceed the  $5^\circ$  limit.

The baseline Concept C at a fixed rail angle of  $17^\circ$  requires automatic return to the upright,  $13^\circ$ , back angle for ejection. This results in a constant thrust vector  $4^\circ$  aft of the seat back, and a DRI limit of 18.

Design Concepts D<sub>1</sub> and E<sub>1</sub> reposition the guide rails to  $30^\circ$  and return the seat back to the  $13^\circ$  upright position for an ejection back angle of  $60^\circ$ . Acceleration thrust vector is a constant  $30^\circ$  forward of the seat back and establishes a DRI limit of 18.

Concepts D<sub>2</sub> and E<sub>2</sub> reposition the guide rails to  $45^\circ$  with a resulting seat back angle of  $75^\circ$  and a DRI limit of 18.

Concept F with a parallel ejection and seat back angle of  $65^\circ$  maintains the DRI limit of 18.

### 8.1.1 Catapult Peak Acceleration and DRI

The existing CKU-5/A catapult has been used as a baseline to determine peak G's associated with DRI limits of 16 and 18. DRI values are affected by the shape of the catapult G-time history. Figure 32 shows an original thrust curve made by averaging catapult test data. Scaled curves are also shown at 150 and 200 percent thrust levels under 10 G field conditions. Spinal axes parallel to the catapult will experience 10 G until thrust exceeds this level and will then be subject to the catapult thrust above 10 G.

The parameter  $\delta$  used in DRI calculations is shown in Figure 33 as a function of time. It may be seen that the  $\delta$  values for typical thrust levels are higher when the model has "settled out" after the 0.3 second delay. Corresponding DRI values are shown in Figure 34. The data shown have been augmented to include the effects of a 0.3 second delay for pre-ejection functions. A peak G of 16.7 results in a DRI of 18.0.

### Increased Thrust Duration

Computer analyses using the thrust variations of Figure 32 indicated that catapult separation occurs at times between 0.25 and 0.35 seconds. These times are dependent on rail angle and thrust levels. The increased times over those of ACES II are caused by the fact that seat first motion does not occur until catapult thrust levels exceed the aircraft acceleration component and by the reduced effective thrust thereafter. The effect of increased catapult burn time has been investigated using the thrust values of Figure 32 with time scales of 120, 150, 170 and 200 percent of catapult thrust duration. Figure 35 shows the parameter  $\delta$  and the DRI values for the 150 percent catapult thrust level. DRI decreases until about 150 percent duration is reached and is then followed by a slow increase in DRI. The present range of catapult separation times occurs at the lower DRI values.

DRI as a function of peak G is shown in Figure 36 for the 100 and 150 percent thrust duration cases. A peak G of 18.0 produces a DRI of 18 at 150 percent duration.

### 8.1.2 Catapult Thrust Levels

A typical acceleration vector diagram for study Concepts D and E is shown in Figure 37. Aircraft accelerations of +10 G<sub>z</sub> and -4 G<sub>x</sub> are combined to give components of 10.7 and 8.5 G for the catapult/ejection and the spinal axes respectively. Peak G in the spinal direction lies between the scaled original and 10 G lines of Figure 34, however, the 10 G line may be used as a conservative limit. For a DRI limit of 18.0, a peak G along the spinal axis of 17.0 permits a catapult peak G of 19.6. According to preliminary estimates of catapult performance this catapult will have a thrust level of 9.5 G for +1 G load factor or level unaccelerated flight conditions.

Figure 38 shows the results of similar analyses for each of the candidate seat concepts. Spinal components due to aircraft G fields range from 5.7 to 10.7 G. The 10 G curve from Figure 32 has been used as a limit in obtaining the peak G/DRI values. At a load factor of +1 G catapult thrust levels range from 7.6 to 12.8 and all are feasible, in combination with increased thrust sustainer rocket motors, for all high-G escape system concepts.

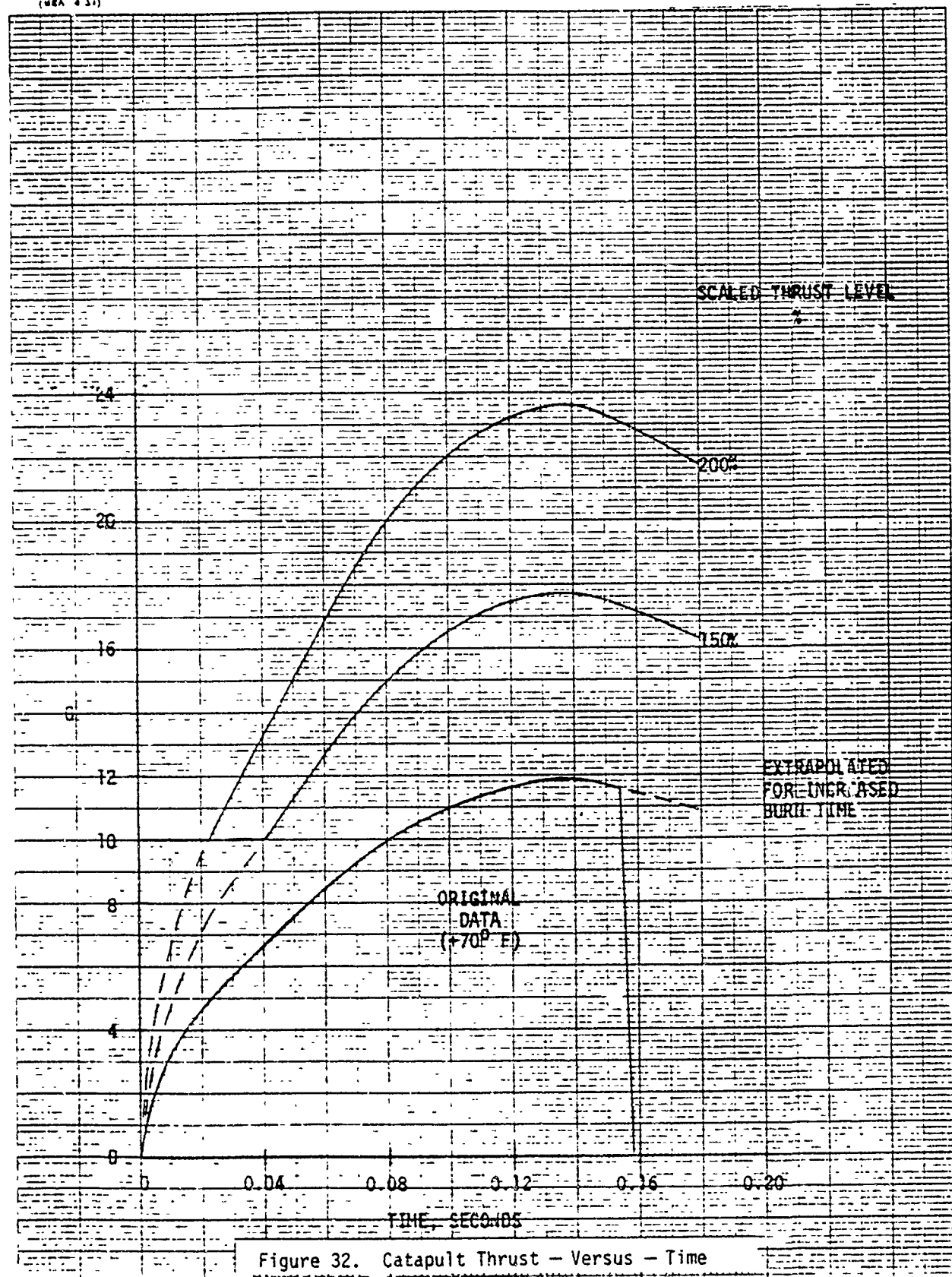


Figure 32. Catapult Thrust - Versus - Time

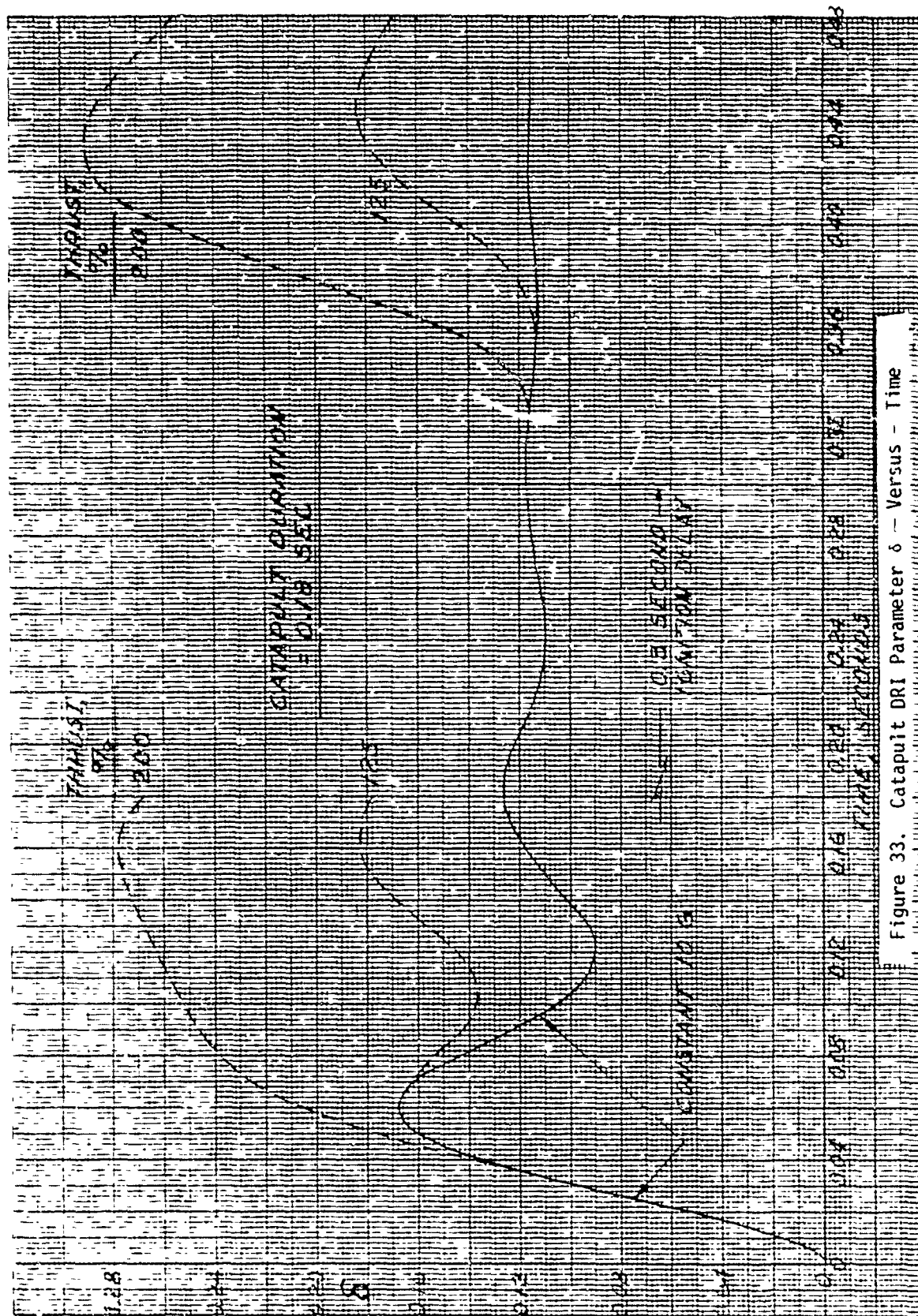
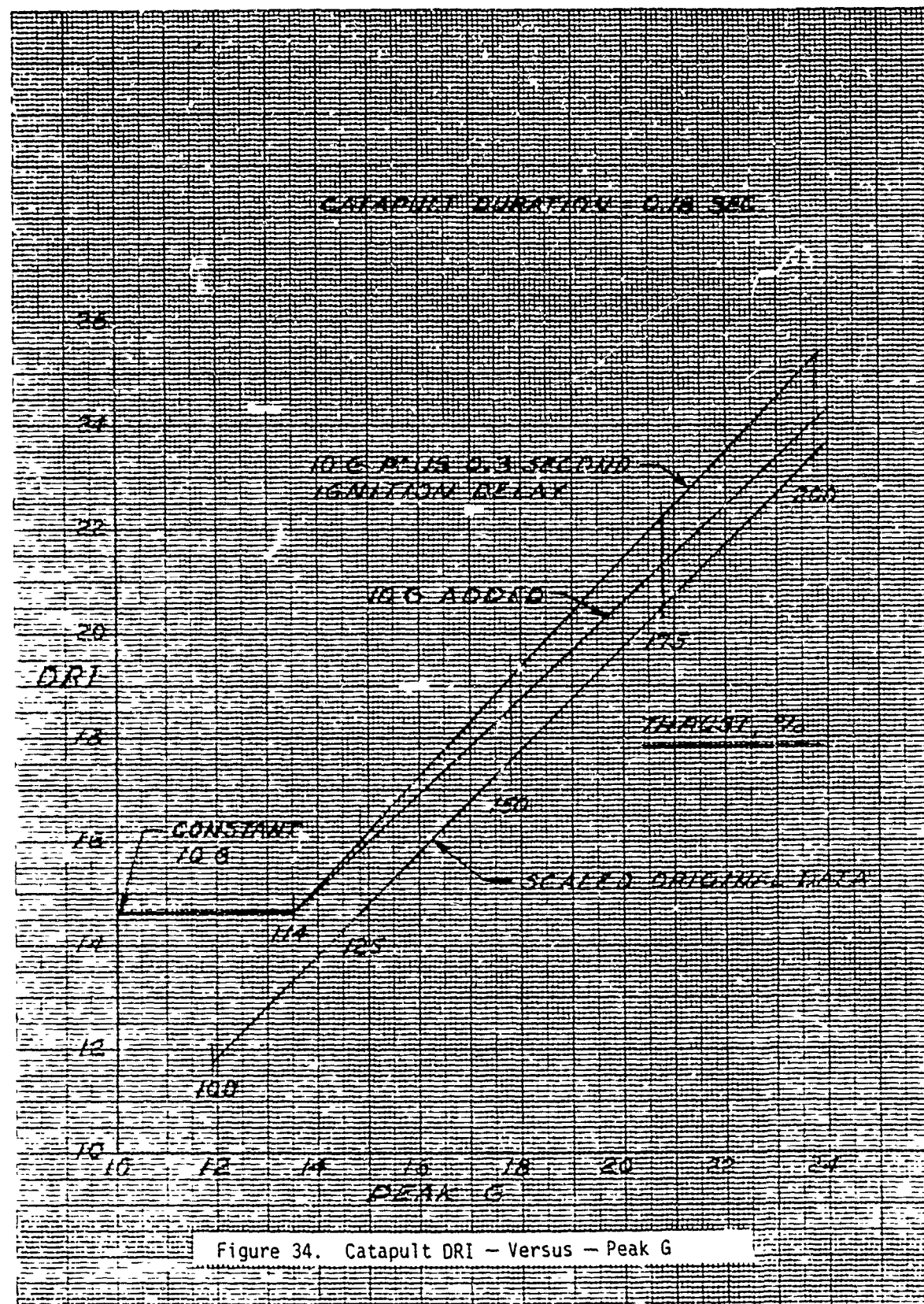


Figure 33. Catapult DRI Parameter 6 - Versus - Time







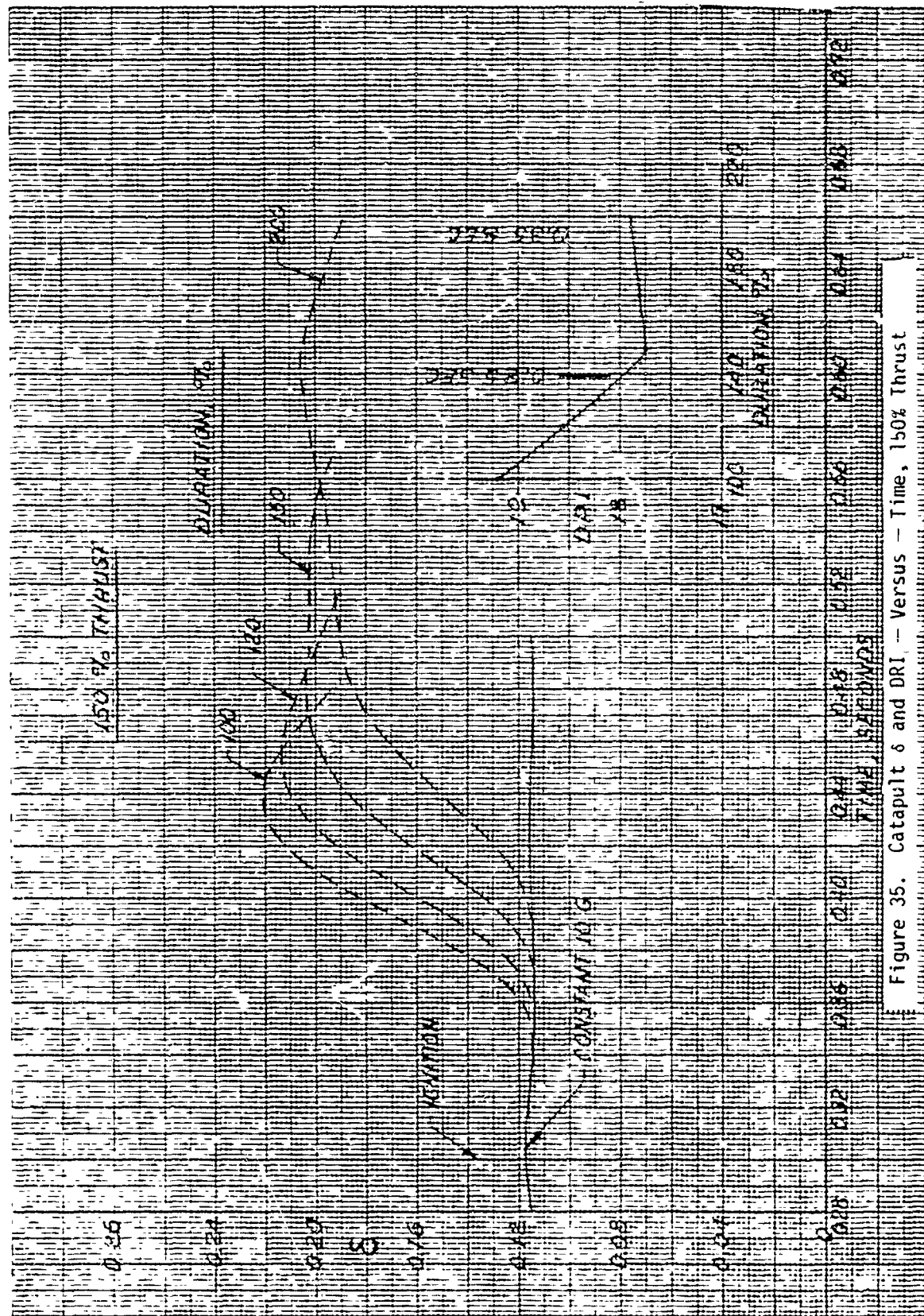


Figure 35. Catapult  $\delta$  and DRI - Versus - Time, 150% Thrust

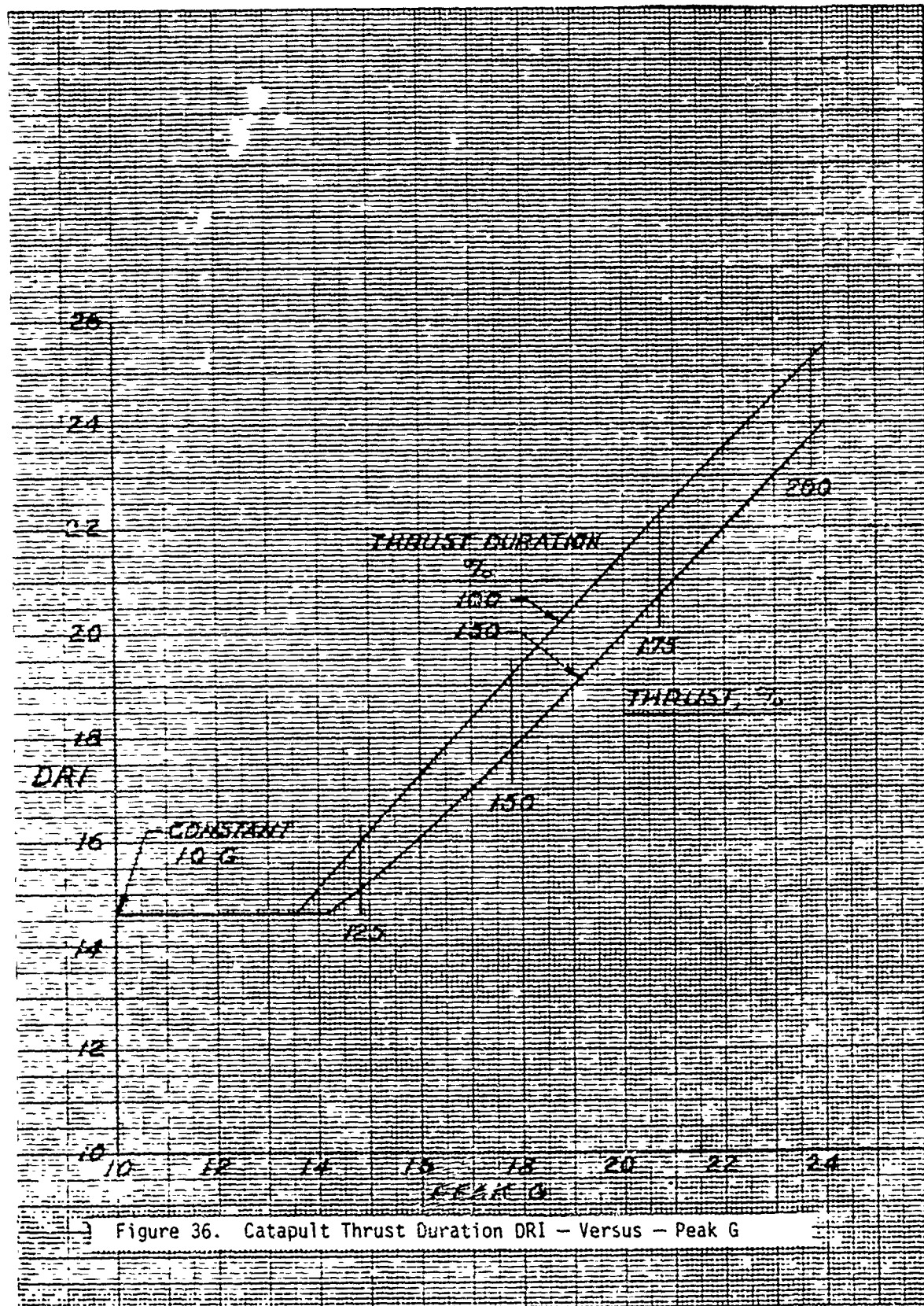


Figure 36. Catapult Thrust Duration DRI - Versus - Peak G

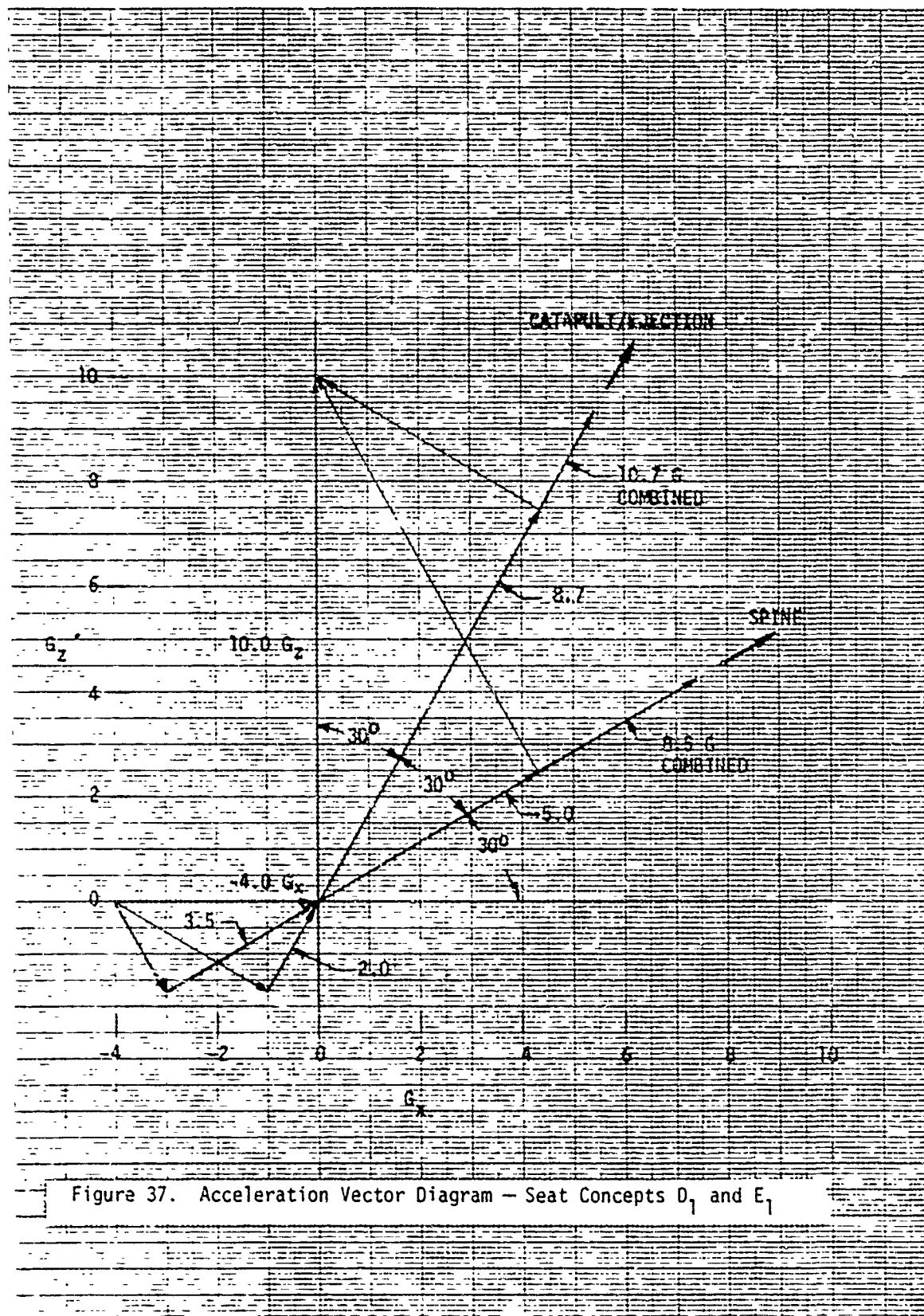


Figure 37. Acceleration Vector Diagram — Seat Concepts  $D_1$  and  $E_1$

SEAT CONCEPT	EJECTION ANGLE (DEG)	SEAT BACK ANGLE (DEG)	SPINAL ACCELERATION COMPONENT (G) (FROM AIRCRAFT)	PEAK G (SPINAL AXIS)	DRI	CATAPULT PEAK G	
						+10 G LOAD FACTOR	+1 G LOAD FACTOR
A (UPRIGHT) (RECLINED)	30°	13°	10.6	15.0	16.0	15.7	7.6
	30°	65°	7.9	17.0	18.0	20.8	10.0
B (UPRIGHT) (RECLINED)	30°	28°	10.7	17.0	18.0	17.0	8.2
	30°	80°	5.7	17.0	18.0	26.4	12.8
C	17°	13°	10.6	17.0	18.0	17.0	8.2
D <sub>1</sub> AND E <sub>1</sub>	30°	60°	8.5	17.0	18.0	19.6	9.5
D <sub>2</sub> AND E <sub>2</sub>	45°	75°	6.5	17.0	18.0	17.6	8.5
F	65°	65°	7.9	17.0	18.0	20.8	10.0

Figure 38. Spinal Components/DRI/Catapult Peak G

## 8.2 EJECTION CLEARANCES

The requirement for high-G escape with the ejection seat in any reclined position, presents problems in providing safe clearances. These problems involve the seat/man/cockpit interface and ejection tail clearances. Cockpit clearances are discussed in the seat concept section of this report. The vertical tail clearance problem is illustrated in Figure 39, which shows a profile outline of the F-16 aircraft with an ejection seat trajectory grid having a point of origin at the cockpit seat/man CG position. The F-16 aircraft presents the most critical tail clearance problem since the tip of the single-tail leading edge is approximately 9 feet closer to the point of origin than the twin tails of the F-15 aircraft. The F-15 twin vertical tail is also shown oriented to the same cockpit CG position.

The ACES II ejection seat performance has been used to develop trajectories representative of conventional ejection seats. The ejection paths for 600 KEAS, level-flight, +1 G load factor ejections are indicated by solid lines for the 32- and 17-degree ejection rail angles of the F-16 and F-15 aircraft respectively. A 17-degree ejection seat trajectory is also shown in this figure for 10 G load factor conditions. This trajectory plot uses the same catapult and rocket forces as the 1 G cases shown. Tail clearances for high-G escape conditions will involve propulsion modifications to increase rocket thrust.

The factors of ejection rail angle, seat back angle, spinal G component, rocket thrust vector, and aerodynamic load effect are closely inter-related as shown in Figure 40 and each affects ejection clearances.

### 8.2.1 Rail Angle Effects

Figure 41 shows the effects of rail angle variation on tail clearance heights for  $-4 G_x/+10 G_z$  aircraft acceleration. In most cases of varying rocket thrust vector angles, tail clearance decreases with increasing rail angle. This variation is much smaller than the loss of height between rocket thrust vector angles of 30 and 45 degrees, illustrating the adverse effects of excessive forward orientation of rocket thrust. The loss of clearance height with increasing rail angle is significant, however, and results in a bias toward the lower angles.

Figure 42 shows rail angle effects for the  $+2 G_x/+10 G_z$  condition. Tail clearance height is again decreased with increasing rail angle. The decreased sensitivity, with variation in rocket thrust vector angle, is evident for this acceleration condition. Tail clearance heights are lowest for the longitudinal position of 32 feet.

### 8.2.2 Rail And Rocket Thrust Vector Angles

The lower limit of rocket thrust vector angle is determined by the  $+2 G_x / +10 G_z$  aircraft load condition because of spinal load limitations. Tail clearance is critical for the same G load condition at these lower vector angles.

The upper limit of potentially usable rocket thrust vector angles is determined by tail clearance height for the  $-4 G_x / +10 G_z$  aircraft load condition. Clearance height is sensitive to thrust vector/seat attitude at the higher thrust vector angles.

The 30 degree rail angle of Concepts  $D_1$  and  $E_1$  has adequate tail clearance height except for the  $-4 G_x$  case. Thrust vector angle range is acceptable but indicates a lower range of permissible angles for pitch control effectiveness.

For a 45 degree rail angle of Concepts  $D_2$  and  $E_2$  a rocket thrust vector angle of 30 degrees results in a range of 14 degrees and an increment of 3.0 spinal  $G_z$  below the 17 G spinal limit. The 45 degree rail angle offers the greatest potential of the rail angles considered. The 45 degree rail angle is the best compromise from a flight dynamics standpoint for the high-G escape systems.

Design Concept F with a spinal angle parallel to the rail angles of 65 degrees exhibits the same spinal G characteristics as that shown for the 30 degree rail angle of Concepts  $D_1$  and  $E_1$  and lower tail clearance heights for all conditions. The 65 degree rail angle represents an upper limit of rail angle selection.

Design Concepts A, B and C require rocket thrust vector angles to maintain spinal G's within acceptable limits, that severely limit tail clearance heights.

### 8.2.3 Parametric Study

A parametric study of tail clearance trajectories contained in Appendix I of Report MDC J7976, is included in this report. The objective of this study is the determination of the effects of aircraft speed and G load, seat propulsion parameters, ejection and rocket thrust vector angles, and aerodynamic effects on tail clearance heights and seat occupant spinal loads.

Rail angle effect plots are not found to be as useful as rocket thrust vector angles in the selection of these variables for the high-G escape system.



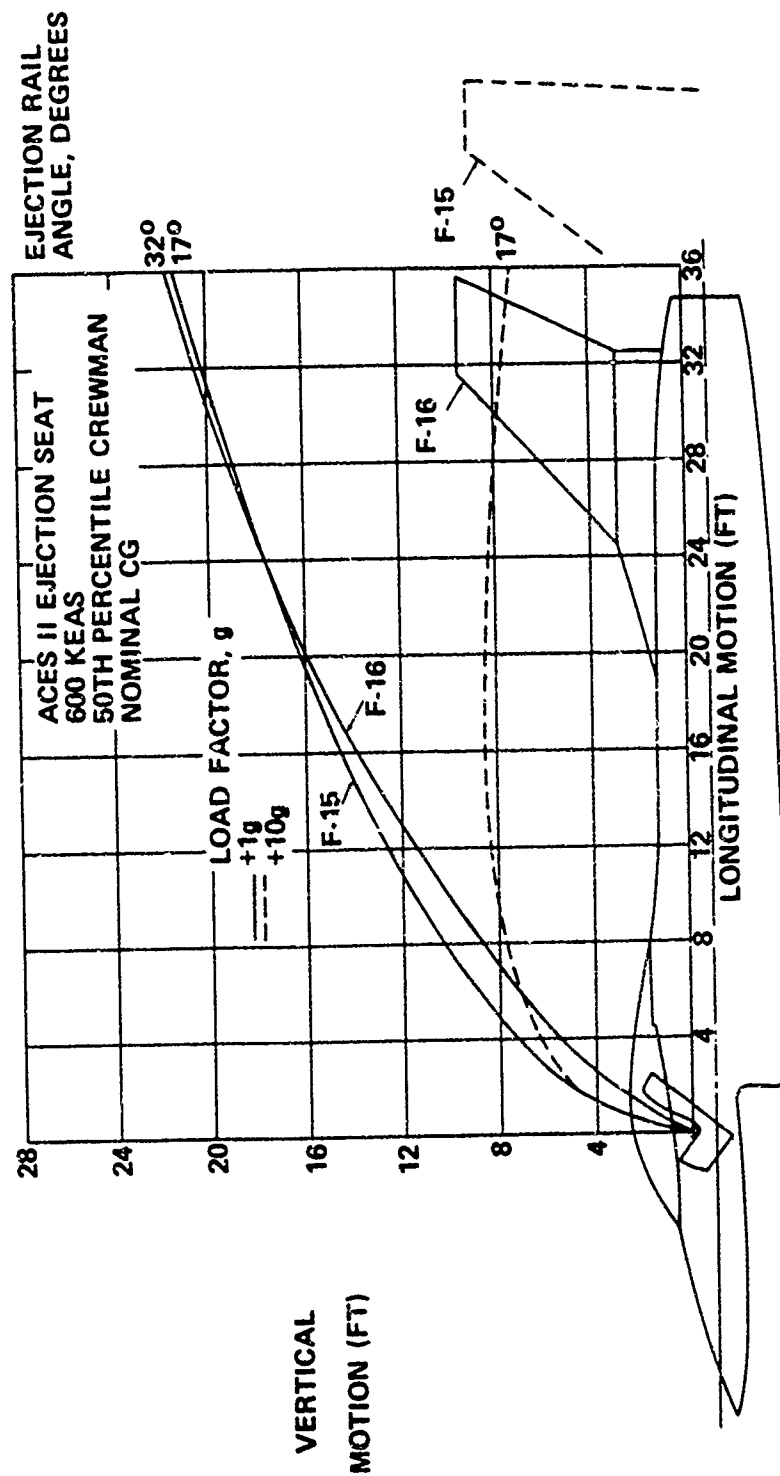


Figure 39. Tail Clearance Effect of +  $G_z$

CONCEPT	EJECTION RAIL ANGLE (DEGREES)	SEAT BACK ANGLE (DEGREES)	MAX. SPINAL G	MIN. THRUST VECTOR (DEGREES)	AIRCRAFT/TAI L CLEARANCE				REQ. THRUST VECTOR FOR ALL CONDITIONS	SPINAL G AT REQ. THRUST VECTOR
					600 KEAS		450 KEAS			
					+2 G <sub>x</sub>	-4 G <sub>x</sub>	+2 G <sub>x</sub>	-4 G <sub>x</sub>		
A	30°	13° 65°	14.9 10.5	*	11.0 FT.	0	12.0 FT.	0	10°	** 23.0
B	30°	28° 80°	19.8 13.4	* 31°	15.0 FT.	20.5 FT.	21.5 FT.	0	15°	** 24.0
C	17°	13°	15.0	45°	9.5 FT.	0	(MARGINAL)	0	0°	** 24.2
D,-E <sub>1</sub>	30°	60°	17.0	30°	15.0 FT.	20.5 FT.	21.5 FT.	0	15°	** 22.4
D <sub>2</sub> -E <sub>2</sub>	45°	75°	17.0	21°	11.5 FT.	20.5 FT.	17.5 FT.	(MARGINAL)	15°	** 19.5
F	65°	65°	17.0	27°	7.0 FT.	15.0 FT.	10.0 FT.	0	150	** 21.4

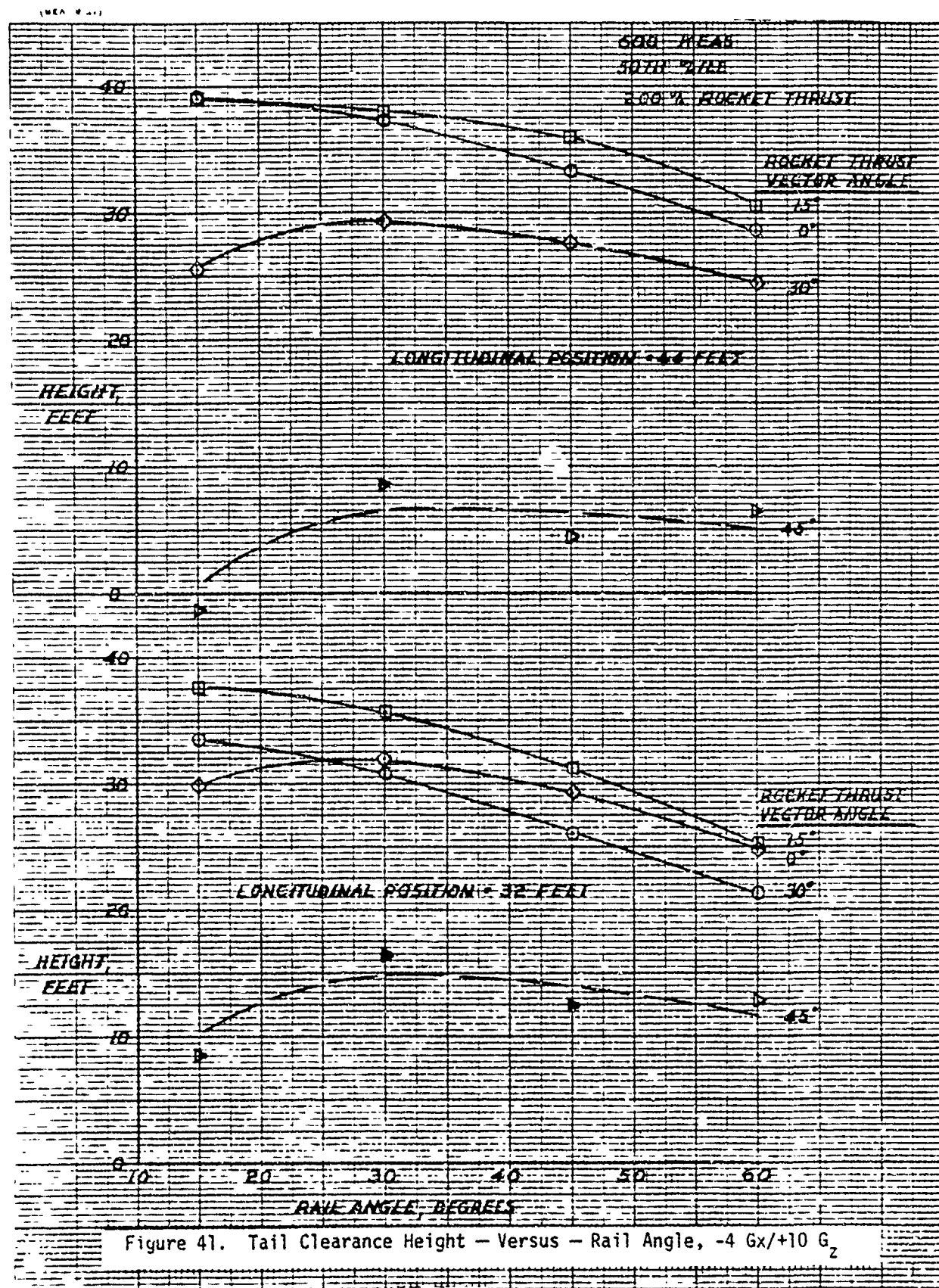
NOTES: \* Thrust vector required for upright and reclined CG Alignment

\*\* Exceeds maximum spinal G

0 Inadequate clearance

Figure 40. Rail Angle/Rocket Thrust Vector/Spinal G- Versus-  
Aircraft Tail Clearance





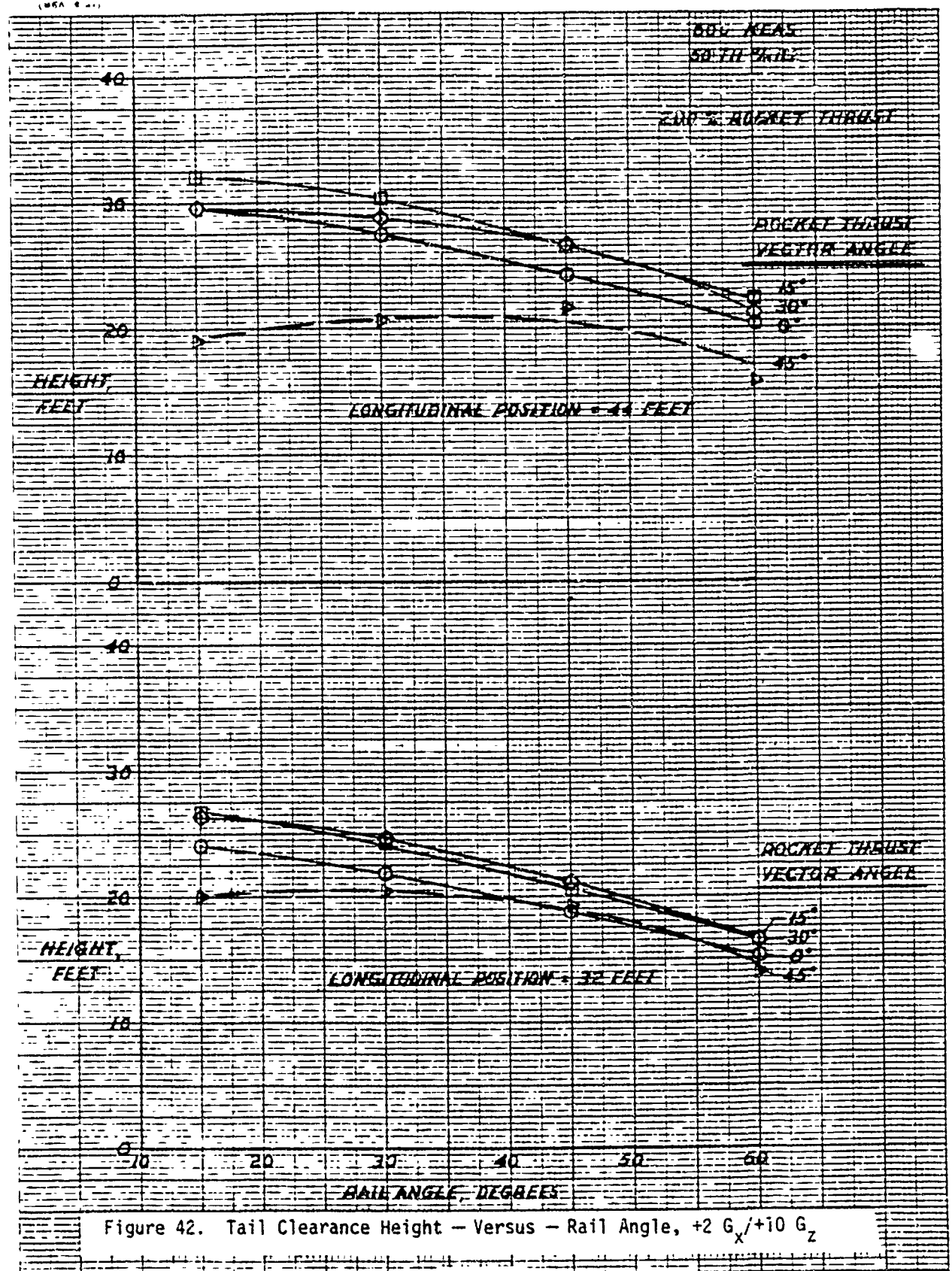


Figure 42. Tail Clearance Height - Versus - Rail Angle, +2 G<sub>x</sub>/+10 G<sub>z</sub>

### 8.3 ESCAPE PERFORMANCE

Analysis of escape performance of all candidate seat concepts in one G level flight, adverse attitude and sink-rate conditions has been made.

The recovery height, above and below ejection altitude, at full inflation of the parachute is as follows:

<u>RECOVERY HEIGHT (FT.)</u>			
<u>CONCEPT</u>	<u>LEVEL FLIGHT</u>	<u>ADVERSE ATTITUDE</u>	<u>SINK RATE</u>
A	+ 112.6	- 170.6	- 83.4
B	+ 115.8	- 173.8	- 80.2
C	+ 114.3	- 172.3	- 81.7
D <sub>1</sub> E <sub>1</sub>	+ 116.0	- 174.0	- 80.0
D <sub>2</sub> E <sub>2</sub>	+ 116.3	- 174.3	- 79.7
F	+ 113.1	- 171.1	- 82.9

#### 8.4 STRUCTURAL ANALYSIS

Candidate seat concepts are required to meet the structural load requirements of MIL-S-9479B. The guide rail support structure and the articulating seat components require load and stress analysis of the affected portions of the seat for flight, ejection and crash conditions. The down latch mechanism for the seat bucket is engaged only for ejection. Therefore, for flight and crash conditions, loads are transmitted from the seat bucket to the fixed seat structure through the articulating segments, gear sectors, and actuating gear motor brake.

The crash condition restraint system ultimate loads of MIL-S-9479B are: 1) forward = 8600 pounds; 2) side = 8600 pounds  $20^{\circ}$  to either side; and 3) down = 1750 pounds. Ejection loads on the seat structure will be less than the crash loads in the downward direction. For design Concept C and F these seat structural loads will be similar to the ACES II ejection seat. For design Concepts A and B reaction loads in the seat structure will be increased by approximately 33 percent due to the increased moment arm from the rail support structure to the CG of the seat and occupant. For design Concepts D<sub>1-2</sub> and E<sub>1-2</sub> this increase will be approximately 92 percent more than the baseline Concept.

The restraint system loads which must be reacted by the articulating segments and gear motor are:

1. Shoulder Harness: 3400 pounds
2. Lap Belt: 3000 pounds
3. Lap Belt Pin: 2600 pounds horizontal  
1500 pounds vertical

These loads are similar to those of the ACES II seat. Side crash loads for the upright position are not transmitted to the positioning system and are comparable to those of the ACES II seat. The side loads will be reacted by the existing seat sides, lap belt and shoulder harness.

Analysis for crash loads applied with the seat in the reclined position shows that current restraint system components will not meet these requirements. Therefore, the crash G forces specified in MIL-S-9479B are applicable for the upright seat position only. Takeoff and landing operations with the seat in the reclined position will require a deviation from the crash load requirements of MIL-S-9479B for the basic restraint harness described in Paragraph 5.1.1 of this report.

## 8.5 WEIGHT ANALYSIS

Weight analysis of each candidate seat concept and individual subsystems for high G escape result in the following estimated weights:

	<u>WEIGHT (LBS)</u>
Basic Restraint Harness	3.3
Contour Bladder Restraint	6.0*
Head/Torso Support	1.6
Powered Twist Torso/Head Support	5.0*
Limb Restraint Strap	4.6
Inflatable Restraint	8.0*
Integral Gear Motor	13.7
Floor Mounted Gear Motor	15.5
Emergency Retraction	7.4
Seat Side Handles	4.2
Center D-Ring - Upward Motion	2.1
Center D-Ring - Downward Motion	2.1
Electrical Initiation	1.0*
Low Boost Phase/High Thrust Rocket	21.1
Twin Sustainer Rocket Motors	38.0*
Two-Stage Rocket Motor	23.0*
Twin Low-Boost Catapults	10.0*
Catapult Pressure Limiting Valve	1.5*
Two-Axis Main Rocket STAPAC	8.0*
Thrust Vector Control (TVC)	6.0*
Gimballed Rocket	18.0*
Inflatable Stabilizer/Decelerator	8.0*
High Thrust Canopy Remover	25.0
Canopy Auxiliary Rocket Motor	15.0*
Canopy Fracturing (SMDC)	5.0*

Weights marked \* are assigned weights. All other weights are estimated.

To provide a comparative weight analysis an average combined subsystem weight of 66.5 pounds has been calculated. This results in the following individual total weight for each seat concept:

SEAT CONCEPT WEIGHT (LBS)

	<u>A</u>	<u>B</u>	<u>C</u>	<u>D<sub>1</sub> D<sub>2</sub></u>	<u>E<sub>1</sub> E<sub>2</sub></u>	<u>F</u>
Basic Seat and Structure	122.6	122.6	122.6	131.0	131.0	134.0
High G Subsystem (average)	66.5	66.5	66.5	66.5	66.5	60.8
Seat Position Retraction	---	---	7.4	7.4	7.4	3.0
Guide Rail Positioning	---	8.5	---	8.5	8.5	11.0
HUD/Windscreen Repositioning	<u>12.0</u>	<u>10.5</u>	---	<u>10.5</u>	---	<u>10.5</u>
TOTAL CONCEPT WEIGHT	201.1	208.1	196.5	223.9	213.4	219.3

Canopy removal system weights have not been included in the total concept weight analysis as their application is not directly related to any particular seat concept, except that the SMDC system does not appear feasible for Concepts A and B where the seat may be ejected in any position.

The estimated total ejected weight for each seat concept will be:

Concept A	164.7 lbs.
Concept B	178.4 lbs.
Concept C	172.1 lbs.
Concept D <sub>1</sub> D <sub>2</sub>	194.2 lbs.
Concept E <sub>1</sub> E <sub>2</sub>	194.2 lbs.
Concept F	191.8 lbs.

Concepts A and C, with fixed guide rails, permit the use of the aircraft floor-mounted positioning gear motor. This reduction in ejection weight is included in the calculations.

## SECTION IX

### CONCEPT SELECTION CRITERIA

Evaluation of high-G ejection seat concepts consists of the following primary criteria elements:

- Safety
- Performance/Capability
- Interface Effects
- Reliability
- Development Risk

#### 9.1 SYSTEM WEIGHTING RATIONALE

Of the five criteria elements, crew safety and system performance are of major importance in the evaluation of emergency escape systems. These elements must be assigned a combined weighting factor greater than the combined subsidiary elements of interface effects, reliability and development risk.

The ratio of assigned weights greater than 50-50 may thus be 55-45, 60-40, 65-35, 70-30, etc. Ratios of 70-30 and greater do not provide a sufficiently wide rating range for meaningful evaluation of the three subsidiary elements, while ratios less than 60-40 result in assigning undue significance to these same elements. A similar rationale is used in assigning weighting factors to sub-categories under each of the primary elements.

In dealing with individual subsystems, crew safety and performance are of equal importance. Each are assigned a weighting factor of 30, for a total weight ratio of 60-40 with the subsidiary elements. For the evaluation of total high G ejection seat system concepts, crew safety is a more significant element than performance/capability. These elements are thus assigned weight factors of 35 and 30 respectively, for a total ratio of 65-35 with subsidiary elements. A similar rationale is used in assigning weighting factors to sub-categories under each of the primary elements.

In the evaluation of the complete high-G seat concepts the major criteria element of Safety consists of the five sub-categories of tail clearance, acceleration/DRI effect, aerodynamic load effect, pre-ejection windblast protection, and ejection repositioning/cockpit clearances. To evaluate crew safety under high-G ejection conditions, the effect of each concept on the interrelated factors of tail clearance and acceleration/DRI are of equal and major importance. Each are assigned a weight factor of 30 for a total weight ratio of 60-40 with the sub-categories of aerodynamic load effects, windblast protection and cockpit clearances, that are not particularly affected by high-G ejection conditions.

In the evaluation of Performance/Capability the sub-categories of upright-level flight, adverse attitude and sink-rate conditions are of equal importance since performance must be evaluated over the full range of flight conditions. Each are thus assigned a weight factor of 33.3.



Interface effect evaluation involves considerations of aircraft compatibility, cockpit volume requirements and aircraft weight effects. Aircraft compatibility is of slightly greater significance than volume and weight effects since compatibility may involve major aircraft structural and component revisions to achieve instrument panel and windscreen repositioning. These considerations result in a 40-30-30 relationship of the three sub-categories.

The evaluation of concept Reliability places equal emphasis on system complexity and the combination of maintainability and the subsidiary element of interlock requirements. In the absence of detailed reliability and failure mode analysis, these sub-categories are simply quantified by the number of component parts involved. This rationale results in a 50-40-10 weighting of these sub-categories.

Evaluations of Development Risk involves the sub-categories of advanced technology requirements, design goal achievability and test and analysis requirements. The sub-category of advanced technology requirements is a more meaningful element since design goal achievability and test/analysis requirements are primarily cost and schedule oriented while new technology deals with advancements in the state-of-the-art. The resulting assigned weight factor ratio is 40-30-30.

## 9.2 RATING RANGE

In order to provide adequate latitude in the evaluation process a wide rating range is used. Weighting factors of the various criteria elements that are capable of being quantified are proportioned between the highest and lowest evaluations, with the lowest evaluation rated at 60 percent of the highest. These include such elements as tail clearance height, acceleration/DRI, escape performance ejection height, aircraft volume and weight, and compatibility and reliability by the number of subsystem and component parts involved.

For selection criteria elements not subject to quantification the following rating method is used:

Superior	100%
Excellent	90%
Good	80%
Fair	70%
Poor	60%



### 9.3 HIGH-G SEAT CONCEPT EVALUATION

Selection criteria evaluation of each of the eight high-G concepts uses the rationale and weighting range discussed in the previous paragraphs.

#### 9.3.1 Safety

The major criteria element of crew safety is weighted at 35 percent. Sub-categories and weighting factors are:

Tail Clearance	30%
Acceleration/DRI Effect	30%
Aerodynamic Load Effect	15%
Windblast Protection	15%
Cockpit Clearances	10%
(TOTAL - 35%)	100%

Tail Clearance - Ejection under the conditions of  $+10 G_z$  at  $+2 G_x/-4 G_x$  at 600 and 450 KEAS is critical to tail clearance. As shown in Figure 40 of Section 8.2, tail clearance is inadequate under  $-4 G_x$  conditions for some of the seat concepts due to limitations on spinal  $G$ 's and resulting rocket thrust vectors. In the evaluation/weighting process, seat Concepts A and C are rated as "poor" since clearance is not acceptable for two of the four noted conditions. Seat Concepts D<sub>2</sub> and E<sub>2</sub> are rated "superior" as adequate clearance is provided under all ejection conditions. All other concepts are rated as "fair". To further differentiate concept rating, +1 and -1 factors are applied for differences in average tail clearance height and for clearances noted as "marginal".

The following weight ratings result:

CONCEPT		RATING
A - Poor	$(30 \times .60) +1$	19.0
B - Fair	$(30 \times .70)$	21.0
C - Poor	$(30 \times .60)$	18.0
D <sub>1</sub> E <sub>1</sub> - Fair	$(30 \times .70)$	21.0
D <sub>2</sub> E <sub>2</sub> - Superior	$(30 \times 1.0) -1$	29.0
F - Fair	$(30 \times .60) -1$	20.0

Acceleration/DRI Effect - Varying seat back angles result in spinal G components from 6.5 G to 10.7 G. These are highest and lowest rated respectively in evaluating DRI effects on crew safety. All seat concepts are proportionally rated between 100 and 60 percent and result in the following weighted ratings:

<u>CONCEPT</u>	<u>BACK ANGLE</u>	<u>SPINAL G</u>	<u>RATING</u>
A	13°	10.6	18.4
B	28°	10.7	(60%) 18.0
C	13°	10.6	18.4
D <sub>1</sub> E <sub>1</sub>	60°	8.5	24.5
D <sub>2</sub> E <sub>2</sub>	75°	6.5	(100%) 30.0
F	65°	7.9	26.0

Aerodynamic Load Effect - Combinations of varying ejection angle, seat back angle and seat attitudes result in aerodynamic loads affecting crew safety. Aerodynamic G loads range from 24.2 G to 27.6 G and are high-and low-rated as shown.

<u>CONCEPT</u>	<u>AERO LOAD (G)</u>	<u>RATING</u>
A	24.2	(100%) 15.0
B	27.3	9.5
C	24.2	(100%) 15.0
D <sub>1</sub> E <sub>1</sub>	27.6	(60%) 9.0
D <sub>2</sub> E <sub>2</sub>	24.9	13.7
F	26.7	10.5

Windblast Protection - Seat concepts that require aircraft windscreen re-positioning for ejection clearance provide windblast protection prior to, and during, ejection from the seat guide rails. These concepts are rated "Excellent" (90%), while seat concepts without pre-ejection windscreen re-positioning are rated as "poor" (60%) for windblast protection. Concepts A, B, D<sub>1</sub>, D<sub>2</sub> and F thus receive a rating of 13.5 (15 x .9), and Concepts C, E<sub>1</sub> and E<sub>2</sub> are rated at 9.0 (15 x .6).

Cockpit Clearances - Varying concept requirements of seat, headrest, guide rail, instrument panel and windscreen pre-ejection positioning affect cockpit clearances and crew safety. Each element is assigned a -1.0 weight factor in the evaluation of cockpit clearances.

CONCEPT	SEAT	HEADREST	RAIL	WIND SCREEN	INSTRUMENT PANEL		RATING
A	0	0	0	-1	-1	(10-2)	8.0
B	0	0	-1	-1	-1	(10-3)	7.0
C	-1	0	0	0	0	(10-1)	9.0
D <sub>1</sub> D <sub>2</sub>	-1	0	-1	-1	-1	(10-4)	6.0
E <sub>1</sub> E <sub>2</sub>	-1	0	-1	0	0	(10-2)	8.0
F	-1	-1	-1	-1	-1	(10-5)	5.0

### 9.3.2 Performance/Capability

Recovery height above and below ejection altitude at full inflation of the recovery parachute is used in the evaluation of performance in upright level flight, adverse attitude and sink-rate conditions. This performance results from variations in ejection rail angle and rocket thrust vector angle for each seat concept. The following recovery heights and ratings are derived for each ejection condition.

#### Upright Level Flight

CONCEPT	RECOVERY HEIGHT (FT.)		RATING
A	+112.6	(60%)	20.0
B	+115.8		31.1
C	+114.3		25.9
D <sub>1</sub> E <sub>1</sub>	+116.0		31.9
D <sub>2</sub> E <sub>2</sub>	+116.3	(100%)	33.3
F	+113.1		21.8

#### Adverse Attitude

A	-170.6	--	(100%)	33.3
B	-173.8			21.7
C	-172.3			27.0
D <sub>1</sub> E <sub>1</sub>	-174.0			21.0
D <sub>2</sub> E <sub>2</sub>	-174.3		(60%)	20.0
F	-171.1			31.2

### Sink Rate

<u>CONCEPT</u>	<u>RECOVERY HEIGHT (FT.)</u>		<u>RATING</u>
A	-83.4	(60%)	20.0
B	-80.2		31.1
C	-81.7		25.9
D <sub>1</sub> E <sub>1</sub>	-80.0		31.9
D <sub>2</sub> E <sub>2</sub>	-79.7	(100%)	33.3
F	-82.9		21.8

### 9.3.3 Interface Effects

The evaluation of each seat concept for aircraft interface effect is determined by considerations of compatibility, volume requirements and total system weight. These sub-categories have a weighted rating of 40, 30, 30 percent respectively.

Aircraft Compatibility - Ejection rail pivoting, instrument panel and windscreen positioning requirements are elements involved in the evaluation of aircraft/seat compatibility. Each element is assigned a -2 weight factor except that rail positioning for all concepts except Concept F is weighted at -1 since rail pivot considerations for these concepts have only minor affect on aircraft compatibility.

<u>CONCEPT</u>	<u>RAIL PIVOT</u>	<u>INSTRUMENT PANEL</u>	<u>WIND SCREEN</u>	<u>TOTAL</u>		<u>RATING</u>
A	0	-2	-2	-4		29.2
B	-1	-2	-2	-5		26.8
C	0	0	0	0	(100%)	40.0
D <sub>1</sub> D <sub>2</sub>	-1	-2	-2	-5		26.8
E <sub>1</sub> E <sub>2</sub>	-1	0	0	-1		37.2
F	-2	-2	-2	-6	(60%)	24.0

Cockpit Volume - The total volume for each seat concept aft of the upright seat-back reference line is rated as shown.

<u>CONCEPT</u>	<u>VOLUME (CU. FT.)</u>		<u>RATING</u>
A	6.8		28.3
B	6.8		28.3
C	4.8	(100%)	30.0
D <sub>1</sub>	10.5		24.7
D <sub>2</sub>	12.5		23.0
E <sub>1</sub>	15.8		20.0
E <sub>2</sub>	17.8	(60%)	18.0
F	7.2		27.9

Aircraft Weight - The weight of each concept affects total aircraft weight and is rated as follows:

<u>CONCEPT</u>	<u>WEIGHT (LBS.)</u>		<u>RATING</u>
A	201		28.0
B	208		24.8
C	196	(100%)	30.0
D <sub>1</sub> D <sub>2</sub>	224	(60%)	18.0
E <sub>1</sub> E <sub>2</sub>	213		22.7
F	219		20.0

#### 9.3.4 Reliability

Sub-categories affecting total system reliability are complexity (50%), maintainability (40%) and interlock requirements (10%). Concept ratings for reliability are noted below.

Complexity - Elements of seat, rail, instrument panel and windscreen positioning subsystems are each assigned a weighting factor -1 for each seat concept. This results in the following weighted rating for complexity evaluations.

<u>CONCEPT</u>	<u>SEAT</u>	<u>RAIL</u>	<u>PANEL</u>	<u>WINDSCREEN</u>	<u>TOTAL</u>	<u>RATING</u>
A	0	0	-1	-1	-2	44.0
B	0	-1	-1	-1	-3	41.0
C	-1	0	0	0	-1	47.0
D <sub>1</sub> D <sub>2</sub>	-1	-1	-1	-1	-4	38.0
E <sub>1</sub> E <sub>2</sub>	-1	-1	0	0	-2	44.0
F	-2	-1	-1	-1	-5	35.0

Maintainability - The primary elements affecting system reliability are the maintainability requirements and accessibility of seat mounted and floor mounted positioning gear motors, the positioning gears and dis-engagement system, and the guide rail positioning motor. Each are assigned a minus rating factor from -1 to -3 and a weighted rating as shown.

CONCEPT	SEAT MOTOR	FLOOR MOTOR	GEARING	RAIL MOTOR	TOTAL	<u>RATING</u>
A	0	-1	-1	0	-2	34.0
B	-3	0	-1	0	-4	28.0
C	0	-1	-1	0	-2	34.0
D <sub>1</sub> D <sub>2</sub>	-3	0	-1	0	-4	28.0
E <sub>1</sub> E <sub>2</sub>	-3	0	-1	0	-4	28.0
F	0	0	0	-1	-1	37.0

Interlock Requirements - Each seat concept except Concept A requires system interlocks to prevent catapult ignition until pre-ejection seat positioning functions are accomplished. These interlock functions affect total system reliability and receive a -1 factor in the evaluation rating.

CONCEPT	SEAT	RAIL	HEADREST	TOTAL	<u>RATING</u>
A	0	0	0	0	10.0
B	0	-1	0	-1	9.0
C	-1	0	0	-1	9.0
D <sub>1</sub> D <sub>2</sub>	-1	-1	0	-2	8.0
E <sub>1</sub> E <sub>2</sub>	-1	-1	0	-2	8.0
F	-1	-1	-1	-3	7.0

#### 9.3.5 Development Risk

The evaluation of development risk involves considerations of advanced technology requirements, design goal achievability and test/analysis requirements. An evaluation weight ratio of 40-30-30 is applied for each element of development risk.

Advanced Technology - Varying degrees of advanced technology are required for rocket thrust and thrust vector control to achieve tail clearance under all ejection conditions while maintaining spinal G components at acceptable levels. To reflect these requirements each seat concept is assigned a minus rating factor of -1 to -5 as shown.

CONCEPT	VECTOR CONTROL	THRUST CONTROL	TOTAL	<u>RATING</u>
A	-4	-4	-8	29.3
B	-2	-2	-4	34.5
C	-4	-5	-9	28.0
D <sub>1</sub> E <sub>1</sub>	-2	-2	-4	34.5
D <sub>2</sub> E <sub>2</sub>	-1	-1	-2	37.2
F	-2	-3	-5	33.2

Design Goal Achievability - Seat concepts are rated in a similar manner, with added considerations of achieving rail, windscreen and panel positioning. Minus rating factors of -0.5 to -4 are assigned to each concept.

CONCEPT	VECTOR CONTROL	THRUST CONTROL	REPOSITIONING R.L. PANEL/WS		TOTAL	<u>RATING</u>
A	-4	-2	0	-1	-7.0	21.0
B	-2	-1	-1	-1	-5.0	23.5
C	-4	-2.5	0	0	-6.5	21.5
D <sub>1</sub>	-2	-1	-1	-1	-5.0	23.5
D <sub>2</sub>	-1	-0.5	-1	-1	-3.5	25.5
E <sub>1</sub>	-2	-1	-1	0	-4.0	24.7
E <sub>2</sub>	-1	-0.5	-1	0	-2.5	25.5
F	-2	-1.5	-2	-1	-6.5	21.5

Test/Analysis Requirements - Minus rating factors of -1 and -2 are applied in a manner similar to the closely related development risk elements of advanced technology and achievability.

CONCEPTS	VECTOR CONTROL	THRUST CONTROL	REPOSITIONING THRUSTERS RAIL PANEL/WS HEADREST			TOTAL	<u>RATING</u>
A	-2	-1	0	-1	0	-4	24.0
B	-2	-1	-1	-1	0	-5	22.5
C	-2	-1	0	0	0	-3	25.5
D <sub>1</sub> D <sub>2</sub>	-2	-1	-1	-1	0	-5	22.5
E <sub>1</sub> E <sub>2</sub>	-2	-1	-1	0	0	-4	24.0
F	-2	-1	-1	-1	-1	-6	21.0

#### 9.4 SELECTION CRITERIA EVALUATION

Evaluation of each candidate seat concept is shown in Figure 43. Selection criteria and evaluation of each subsystem follows the same system weighting rationale and rating range as seat concept evaluations. These evaluations are shown in Figure 44 through 49.



	WEIGHTING (%)	HIGH-G SEAT CONCEPTS							
		A	B	C	D <sub>1</sub>	D <sub>2</sub>	E <sub>1</sub>	E <sub>2</sub>	F
1.0 SAFETY	35	25.9	24.1	24.3	26.0	32.6	25.0	31.7	26.6
1.1 TAIL CLEARANCE	30	19.0	21.0	18.0	21.0	30.0	21.0	30.0	20.0
1.2 ACCELERATION/DRI EFFECT	30	18.4	18.0	18.4	24.5	30.0	24.5	30.0	26.0
1.3 AERODYNAMIC LOAD EFFECT	15	15.0	9.5	15.0	9.0	13.7	9.0	13.7	10.5
1.4 WINDBLAST PROTECTION	15	13.5	13.5	9.0	13.5	13.5	9.0	9.0	13.5
1.5 COCKPIT CLEARANCE	10	8.0	7.0	9.0	6.0	6.0	8.0	8.0	6.0
	100	73.9	69.0	69.4	74.0	93.2	71.5	90.7	76.0
2.0 PERFORMANCE/CAPABILITY	30	22.0	25.2	23.6	25.4	26.0	25.4	26.0	22.4
2.1 UPRIGHT-LEVEL FLIGHT	33.3	20.0	31.1	25.9	31.9	33.3	31.9	33.3	21.8
2.2 ADVERSE ATTITUDE	33.3	33.3	21.7	27.0	21.0	20.0	21.0	20.0	31.2
2.3 SINK-RATE	33.3	20.0	31.1	25.7	31.9	33.3	31.9	33.3	21.8
	100	73.3	83.9	78.8	84.8	86.6	84.8	86.6	74.8
3.0 INTERFACE EFFECTS	15	12.8	12.0	15.0	10.4	10.2	12.0	11.7	10.8
3.1 AIRCRAFT COMPATIBILITY	40	29.2	26.8	40.0	26.8	26.8	37.2	37.2	24.0
3.2 VOLUME REQUIREMENT	30	28.3	28.3	30.0	24.7	23.0	20.0	18.0	27.9
3.3 AIRCRAFT WEIGHT	30	28.0	24.8	30.0	18.0	18.0	22.7	22.7	20.0
	100	85.5	79.9	100.0	69.5	67.8	79.9	77.9	71.9
4.0 RELIABILITY	10	8.8	7.8	9.0	7.4	7.4	8.0	8.0	7.9
4.1 SYSTEM COMPLEXITY	50	44.0	41.0	47.0	38.0	38.0	44.0	44.0	35.0
4.2 MAINTAINABILITY	40	34.0	28.0	34.0	28.0	28.0	28.0	28.0	37.0
4.3 INTERLOCK REQUIREMENTS	10	10.0	9.0	9.0	8.0	8.0	8.0	8.0	7.0
	100	88.0	78.0	90.0	74.0	74.0	80.0	80.0	79.0
5.0 DEVELOPMENT RISK	10	7.4	8.1	7.5	8.1	8.5	8.3	8.8	7.6
5.1 ADVANCED TECHNOLOGY	40	29.3	34.5	28.0	34.5	37.2	34.5	37.2	33.2
5.2 DESIGN GOAL ACHIEVABILITY	30	21.0	23.5	21.5	23.5	25.5	24.7	26.5	21.5
5.3 TEST/ANALYSIS REQUIREMENTS	30	24.0	22.5	25.5	22.5	22.5	24.0	24.0	21.0
	100	74.3	80.5	75.0	80.5	85.2	83.2	87.7	75.7
EVALUATION	100	76.9	77.2	79.4	77.3	84.7	78.7	86.2	75.3

Figure 43. High-G Seat Concepts Selection Criteria Evaluation

CONCEPT 1 - BASIC RESTRAINT HARNESS  
 - LIMB RESTRAINT STRAPS  
 - HEAD/TORSO SUPPORT

CONCEPT 2 - CONTOUR BLADDER  
 - INFLATABLE RESTRAINT  
 - POWERED TWIST TORSO/HEAD SUPPORT

EVALUATION FACTORS	WEIGHTING (%)		EVALUATION			
			CONCEPT 1		CONCEPT 2	
1.0 SAFETY		30		24.3		28.1
1.1 INJURY PROTECTION	35		31.5		35.0	
1.2 EJECTION ENTANGLEMENT PROTECTION	25		17.5		22.5	
1.3 IN-FLIGHT ENTANGLEMENT PROTECTION	20		16.0		18.0	
1.4 GROUND EMERGENCY RELEASE	20		16.0		18.0	
	100		81.0		93.5	
2.0 PERFORMANCE/CAPABILITY		30		24.9		27.3
2.1 IN-FLIGHT SUPPORT/RESTRAINT	30		24.0		27.0	
2.2 EJECTION LIMB RESTRAINT	30		27.0		27.0	
2.3 CREW MOBILITY	15		12.0		13.5	
2.4 CREW COMFORT	15		12.0		13.5	
2.5 PRE-FLIGHT CONNECTIONS	10		8.0		10.0	
	100		83.0		91.0	
3.0 INTERFACE EFFECTS		15		12.6		12.2
3.1 INTERNAL VISION	25		22.5		22.5	
3.2 EXTERNAL VISION	25		17.5		20.0	
3.3 FUNCTIONAL REACH	25		22.5		22.5	
3.4 SEAT COMPATIBILITY	15		13.5		10.5	
3.5 WEIGHT	10		8.0		6.0	
	100		84.0		81.5	
4.0 RELIABILITY		15		12.2		12.0
4.1 SYSTEM COMPLEXITY	30		27.0		21.0	
4.2 MAINTAINABILITY	30		24.0		21.0	
4.3 MIS-RIGGING PROTECTION	20		14.0		20.0	
4.4 AUTOMATIC RELEASE	20		16.0		18.0	
	100		81.0		80.0	
5.0 DEVELOPMENT RISK		10		9.4		7.1
5.1 ADVANCED TECHNOLOGY REQUIREMENTS	40		40.0		32.0	
5.2 DESIGN GOAL ACHIEVABILITY	30		27.0		21.0	
5.3 TEST/ANALYSIS REQUIREMENTS	30		27.0		18.0	
	100		94.0		71.0	
EVALUATION		100		83.4		86.7

Figure 44. Support/Restraint Subsystems — Selection Criteria Evaluation

CONCEPT 1 - INTEGRAL GEAR MOTOR

CONCEPT 2 - FLOOR MOUNTED GEAR MOTOR

EVALUATION FACTORS	WEIGHTING (%)		EVALUATION			
			CONCEPT 1		CONCEPT 2	
1.0 SAFETY		30		27.0		27.0
2.0 PERFORMANCE/CAPABILITY		30		27.0		27.0
3.0 INTERFACE EFFECTS		15		12.4		11.7
3.1 SEAT COMPATIBILITY	30		24.0		27.0	
3.2 COCKPIT VOLUME	25		25.0		17.5	
3.3 AIRCRAFT WEIGHT	25		20.0		17.5	
3.4 EJECTION WEIGHT	20		14.0		16.0	
	<u>100</u>		<u>83.0</u>		<u>78.0</u>	
4.0 RELIABILITY		15		13.5		12.0
4.1 SYSTEM COMPLEXITY	60		54.0		48.0	
4.2 MAINTAINABILITY	40		36.0		32.0	
	<u>100</u>		<u>90.0</u>		<u>80.0</u>	
5.0 DEVELOPMENT RISK		10		9.0		8.0
EVALUATION		100		88.9		85.7

Figure 45. Seat Positioning Subsystems - Selection Criteria Evaluation

CONCEPT 1 - CENTER D-RING - UPWARD MOTION

CONCEPT 2 - CENTER D-RING - DOWNWARD MOTION

CONCEPT 3 - ELECTRICAL INITIATION

EVALUATION FACTORS	WEIGHTING (%)		EVALUATION			
			CONCEPT 1	CONCEPT 2	CONCEPT 3	
1.0 SAFETY		30		25.5		24.0
1.1 EJECTION CLEARANCES	50		40.0		45.0	40.0
1.2 INADVERTENT ACTUATION	50		45.0		40.0	40.0
	100		85.0		85.0	80.0
2.0 PERFORMANCE/CAPABILITY		30		22.5		25.5
2.1 ACTUATION UNDER HIGH G LOADS	50		30.0		45.0	45.0
2.2 FUNCTIONAL REACH	50		45.0		45.0	40.0
	100		75.0		90.0	85.0
3.0 INTERFACE EFFECTS		15		12.9		13.2
3.1 EJECTION RESTRAINT COMPATIBILITY	40		32.0		36.0	28.0
3.2 SEAT COMPATIBILITY	30		27.0		27.0	30.0
3.3 WEIGHT	30		27.0		27.0	30.0
	100		86.0		90.0	88.0
4.0 RELIABILITY		15		12.0		13.5
4.1 SYSTEM COMPLEXITY	60		48.0		48.0	64.0
4.2 MAINTAINABILITY	40		32.0		32.0	36.0
	100		80.0		80.0	90.0
5.0 DEVELOPMENT RISK		10		10.0		9.1
5.1 ADVANCED TECHNOLOGY REQUIREMENTS	40		40.0		40.0	40.0
5.2 DESIGN GOAL ACHIEVABILITY	30		30.0		30.0	24.0
5.3 TEST/ANALYSIS REQUIREMENTS	30		30.0		27.0	27.0
	100		100.0		97.0	91.0
EVALUATION		100	82.9		87.7	85.3

Figure 46. Ejection Initiation Subsystems - Selection Criteria Evaluation

CONCEPT 1 - TWO-AXIS MAIN ROCKET STAPAC

CONCEPT 2 - THRUST VECTOR CONTROL (TVC)

CONCEPT 3 - GIMBALLED ROCKET

EVALUATION FACTORS	WEIGHTING (%)		EVALUATION					
			CONCEPT 1		CONCEPT 2		CONCEPT 3	
1.0 SAFETY		30		27.0		27.0		27.0
2.0 PERFORMANCE/CAPABILITY		30		24.3		25.6		27.1
2.1 PITCH CONTROL	40			36.0		36.0		36.0
2.2 YAW CONTROL	40			36.0		36.0		36.0
2.3 ROLL CONTROL	15			9.0		13.5		13.5
2.4 VERTICAL SEEKING CAPABILITY	5			0.0		0.0		5.0
	100			81.0		85.5		90.5
3.0 INTERFACE EFFECTS		15		11.5		13.5		11.0
3.1 SEAT COMPATIBILITY	65			52.0		58.5		45.5
3.2 WEIGHT	35			24.5		31.5		28.0
	100			76.5		90.0		73.5
4.0 RELIABILITY		15		12.6		10.5		9.6
4.1 SYSTEM COMPLEXITY	60			48.0		42.0		36.0
4.2 MAINTAINABILITY	40			36.0		28.0		28.0
	100			84.0		70.0		64.0
5.0 DEVELOPMENT RISK		10		9.1		8.1		7.1
5.1 ADVANCED TECHNOLOGY REQUIREMENTS	40			40.0		36.0		32.0
5.2 DESIGN GOAL ACHIEVABILITY	30			27.0		24.0		21.0
5.3 TEST/ANALYSIS REQUIREMENTS	30			24.0		21.0		18.0
	100			91.0		81.0		71.0
EVALUATION		100		84.5		84.7		81.8

Figure 47. Seat Stabilization Subsystems — Selection Criteria Evaluation

CONCEPT 1 - TWO-AXIS MAIN ROCKET STAPAC

CONCEPT 2 - THRUST VECTOR CONTROL (TVC)

CONCEPT 3 - GIMBALLED ROCKET

EVALUATION FACTORS	WEIGHTING (%)		EVALUATION					
			CONCEPT 1		CONCEPT 2		CONCEPT 3	
1.0 SAFETY		30		27.0		27.0		27.0
2.0 PERFORMANCE/CAPABILITY		30		24.3		25.6		27.1
2.1 PITCH CONTROL	40		36.0		36.0		36.0	
2.2 YAW CONTROL	40		36.0		36.0		36.0	
2.3 ROLL CONTROL	15		9.0		13.5		13.5	
2.4 VERTICAL SEEKING CAPABILITY	5		0.0		0.0		5.0	
	100		81.0		85.5		90.5	
3.0 INTERFACE EFFECTS		15		11.5		13.5		11.0
3.1 SEAT COMPATIBILITY	65		52.0		58.5		45.5	
3.2 WEIGHT	35		24.5		31.5		28.0	
	100		76.5		90.0		73.5	
4.0 RELIABILITY		15		12.6		10.5		9.6
4.1 SYSTEM COMPLEXITY	60		48.0		42.0		36.0	
4.2 MAINTAINABILITY	40		36.0		28.0		28.0	
	100		84.0		70.0		64.0	
5.0 DEVELOPMENT RISK		10		9.1		8.1		7.1
5.1 ADVANCED TECHNOLOGY REQUIREMENTS	40		40.0		36.0		32.0	
5.2 DESIGN GOAL ACHIEVABILITY	30		27.0		24.0		21.0	
5.3 TEST/ANALYSIS REQUIREMENTS	30		24.0		21.0		18.0	
	100		91.0		81.0		71.0	
EVALUATION		100	84.5		84.7		81.8	

Figure 47. Seat Stabilization Subsystems — Selection Criteria Evaluation

CONCEPT 1 - LOW BOOST PHASE/HIGH THRUST ROCKET

CONCEPT 2 - TWIN SUSTAINER ROCKET MOTORS

CONCEPT 3 - TWO-STAGE ROCKET MOTORS

EVALUATION FACTORS	WEIGHTING (%)		EVALUATION					
			CONCEPT 1		CONCEPT 2		CONCEPT 3	
1.0 SAFETY		30		25.8		27.0		27.0
1.1 ACCELERATION LIMITS	35		28.0		31.5		31.5	
1.2 DRI EFFECT	35		28.0		31.5		31.5	
1.3 TAIL CLEARANCE	30		30.0		27.0		27.0	
	100		86.0		90.0		90.0	
2.0 PERFORMANCE/CAPABILITY		30		24.9		24.9		24.9
2.1 UPRIGHT-LEVEL FLIGHT	33		29.9		26.6		26.6	
2.2 ADVERSE ATTITUDE	33		23.3		29.9		29.9	
2.3 SINK-RATE	33		29.9		26.6		25.6	
	100		83.1		83.1		83.1	
3.0 INTERFACE EFFECTS		15		14.0		10.5		13.7
3.1 SEAT COMPATIBILITY	65		58.5		45.5		58.5	
3.2 WEIGHT	35		35.0		24.5		33.2	
	100		93.5		70.0		91.7	
4.0 RELIABILITY		15		15.0		12.6		11.7
4.1 SYSTEM COMPLEXITY	60		60.0		48.0		42.0	
4.2 MAINTAINABILITY	40		40.0		36.0		36.0	
	100		100.0		84.0		78.0	
5.0 DEVELOPMENT RISK		10		9.4		7.7		
5.1 ADVANCED TECHNOLOGY REQUIREMENTS	40		40.0		32.0		25.0	
5.2 DESIGN GOAL ACHIEVABILITY	30		27.0		24.0		24.0	
5.3 TEST/ANALYSIS REQUIREMENTS	30		27.0		21.0		21.0	
	100		94.0		77.0		73.0	
EVALUATION		100	89.1		82.7		84.6	

Figure 48. Ejection Propulsion Subsystems — Selection Criteria Evaluation

CONCEPT 1 - HIGH THRUST REMOVER

CONCEPT 2 - AUXILIARY ROCKET MOTORS

CONCEPT 3 - CANOPY FRACTURING (SMDC)

EVALUATION FACTORS	WEIGHTING (%)		EVALUATION			
			CONCEPT 1		CONCEPT 2	
1.0 SAFETY		30		25.5		22.8
1.1 INJURY PROTECTION	40		40.0		40.0	28.0
1.2 WINDBLAST PROTECTION	30		18.0		18.0	27.0
1.3 GROUND EMERGENCY EGRESS	30		27.0		24.0	21.0
	100		85.0		82.0	76.0
2.0 PERFORMANCE/CAPABILITY		30		25.8		26.4
2.1 CANOPY REMOVAL UNDER HIGH-G	60		54.0		54.0	48.0
2.2 PRE-EJECTION TIME DELAY	40		32.0		32.0	40.0
	100		86.0		86.0	88.0
3.0 INTERFACE EFFECTS		15		11.7		12.3
3.1 SEAT CONCEPT COMPATIBILITY	40		36.0		36.0	28.0
3.2 AIRCRAFT/CANOPY STRUCTURAL EFFECT	30		21.0		24.0	27.0
3.3 WEIGHT	30		21.0		24.6	27.0
	100		78.0		84.6	82.0
4.0 RELIABILITY		15		13.5		11.4
4.1 SYSTEM COMPLEXITY	60		54.0		48.0	48.0
4.2 MAINTAINABILITY	40		36.0		32.0	28.0
	100		90.0		80.0	76.0
5.0 DEVELOPMENT RISK		10		9.4		8.1
5.1 ADVANCED TECHNOLOGY REQUIREMENTS	40		40.0		40.0	36.0
5.2 DESIGN GOAL ACHIEVABILITY	30		30.0		30.0	27.0
5.3 TEST/ANALYSIS REQUIREMENTS	30		24.0		21.0	18.0
	100		94.0		91.0	81.0
EVALUATION		100		85.9		81.0

Figure 49. Canopy Jettison Subsystems - Selection Criteria Evaluation



## SECTION X

### SELECTED CONCEPT FOR HIGH-G ESCAPE

Seat Concept D<sub>2</sub> has been selected as the design concept for final definition and analysis. This selection is based upon the evaluation ratings of seat selection criteria and on the parametric study of tail clearance trajectories for high-G escape conditions. This concept has an ejection rail angle of 45-degrees and a seat-back spinal angle of 75-degrees. Improved tail clearance over other candidate concepts and minimal spinal loading is achieved with this concept. Rocket thrust vector angles provide safe ejection clearances under all aircraft G-load conditions.

Concept E<sub>2</sub> incorporates the same ejection and seat-back angles and exhibits the same tail clearance trajectories and spinal loading characteristics as the selected concept. Although Concept E<sub>2</sub> rates slightly higher in the evaluation ratings, Concept D<sub>2</sub> rates highest in safety and requires 5.3 cu. ft. less cockpit volume. Pre-ejection windblast protection is provided with the selected concept by repositioning of the aircraft windscreen. This protection is not inherent in the E<sub>2</sub> design concept.

These considerations lead to the selection of Concept D<sub>2</sub> for high-G escape.

#### 10.1 SELECTED CONCEPT DEFINITION

The selected concept for high-G escape consists of an articulating ejection seat providing a multi-position range of seat back angles from a 13-degree normal upright position to a reclined back angle position of 65-degrees. Ejection initiation returns the seat to the 13-degree back angle from any reclined position and repositions the seat guide rails to a 45-degree ejection angle. This repositioning results in an ejection seat-back spinal angle of 75-degrees. This configuration is shown in Figure 50 and consists of the following selected subsystems.

##### 10.1.1 Seat Positioning System

The positioning system is integrated into the basic ejection seat structure by the addition of the articulating backrest and shoulder support, the seat pan and bucket, and the gear motor assembly unit. Positioning motion of the seat pan is controlled by a four-bar linkage consisting of the seat back, bucket, primary seat structure and lower links. The lower links are integral with gear sectors driven by a pinion gear and cross shaft assembly that is part of an integral gear motor unit. This arrangement provides lateral stability of the articulating components and maintains the structural integrity of the basic seat. This system is described in detail in Section 5.2 of this report.

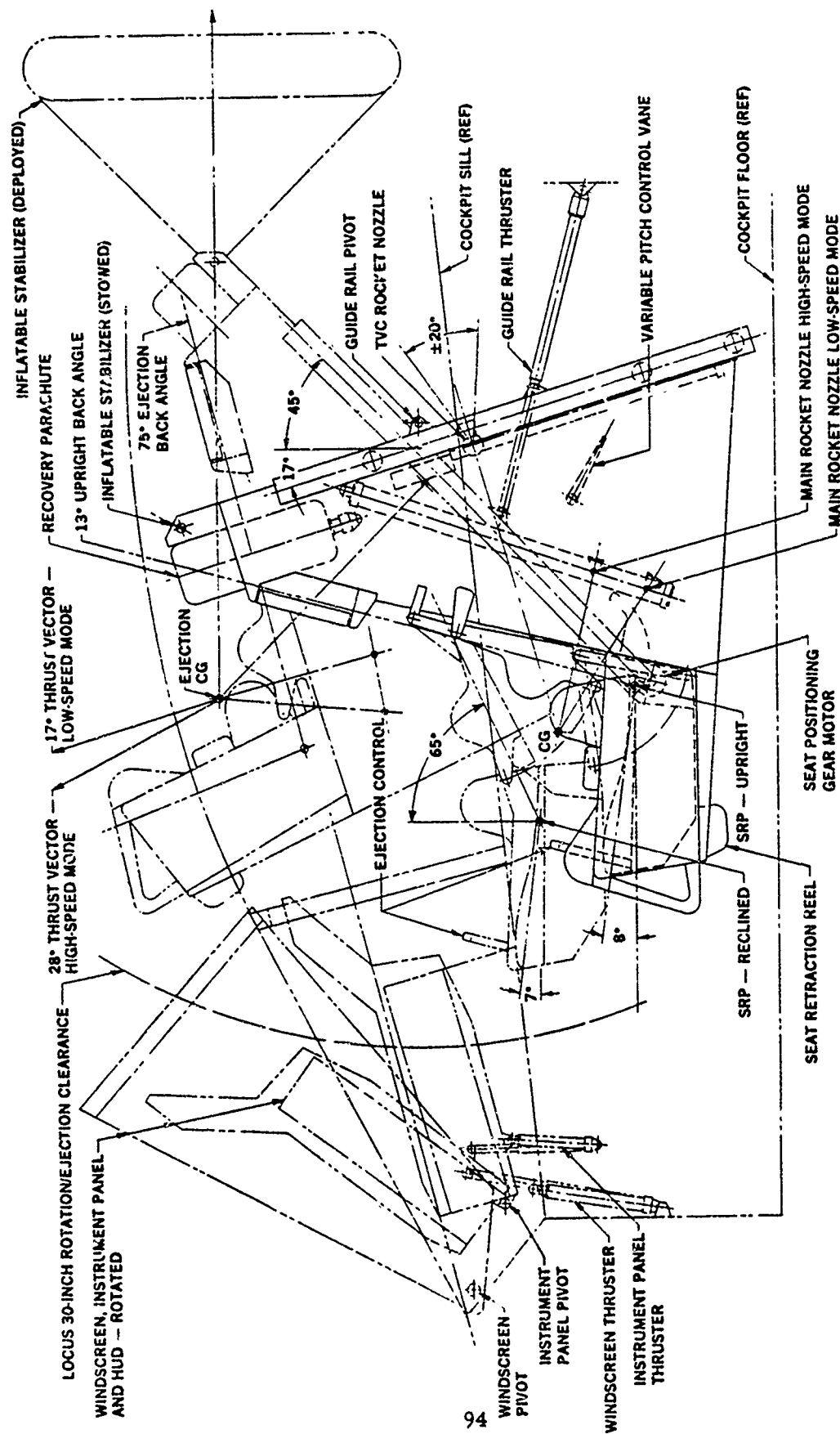


Figure 50. High-G Ejection Seat Selected Concept Configuration

### 10.1.2 Crew Restraint System

Normal crew support and ejection limb restraint is provided by an inflatable torso and limb fixation system. The articulating backrest consists of three segments which have projections to retain and support the body. One segment encloses the shoulders while the two lower segments enclose the upper and lower torso. The projecting portions are fitted with a contour and inflation bladder system. The contour bladder system also provides restraint for the thighs and forearms. The bladder system is contained in a trough which forms the arm support. When the system is activated, the bladder system holds the limbs firmly in place, as further described in Section 5.1.2.

### 10.1.3 Ejection Initiation/Sequencing

A center D-ring firing control initiates ejection by applying the operating force in a downward direction. This control requires a two-motion, squeeze and push, operation to prevent inadvertent operation. The control is accessible to the 5th through 95th percentile range of pilots from any seat position, with ease of actuation under all multi-axis G conditions.

A schematic of the complete ejection initiation system, including all pre-ejection functions of the aircraft sequencing systems, is shown in Figure 51. Event/time sequencing is keyed to the system schematic as shown:

<u>EVENT</u>	<u>TIME (SECS.)</u>
1. Ejection initiation.	0.000
2. Gear Motor Pinion Puller disconnection	0.001
3. Windscreen Thruster initiation	0.001
4. Canopy Thruster initiation	0.001
5. Seat Retraction Reel initiation	0.002
6. Windscreen repositioned	0.100
7. Instrument Panel Thruster initiation	0.101
8. Instrument Panel repositioned	0.200
9. Seat retraction to upright position	0.200
10. Seat Position/Instrument Panel Interlock release	0.202
11. Guide Rail Thruster initiation	0.202
12. Guide Rails repositioned	0.300
13. Canopy jettisoned	0.300
14. Canopy/Guide Rail interlock release	0.302
15. Rocket Catapult initiation	0.302

<u>EVENT</u>	<u>TIME (SECS.)</u>
1. Ejection initiation.	0.000
2. Gear Motor Pinion Puller disconnection	0.001
3. Windscreen Thruster initiation	0.001
4. Canopy Thruster initiation	0.001
5. Seat Retraction Reel initiation	0.002
6. Windscreen repositioned	0.100
7. Instrument Panel Thruster initiation	0.101
8. Instrument Panel repositioned	0.200
9. Seat retraction to upright position	0.200
10. Seat Position/Instrument Panel Interlock release	0.202
11. Guide Rail Thruster initiation	0.202
12. Guide Rails repositioned	0.300
13. Canopy jettisoned	0.300
14. Canopy/Guide Rail interlock release	0.302
15. Rocket Catapult initiation	0.302



#### 10.1.4 Ejection Propulsion System

Two sustainer rocket motors are used for the propulsion system of the selected seat concept. The main rocket provides 4100 pound of thrust at thrust vector angles of 15-degrees aft of the vertical and 5-degrees forward of the vertical for high and low speed modes respectively. This mode selection is provided by two rocket nozzles that are opened selectively by an aircraft speed-mode sensing unit.

The second sustainer rocket provides 3300 pounds of thrust at a nominal thrust vector angle of 45-degrees through a single thrust vector control nozzle for pitch control. These rockets are mounted in tandem on the longitudinal seat centerline as shown in the seat configuration of Figure 50. The resultant thrust and vector angles of the combined rockets provide 7200 pounds of thrust at a 28-degree vector angle in the 600 KEAS high-speed mode, and 6700 pounds of thrust at a vector angle of 17-degrees in the zero to 450 KEAS low-speed mode. These combined thrusts and vector angles maintain spinal G loading within the 17 G limit under all ejection conditions.

Catapult Thrust - The catapult boost phase cartridge unit is integral with the thrust vector control rocket mounted parallel with the ejection guide rails. The catapult thrust level results in a peak G of 8.5 under +1 G<sub>z</sub> aircraft load factor conditions, and a thrust of 17.6 G under +10 G<sub>z</sub> load factor conditions. Spinal G components are within the 17 G limit for a maximum DRI value of 18.0. Catapult boost phase thrust duration is 150 percent of the CKU-5/A catapult burn time.

#### 10.1.5 Seat Stabilization

The selected concept seat is stabilized in pitch and yaw by the thrust vector control rocket, an inflatable stabilizer/decelerator and a variable pitch control vane. These three systems, in combination, limit seat instability to damped oscillations of  $\pm 5$ -degrees.

Thrust Vector Control (TVC) - A two-axis hydrofluidic TVC is used with the secondary, 3300 pound thrust, sustainer rocket. This system provides  $\pm 20$  degrees of deflection of the variable nozzle in the pitch and yaw axes.

This TVC concept consists of attitude stabilization controllers and an internally actuated nozzle. The controllers obtain their power from the main rocket. The nozzle provides 20 degrees of deflection with less than 150 in-lb actuation torque. The integrated fluidic circuit contains a rate sensor, integrator and a position control valve. The control valve drives the nozzle with hydraulic pressure fed into piston-like bladders around the nozzle. Position transducers on the nozzle feed back pressure signals proportional to nozzle angle. This system is further described in Section 5.5.3 of this report.

Inflatable Stabilizer/Decelerator - An inflatable stabilizing structure replaces the conventional drogue parachute to provide more effective yaw and pitch stability. The inflatable system is stowed in a container on the upper seat structure as shown in Figure 50. During ejection a pyrotechnic gas generator is initiated just prior to seat/rail separation. The gas generator inflates the structure to approximately 12 psi in 30 milliseconds at any air speed. The required stabilizing forces are applied to the seat before the degree of seat rotation becomes a problem. Wind-tunnel testing and design analysis will be required to select final configuration providing the best aerodynamic shape compatible with internal gas shaping forces and stowage considerations.

Pitch Control Vane - A variable pitch control vane is mounted on the lower portion of the sub-structure aft of the primary seat structure. This vane provides an 0.92 sq. ft. of drag area at an effective moment arm 37.0 inches below the center of pressure of the basic seat. Two-speed mode operation of the pitch vane is provided by a thruster unit operating in conjunction with the speed mode sensing unit that controls nozzle selection of the main rocket. Rotation of the vane to a position normal to aero drag forces results in a forward pitch moment of the seat.

In the low-speed mode the vane is not actuated and does not affect normal TVC control of seat pitch moments. This results in the more vertical rocket thrust vectors desirable for tail clearance under adverse high-G conditions at low aircraft speeds.

In the high-speed mode (450 to 600 KEAS) the vane is actuated to provide additional forward pitch moments to assist the TVC rocket system. This effectively reduces initial TVC vertical rocket thrust vectors required to correct aero-induced aft seat pitch and reduces spinal G loading under high speed conditions.

#### 10.1.6 Canopy Jettison System

Canopy jettison under all high-G ejection conditions is provided by a 10,000 pound thrust pyrotechnic canopy remover. Operating characteristics of this unit are fully described in Section 5.6.1 of this report.



## 10.2 SELECTED CONCEPT ANALYSIS

The selected ejection seat concept has been analyzed to determine seat/cockpit/canopy interface effects, tail clearance ejection trajectories, and escape performance

### 10.2.1 Seat/Cockpit/Canopy Interfaces

Safe cockpit ejection clearances are provided with the selected concept by returning the seat to the upright position and by rotation of the instrument panel and aircraft windscreen clear of the ejection path as part of the pre-ejection functions. Repositioning of the ejection guide rails to the 45-degree ejection angle requires a swept cockpit volume of 12.5 cu. ft. aft of the seat back reference plane.

In the normal and reclined seat positions adequate clearance is provided under the closed cockpit canopy for the recovery parachute and inflatable stabilizer stowage containers located aft and above the seat headrest. Canopy jettison by the increased thrust canopy remover insures clearance of the ejection path prior to seat rocket catapult ignition under maximum  $G_z$  conditions.

### 10.2.2 Ejection Tail Clearances

The two-mode rocket thrust vector system provides safe ejection tail clearances and spinal G limits under all ejection conditions. As shown in Figures 52 and 53 the leading edge of the F-16 tail at a longitudinal position of 32 feet, and the trailing edge of the F-15 tail at a longitudinal position of 44 feet, represent the critical points for tail clearance trajectories.

In the high-speed mode at 600 KEAS, shown in Figure 52, the resultant rocket thrust of 7200 pounds at a vector angle of 28-degrees provides an ejection height of 19 feet at the 32 foot longitudinal position and 24 feet at the 44 foot longitudinal position under  $+2 G_x/+10 G_z$  load conditions. Under  $-4 G_x/+10 G_z$  conditions ejection heights are 27.5 feet and 29 feet respectively.

In the low-speed mode at 450 KEAS, rocket thrust is 6700 pounds and vector angle is 17-degrees. As shown in Figure 53 ejection heights are 23 feet and 27.5 feet at the 32 and 44 foot positions respectively under  $+2 G_x/+10 G_y$  load conditions. Under  $-4 G_x/+10 G_y$  conditions ejection heights are 29 feet and 21.5 feet at the respective longitudinal positions.

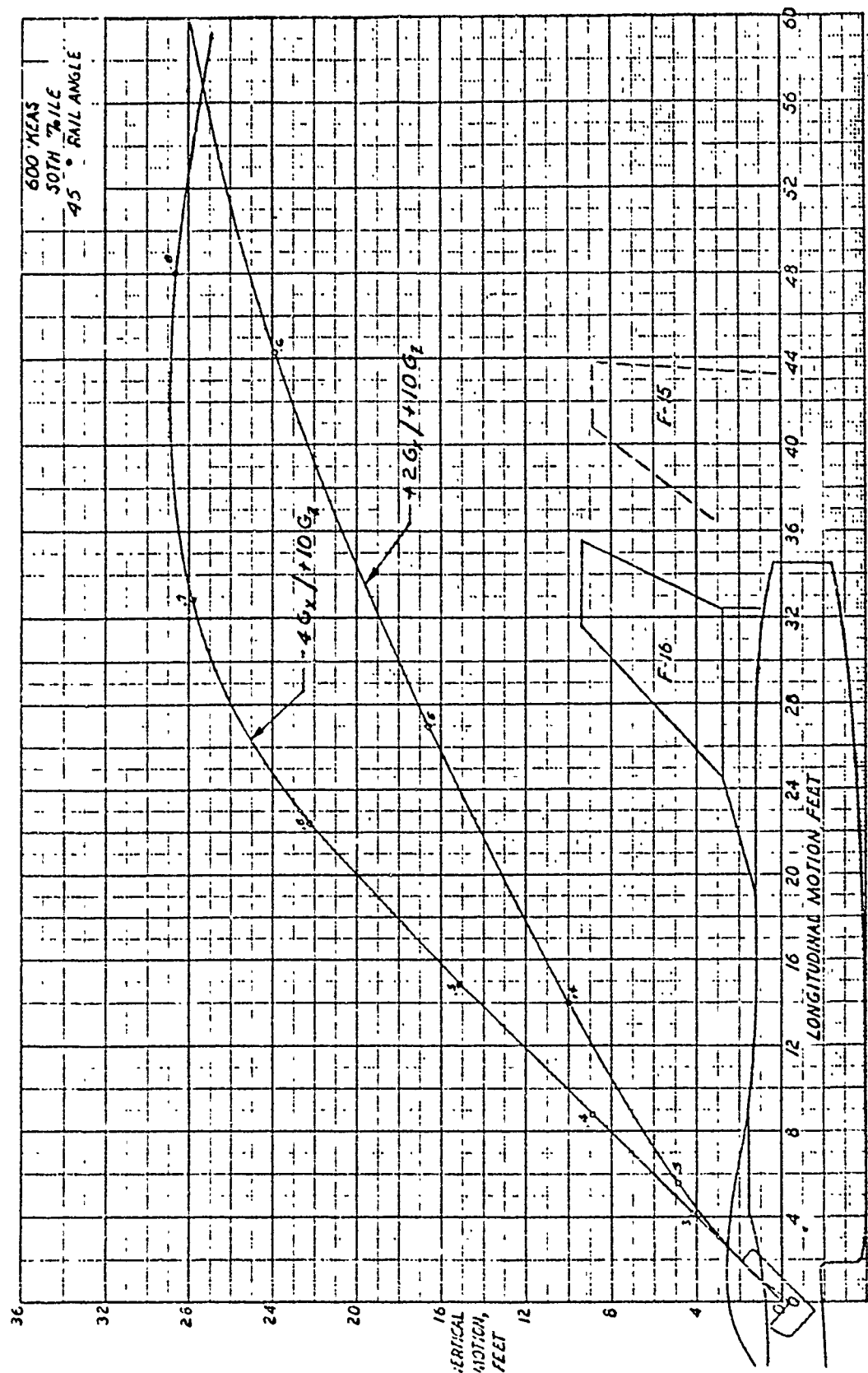


Figure 52. Selected Concept Tail Clearance Trajectories, High-G Speed Mode

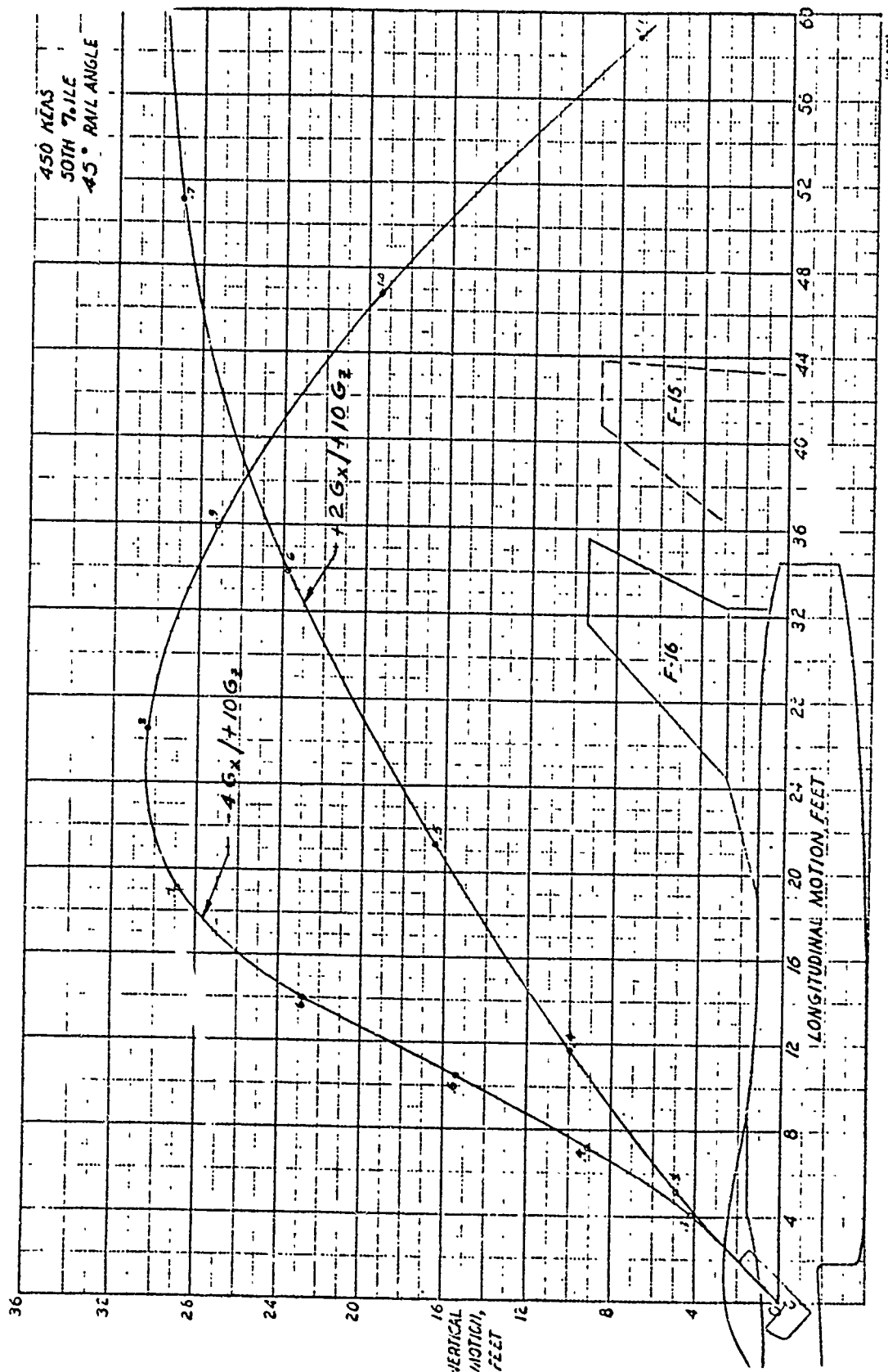


Figure 53. Selected Concept Tail Clearance Trajectories, Low-Speed Mode

### 10.2.3 Escape Performance

Escape performance of the selected seat in the low-speed mode at 150 KEAS has been determined for upright level flight, inverted attitude, and 10,000 fpm sink-rate conditions. Recovery height, above and below ejection altitude, at full inflation of the recovery parachute is as follows:

Level Flight	(+)	179 ft.
Inverted Attitude	(-)	203 ft.
Sink-Rate	(-)	59 ft.

## SECTION XI

### CONCLUSIONS AND RECOMMENDATIONS

An ejection seat design concept has been selected to meet all requirements for high-G escape. This selection is based on detailed study and analysis of all major subsystems and their integration into the basic seat concept. From this analysis, and from a parametric study of tail clearance trajectories, it is concluded that safe ejection from advanced flight vehicles operating at high acceleration loads may be accomplished with the selected High-G Ejection Seat.

These studies have further identified critical areas in computer analysis of high-speed trajectories. The establishment of precise rocket thrust vectors and the proportional thrust of main and thrust vector control rockets requires the availability of well-defined aerodynamic coefficients. Reasonable estimates of lift and drag coefficients have been made for the selected design concept from data established for the ACES II ejection seat. These coefficients yield valid test data and permit definitive trajectory analyses only for ejection seat systems similar to the ACES II configuration.

Further analysis, beyond the scope of this study, is recommended to establish aerodynamic coefficients based on wind-tunnel test data to verify the validity of these coefficients. Pitching moment coefficients can then determine the amount of control required for the propulsion/stabilization system and coefficient trend.

Additional analysis is required to assess the performance of the rocket catapult when actuated in a high-G environment. The Aerospace Medical Research Laboratory at Wright-Patterson Air Force Base, Ohio recently completed a series of tests on catapults in which the payload was subjected to sustained accelerations of up to 9 G's. The results of these tests require analysis to determine if catapults perform as predicted in this report.

The concepts generated in this study are based on the crew member going through a number of position changes prior to ejection. During repositioning, the crew member is subjected to high angular accelerations in addition to the aircraft G's. Analysis is required to determine if human tolerance limits are exceeded under these conditions.

APPENDIX  
PARAMETRIC STUDY OF TAIL CLEARANCE  
TRAJECTORIES FOR HIGH G ESCAPE CONDITIONS

## SECTION I

### INTRODUCTION

A systematic study of tail clearance trajectories provides an aid in the selection of concept configuration characteristics for high-G escape. The study objective is the determination of the effects of aircraft speed and G loads and seat propulsion parameters on tail clearance height and seat occupant spinal loads.

ACES II ejection seat data, with appropriate modifications, are used for seat characteristics.

Pitch variations are reduced to usable levels to promote the understanding of parametric variations in ejection rail and rocket thrust vector angles. The drogue parachute is eliminated and aerodynamic and rocket pitch moments are set to zero. Seat attitude is controlled by the ACES II seat STAPAC pitch control rocket.

This approach eliminates the large pitch variations associated with high-speed aerodynamic instability and results in small variations representative of the larger propulsion pitch control systems required for high-G escape.

## SECTION II

### INITIAL CONDITIONS

#### 2.1 AIRCRAFT SPEED AND LOADS

A speed of 600 KEAS at initiation of ejection is used in the major portion of the study. Additional trajectories at ejection speeds of 450 and 300 KEAS are included.

An aircraft load factor of  $+10 G_z$  is used in all cases. Aircraft longitudinal accelerations of  $+2 G_x$  (thrust) and  $-4 G_x$  (drag) are used in combination with  $+10 G_z$  for most cases. Some trajectory studies are made at  $+10 G_z$ ,  $0 G_x$  to provide a check on the criticality of this condition.

#### 2.2 PRE-EJECTION PHASE

The aircraft is assumed to be at the bottom of a pullout at the initiation of ejection. The catapult is ignited after a 0.3 second delay for pre-ejection functions. Catapult separation occurs approximately 0.20 to 0.25 seconds after catapult ignition. Seat/aircraft separation follows at 0.22 to 0.27 seconds.

All trajectories shown are for the  $+10 G_z$  aircraft load factor. This requires angles of attack from about 6 degrees at sea level to 24 degrees at 30,000 feet for the F-15 aircraft. The minimum angle of attack of 6 degrees is used for the subject trajectories. Higher aircraft angles of attack introduce indeterminate aerodynamic coefficients for the seat in the vicinity of the aircraft fuselage.

The aircraft is assumed to maintain constant attitude and acceleration during the tail-clearance portion of the trajectory. The vertical acceleration and catapult velocity increment cause the initial horizontal flight path angle of the seat to increase to about 13 degrees for the  $-4 G_x$  case at



seat/aircraft separation. The  $-4 G_x$  deceleration causes a decrease in dynamic pressure from an initial value of 1220 psi to about 1000 psi at seat/aircraft separation with beneficial effects for tail clearance and spinal forces. For the  $+2 G_x$  case, the aircraft accelerates to a dynamic pressure of about 1250 psi at separation, resulting in increased spinal loads.

## SECTION III

### PARAMETRIC CONSIDERATIONS

#### 3.1 SEAT CONFIGURATION

Seat data are basically those of ACES II. Ejected weight for the 50th percentile crewman plus seat is 363 pounds. Ejection rail and spinal angles are all aft with respect to the aircraft vertical. Rocket thrust vectors are all forward with respect to the aircraft vertical. Pitch and flight-path angles are given with respect to the earth horizontal. Angle of attack is given with respect to the flight path.

#### 3.2 SPINAL ANGLE AND LOAD

Peak spinal acceleration during the catapult phase is limited to 17.0 G. The same value applies to the rocket phase of the trajectory. Spinal  $G_z$  for the range of rail angles is from 1.0 to 5.0 G less than the 17.0 G limit. This margin is sufficient to maintain the 18.0 DRI limit for detailed analysis of this parameter during the rocket portion of the trajectory.

A seat-back/spinal angle of 30 degrees aft of the rail axis is used for most cases. This angle is a practical limit for seat articulation during the pre-ejection period. Some trajectories are run at a 30-degree rail angle with a 90-degree spinal angle, or 60 degrees aft of the rail, to determine the effect of variations in this parameter.

### 3.3 CATAPULT PERFORMANCE

Figure 54 shows the variation of catapult peak G under impressed G fields. This curve is used to determine peak G for catapult performance in less than maximum G fields.

Figure 55 shows the variation of catapult impressed G field with rail angle. A constant spinal angle of 30 degrees aft of the rail is used for all rail angles. A peak spinal  $G_z$  of 17.0 permits a catapult peak G of 19.6 for the  $-4 G_x/+10 G_z$  aircraft load condition at all rail angles.

Impressed G fields for 0.0, +2 and  $-4 G_x$  conditions are shown in the lower curves of Figure 55. The values from the  $-4$  and  $+2 G_x$  curves at each rail angle are applied to the curve of Figure 54 to give the peak G trend shown for the  $+2 G_x/10 G_z$  condition.

Although peak G for the  $+2 G_x$  condition is reduced with increasing rail angle, the differential between peak and impressed G curves remains fairly constant at 9 to 10 G. A similar situation prevails for the  $-4 G_x$  case. Catapult performance is therefore not strongly affected by rail angle.

Catapult duration for all trajectories is 150 percent of the CKU-5/A catapult burn time except for the 34-G catapult noted in Section 5.4, which maintains a 100 percent burn time duration for a spinal angle of 90 degrees.

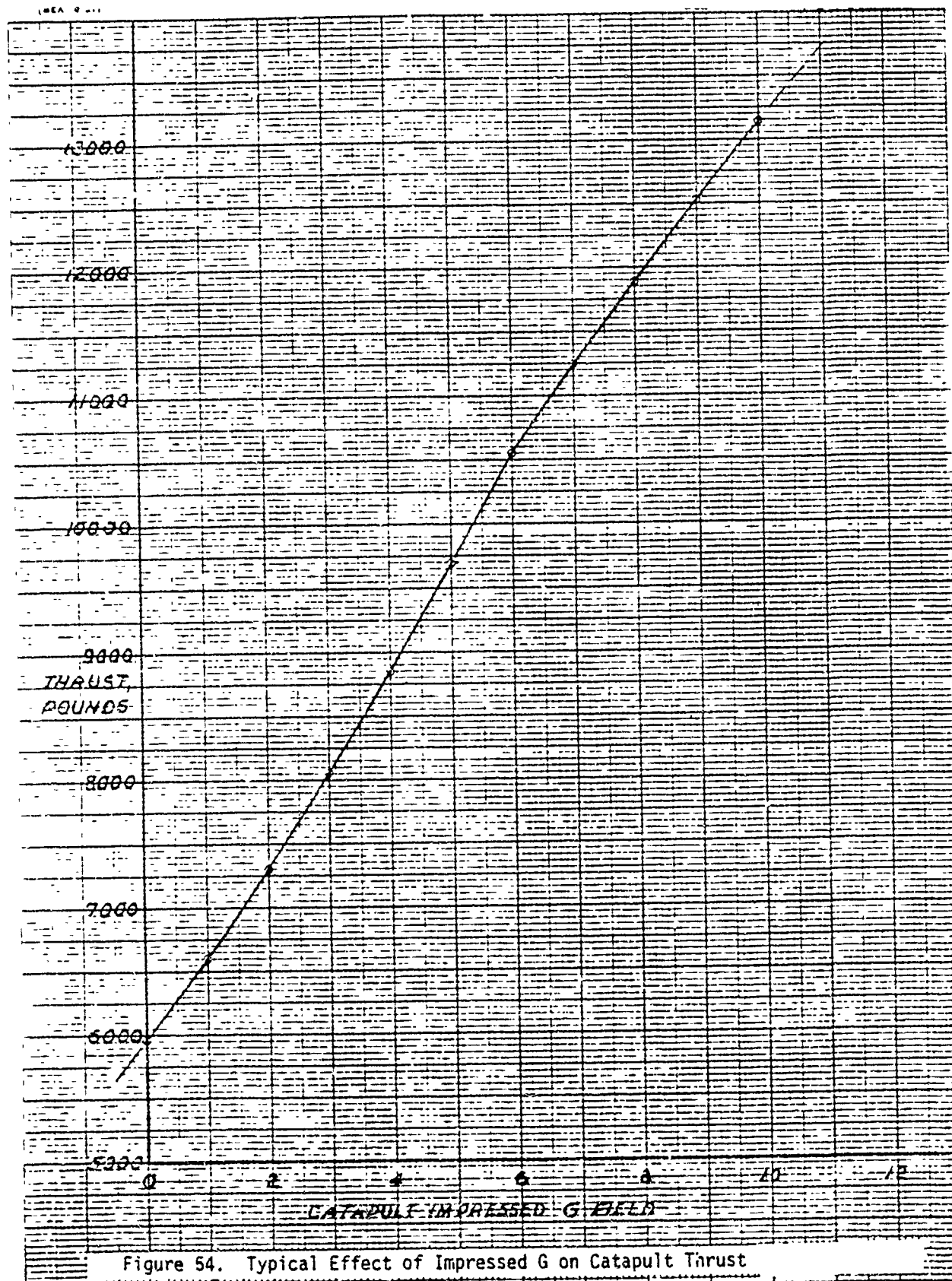


Figure 54. Typical Effect of Impressed G on Catapult Thrust

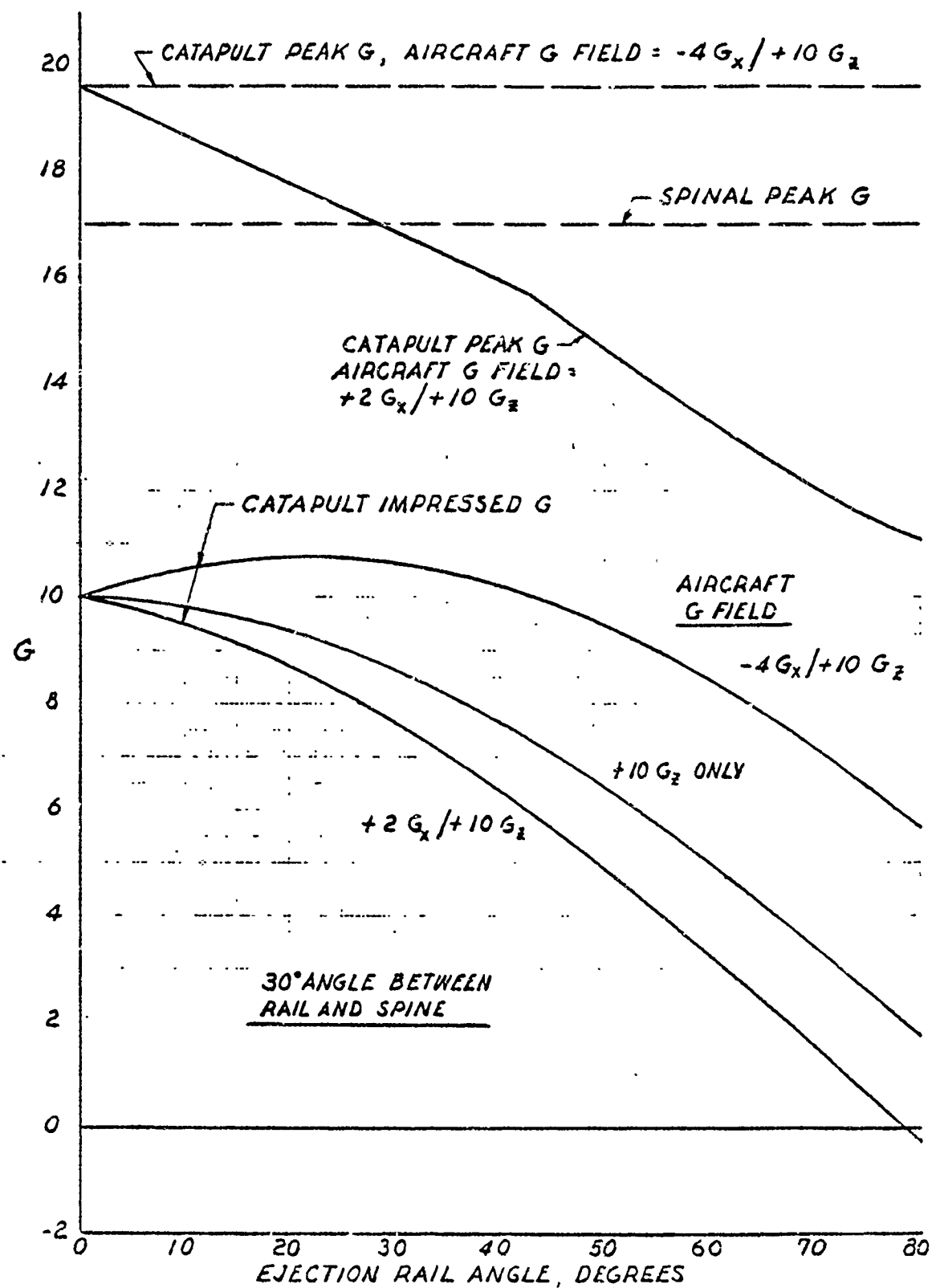


Figure 55. Catapult Impressed G Effects

### 3.4 ROCKET THRUST

Rocket thrust variation methods are shown in Figure 56. Thrust level is increased by multiplying all values by the appropriate percentage. To attain consistent trends at seat/aircraft separation, which occurs near the initial thrust peak, the duration of the thrust peak is held constant. Thrust duration is increased by extending the flat portion of the curve as typified by the 150 percent level. A thrust duration of 100 percent of the CKU-5/A rocket is used for all trajectories.

### 3.5 AERODYNAMIC COEFFICIENTS

The lift and drag coefficients used for the rocket phase of trajectory analysis are derived from the axial and normal force coefficients of Reference 41. Seat/aircraft separation occurs at Mach numbers between  $M = 0.8$  and  $0.9$ , with  $M$  decreasing to about  $0.6$  at tail clearance.

Figures 57 and 58 show lift and drag coefficients versus angle-of-attack,  $\alpha$ , at Mach numbers of  $0.6$  and  $0.9$ . The solid line drawn through the circles is that used for simulation in the H5HC computer program.

Also shown in the Figures are  $C_D$  and  $C_L$  for the F-106 seat based on  $C_A$  and  $C_N$  from Reference 42. A close correlation may be observed for  $C_L$  data.  $C_D$  for the F-106 seat is 5 to 10 percent lower than that used for ACES II but the reference area ratio is  $8.25/7.8$  (F-106/ACES II) or  $1.06$ . Drag force is nearly equal for both seats.



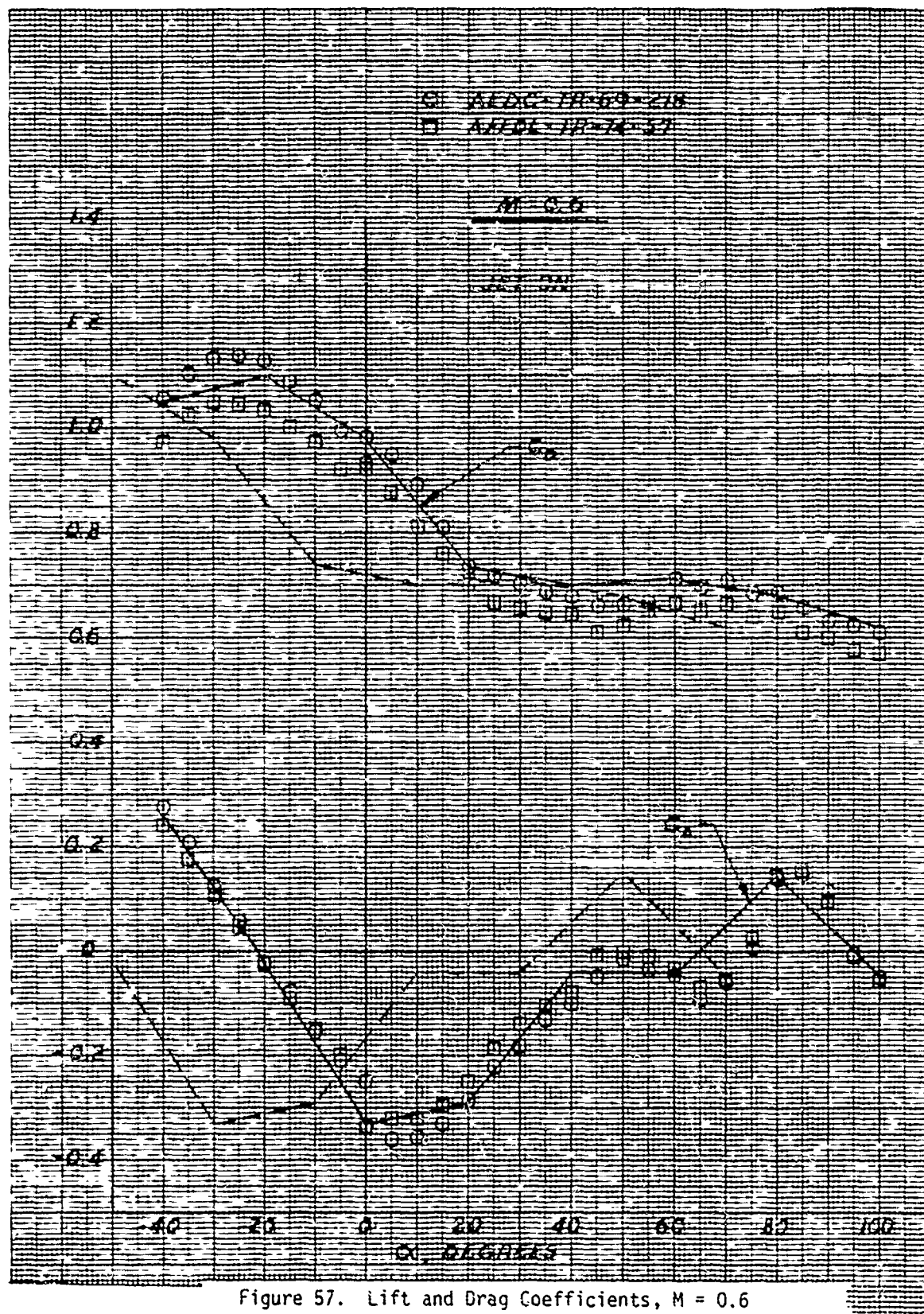
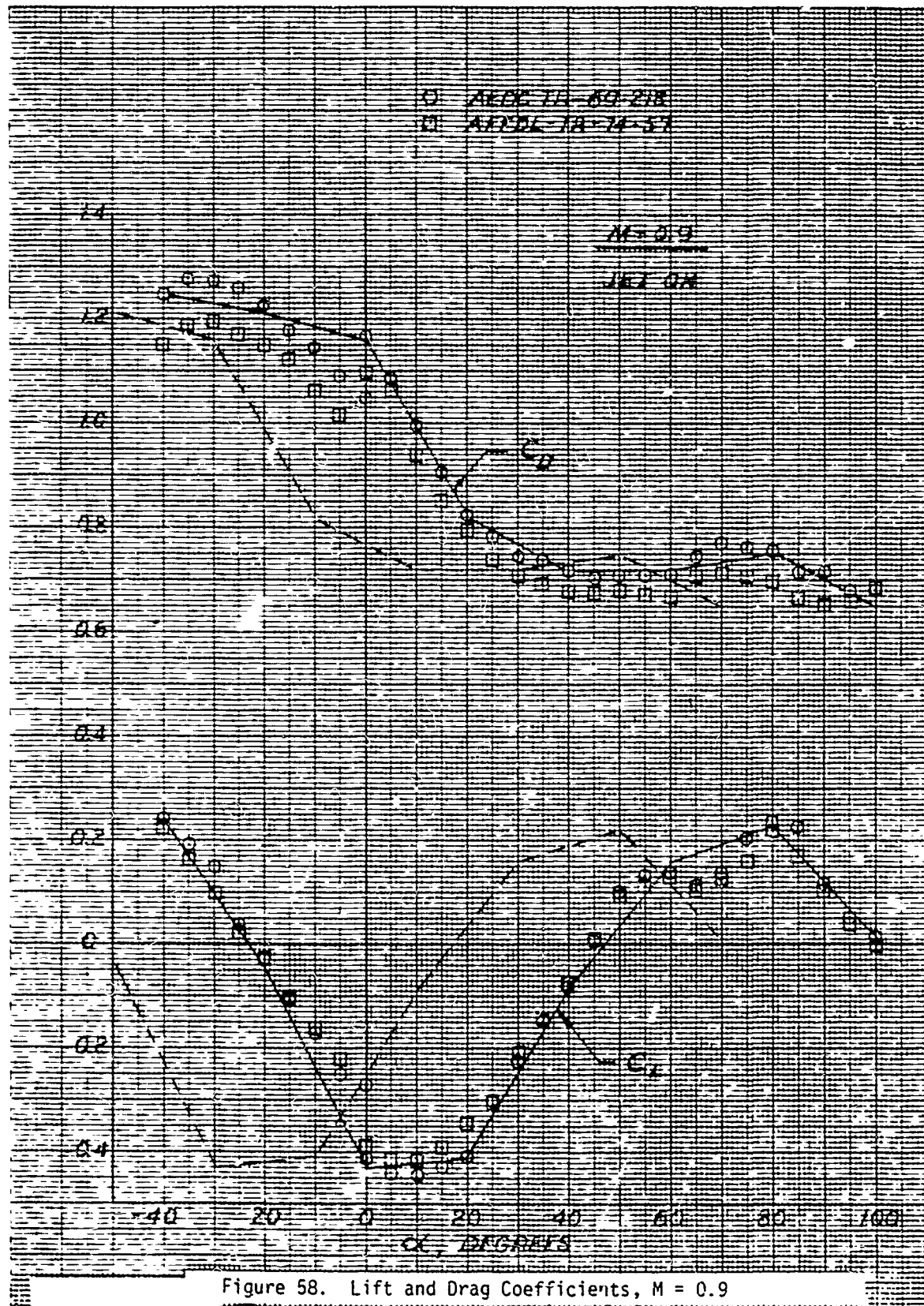


Figure 57. Lift and Drag Coefficients,  $M = 0.6$





Past work with the H5HC program has required reduction of the negative lift coefficients to about 20 percent of their original values to simulate actual test trajectories for the ACES II ejection seat. Additional evidence for negative lift reduction near the aircraft fuselage is shown in Figure 59. These preliminary data were obtained from wind tunnel test data of the B-1 Division of Rockwell International as part of the ACES II/B-1 test program. An increment of +0.2 in normal force coefficient,  $C_N$ , is indicated up to 6 feet from the fuselage. The data shown are for the rocket-off condition. The  $C_L$  data of Figures 57 and 58 are multiplied by a factor of 0.2 for this study.

Some reduction in drag is shown near the fuselage and would be beneficial in reducing spinal loading. This effect is not used for the present study due to the uncertainty of application to fuselage configurations different than that of the B-1 aircraft. The H5HC program uses the rail/ejection axis as a basis for pitch and angle-of-attack computation. When the form of the seat is rotated with respect to rails, the coefficients are shifted accordingly. With the seat rotated 30 degrees aft of the rails, the  $C_L$  and  $C_D$  data are displaced -30 degrees as shown by the dashed line of Figures 57 and 58. This shift is used for all cases in the parametric study.

In summary of the aerodynamic drag coefficient situation, the shifted  $C_D$  varies between 0.65 and 0.75 in the angle-of-attack range from 0 to 70 degrees encountered in the parametric study. This essentially flat trend indicates that rail and thrust angle effects are relatively independent of angle-of-attack variations.

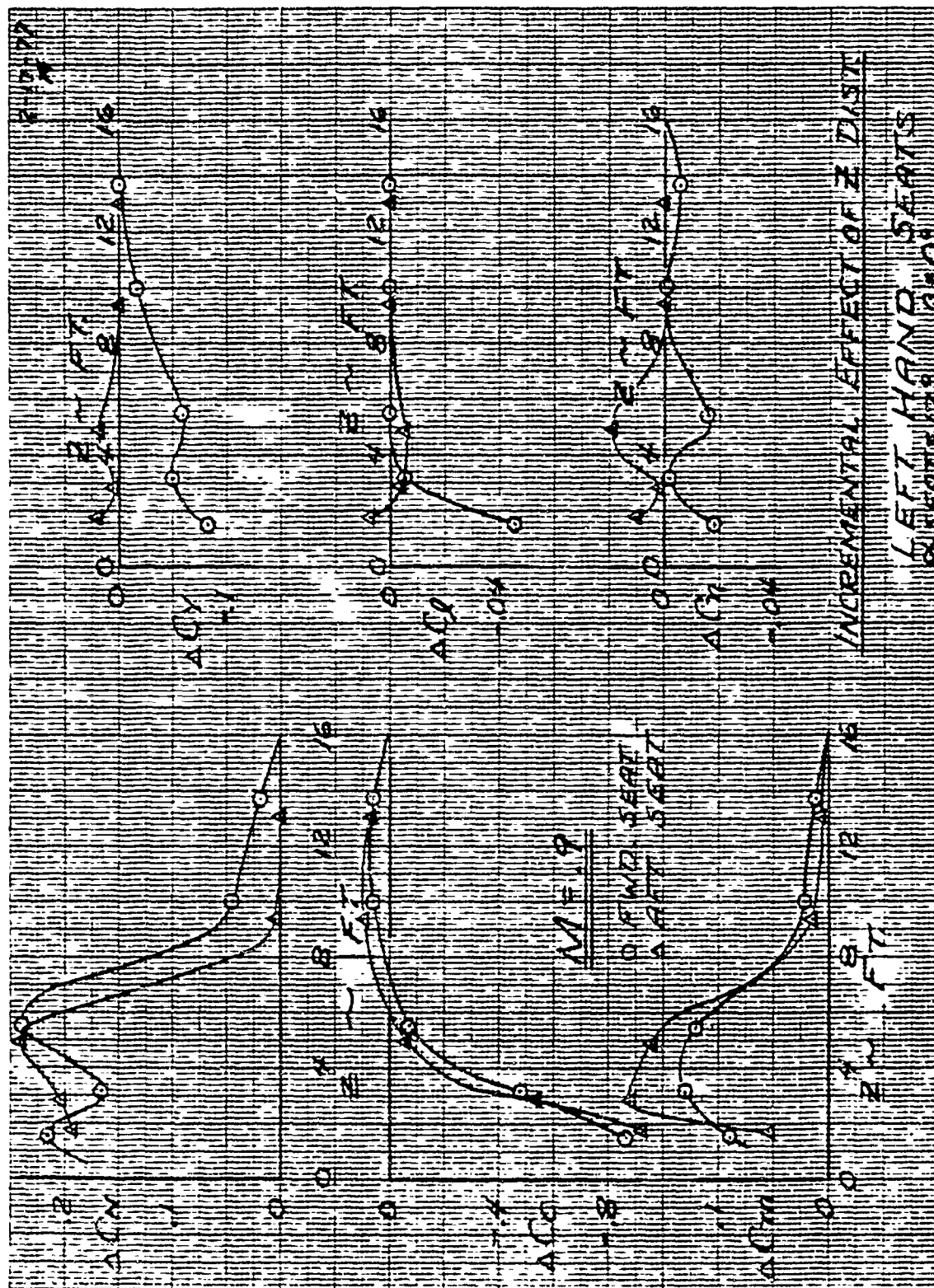


Figure 59. ACES/B1 Seat Test Data

The 20 percent factor reduces lift to a range of about  $\pm 1$  G. The effects of lift on spinal forces are analyzed by means of acceleration vector diagrams for variations in rail, seat-back and rocket thrust vector angles.

The 600 - KEAS condition results in a Mach number of 0.91 at sea level. At 30,000 feet altitude, Mach number is 1.67. There is an increase in drag coefficient of 10 to 15 percent from  $M = .9$  to  $M = 1.5$  resulting in a corresponding increase in drag for the same equivalent airspeed.

The F-15 airplane at 30,000 feet requires an angle-of-attack of 24 degrees at 600 KEAS to maintain 10  $G_z$  load factor. At this altitude the aircraft fuselage tends to blanket the seat with resulting reduction of dynamic pressure and drag force. The magnitude of this reduction is not known but drag will be less under such conditions than at lower angles of attack at low altitudes. In addition, the vertical component of drag with respect to the aircraft increases with angle-of-attack and is more effective in propelling the seat away from the aircraft under the +10  $G_z$  condition. Study of tail clearance trajectories at high angle-of-attack conditions is of little value in the parametric study without precise data on aerodynamic coefficients in this regime.

### 3.6 ATTITUDE CONTROL

ACES II high-speed test data have shown that the seat can rotate in pitch as much as 30 degrees forward or 40 degrees aft before drogue control of pitch attitude becomes effective. These motions are caused by seat tip-off forces and aero pitch instability. Forward or aft direction is determined by center of gravity and pressure differences for varying crew percentile sizes.

Drogue parachute effects are not used in the study in order to determine trajectory variations due to seat aero forces alone. Large seat attitude variations are eliminated from the parametric study by setting aerodynamic pitching moments to zero and by placing centers of gravity and pressure on the rocket thrust centerline. Pitch rates from seat tip-off are controlled by the STAPAC pitch control system. Seat attitudes during rocket burning are held to an average angle near the rail angle. An alternate approach of eliminating all pitch motions and fixing seat attitude at rail angle is not used. The tip-off/STAPAC control approach provides better simulation of High-G escape systems.

### 3.7 ATTITUDE/TIME HISTORIES

Figures 60-A and -B show pitch and angle-of-attack time histories for a 30-degree rail angle with 150 percent rocket thrust. The excess of aft aero moment over forward thrust moment causes an aft tip-off which is controlled by the STAPAC system until burnout. The seat then pitches at the constant rate prevailing at burnout.

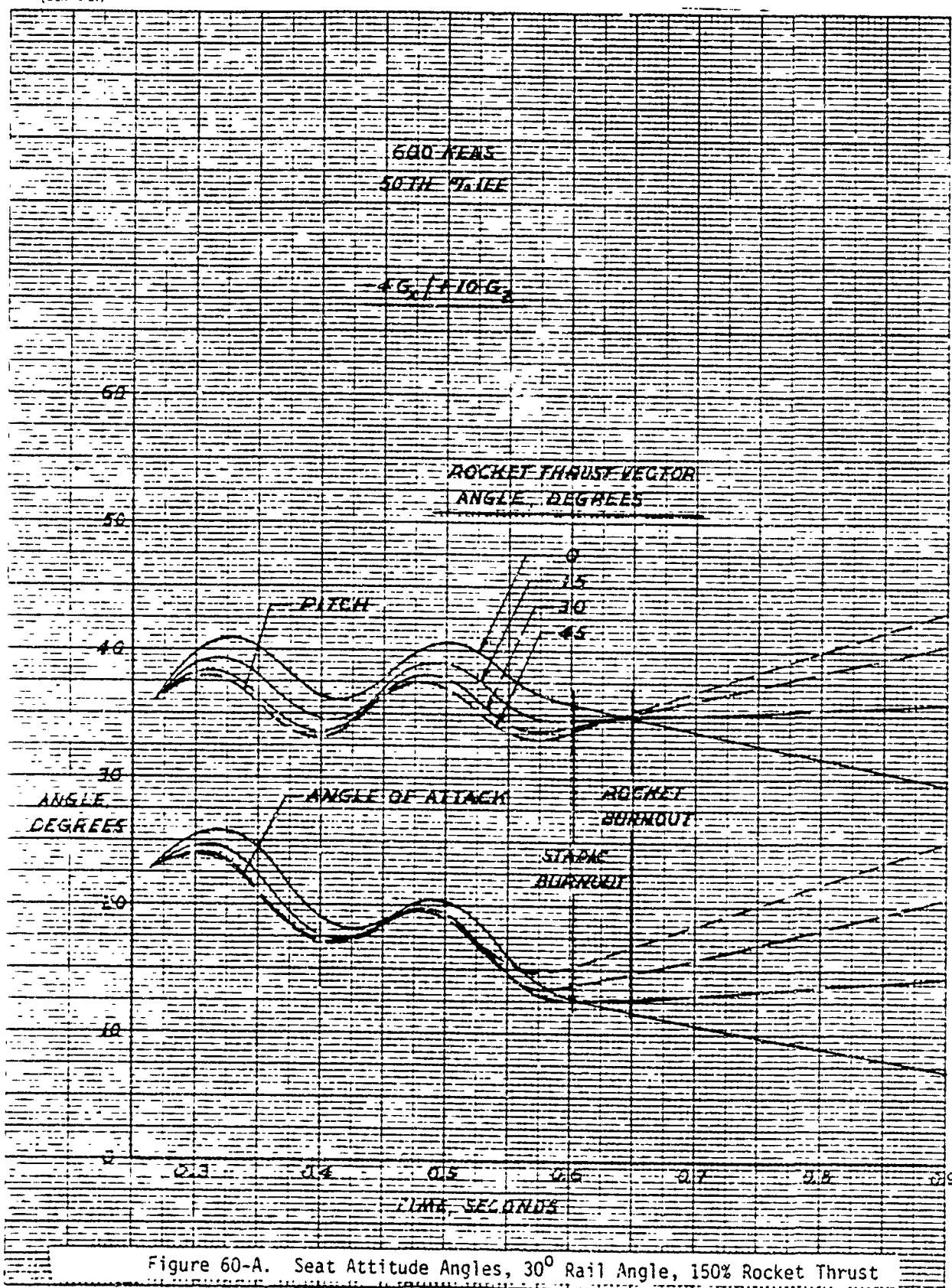


Figure 60-A. Seat Attitude Angles, 30° Rail Angle, 150% Rocket Thrust

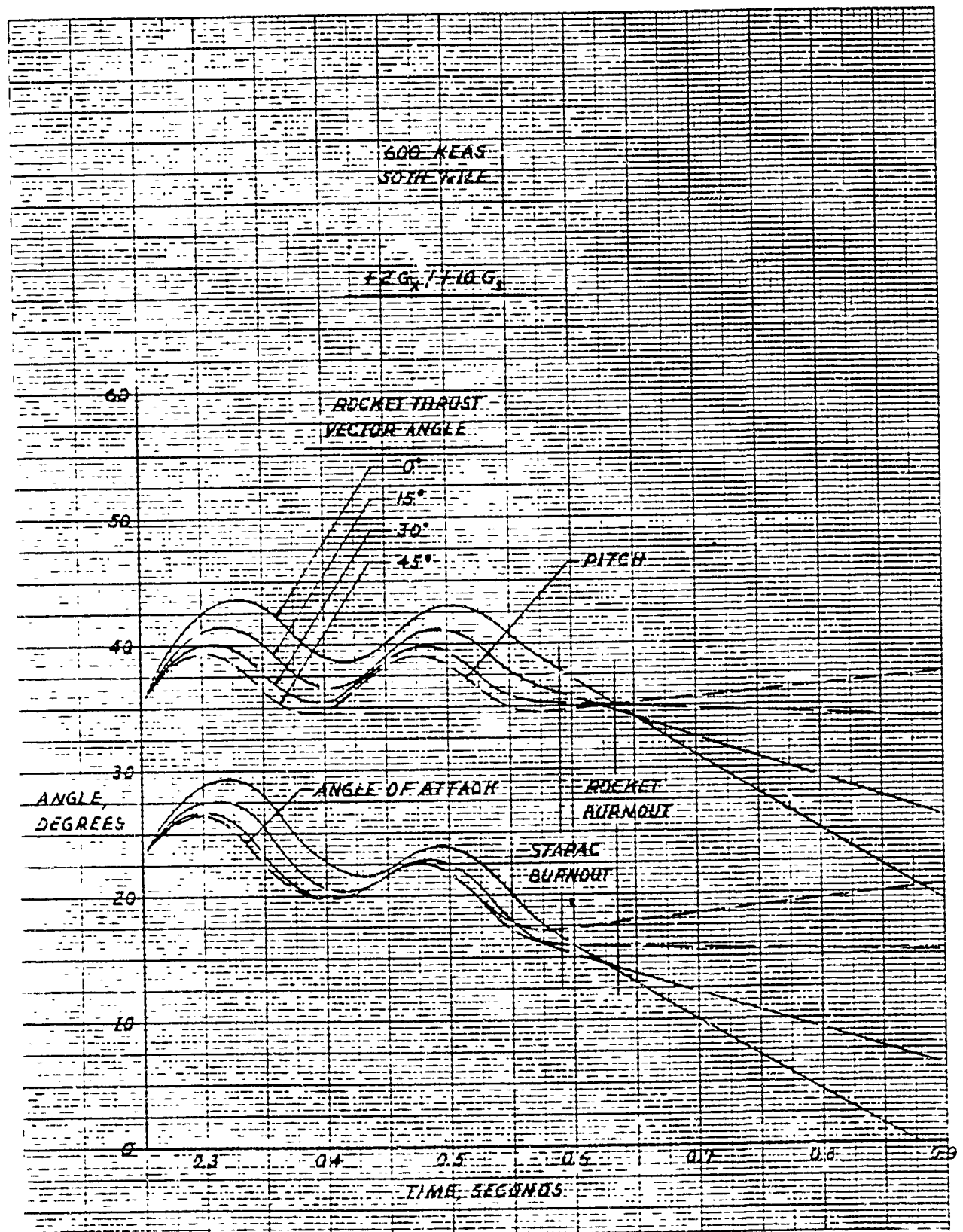


Figure 60-8. Seat Attitude Angles, 30° Rail Angle, 150% Rocket Thrust



Control of seat attitude by extending STAPAC burn-time beyond rocket burnout is not used in the study. The relatively constant nature of the aero coefficient curves previously shown in Figures 57 and 58 do not produce significant changes in aero forces and correspondingly small changes in the flight path at varying angles-of-attack. Rocket burnout usually occurs just before or during the time that the seat is over the tail for trajectories with adequate tail clearance. The remainder of the trajectory does not affect tail clearance.

Aft tip-off is greater for the +2  $G_x$ /10  $G_z$  case. The higher speed at seat aircraft separation results in an increase of aero moment over thrust moment. The decrease in aft tip-off as thrust vector is inclined forward is a result of increasing thrust moment over aero moment.

Figures 61-A and -B show attitude time histories for the 30 degree rail angle with 200 percent rocket thrust. Tip-off rates and angles are lower because of the increased thrust. For the -4  $G_x$  condition, the tip-off rate for the 45-degree case is too low to cause STAPAC nozzle movement, resulting in the lack of oscillation shown.



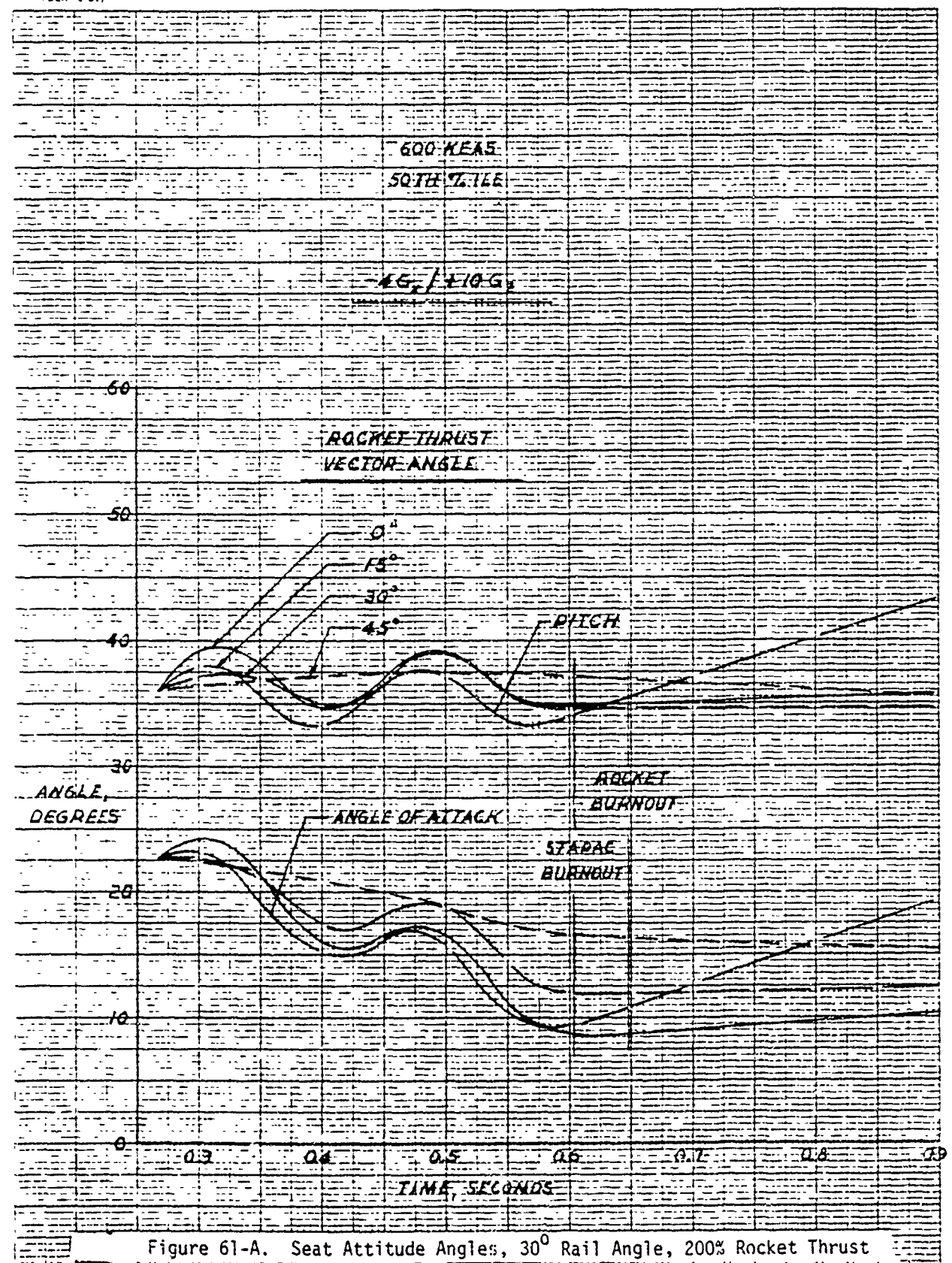


Figure 61-A. Seat Attitude Angles, 30° Rail Angle, 200% Rocket Thrust

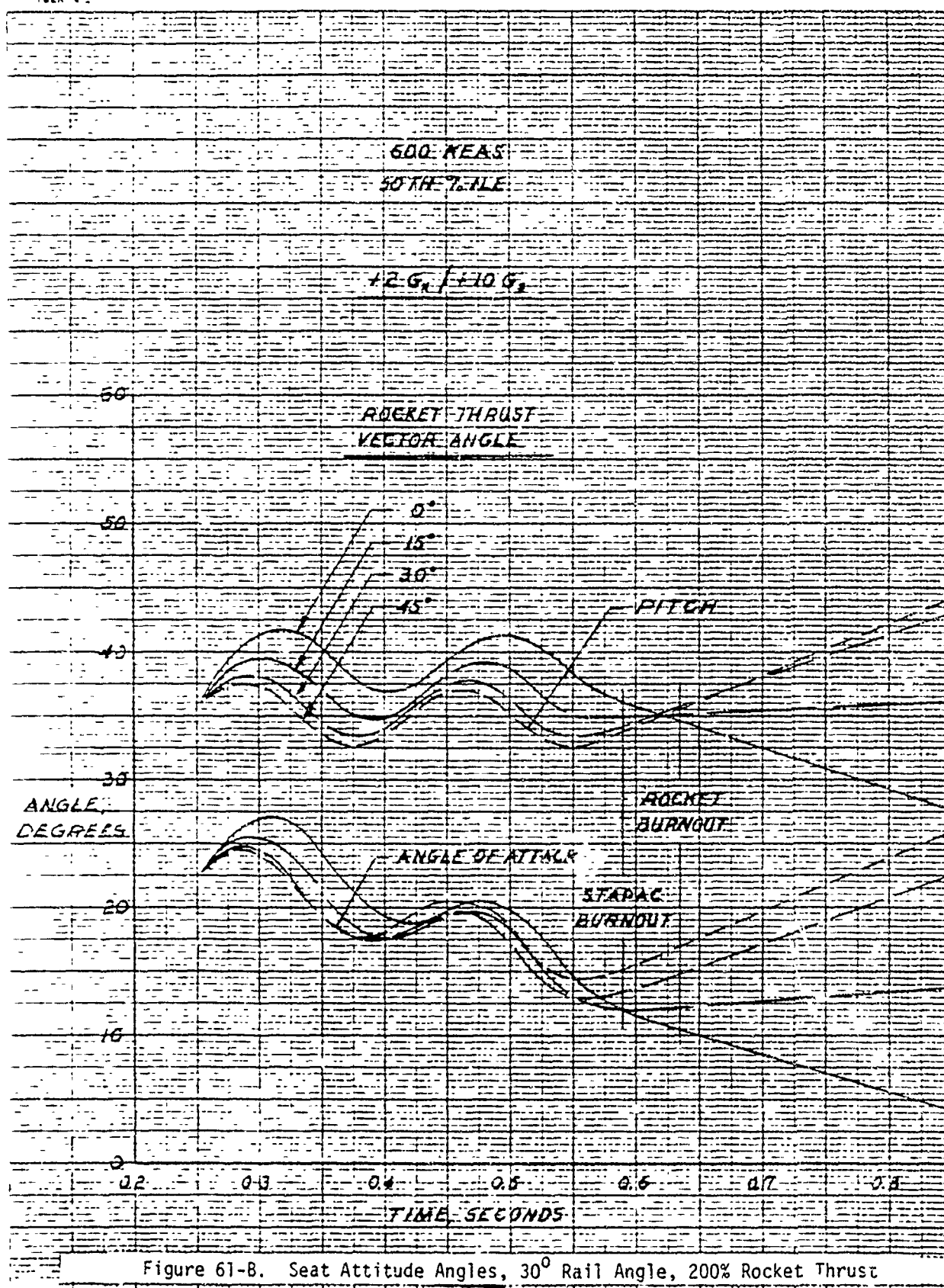


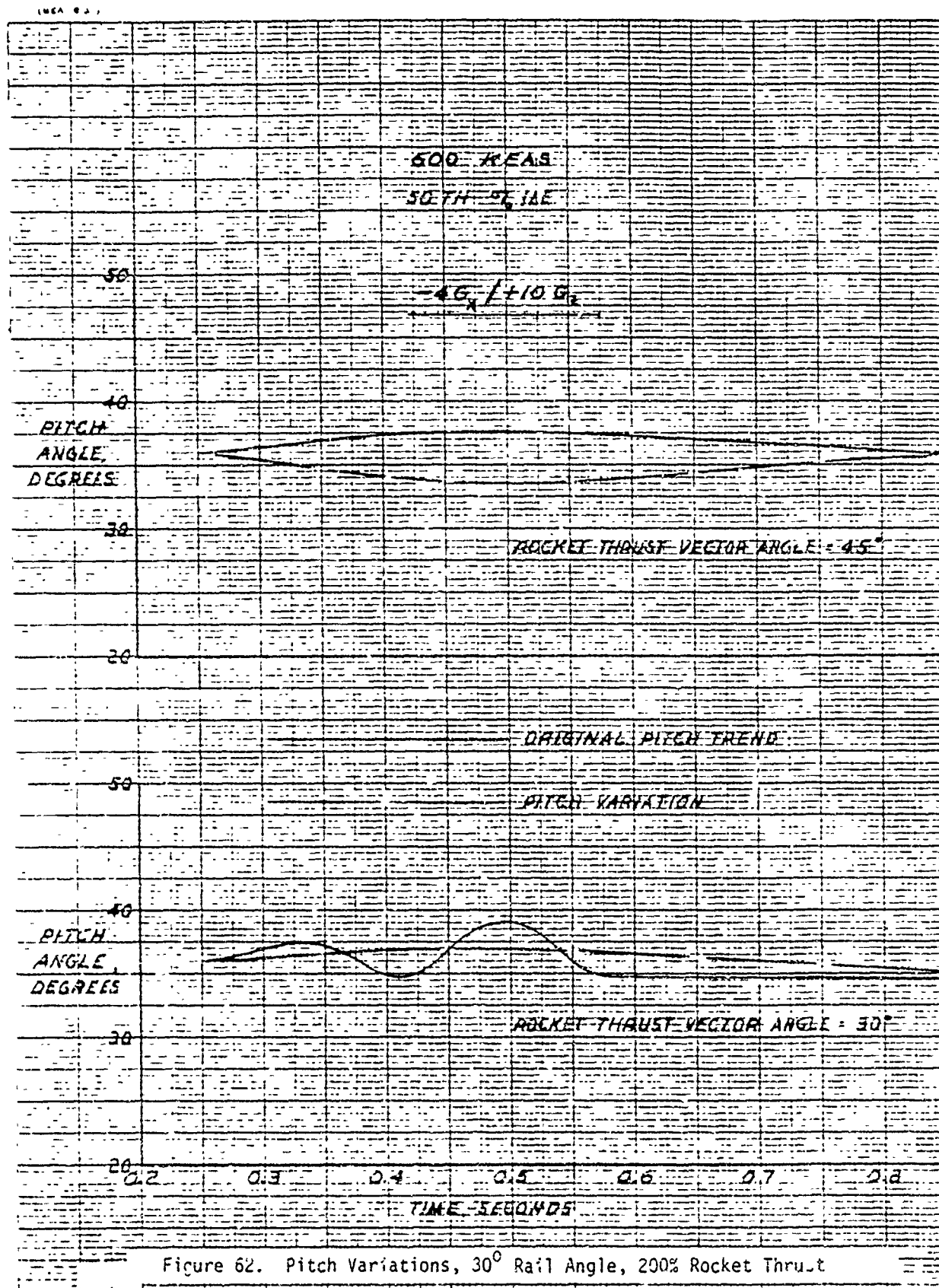
Figure 61-B. Seat Attitude Angles, 30° Rail Angle, 200% Rocket Thrust

### 3.8 PITCH VARIATIONS

The effect of a small change in tip-off rate on pitch time history is shown in Figure 62 for the 200 percent rocket thrust level. The solid lines indicate the trends for 30 and 45 degree rocket thrust vector cases previously shown in Figure 61-A at  $-4 G_x$ . The dashed curves result from a small change in speed reducing aerodynamic forces sufficiently to lower tip-off rates.

The corresponding trajectories are shown in Figure 63. In the 45-degree thrust vector angle case, the more forward pitch of tip-off causes a steeper trajectory with decreased height in the vicinity of the tail. At a thrust vector angle of 30 degrees, STAPAC is not activated and a pitch variation trend without oscillation results.

A range of thrust vector angles between 30 and 45 degrees defines the critical tail clearance region for a 30 degree rail angle under  $-4 G_x$  conditions. This holds true for the higher rail angles studied. The trajectories at these thrust vector angles indicate that changes in pitch produce changes in the trajectory equivalent to those caused by the vector angle. A design thrust vector angle of 30 degrees which pitches forward 15 degrees will have a steep, low trajectory similar to that of the 45 degree thrust vector angle. Pitch control or control of thrust vector orientation in space is necessary to prevent undesirable forward inclination of the thrust vector.



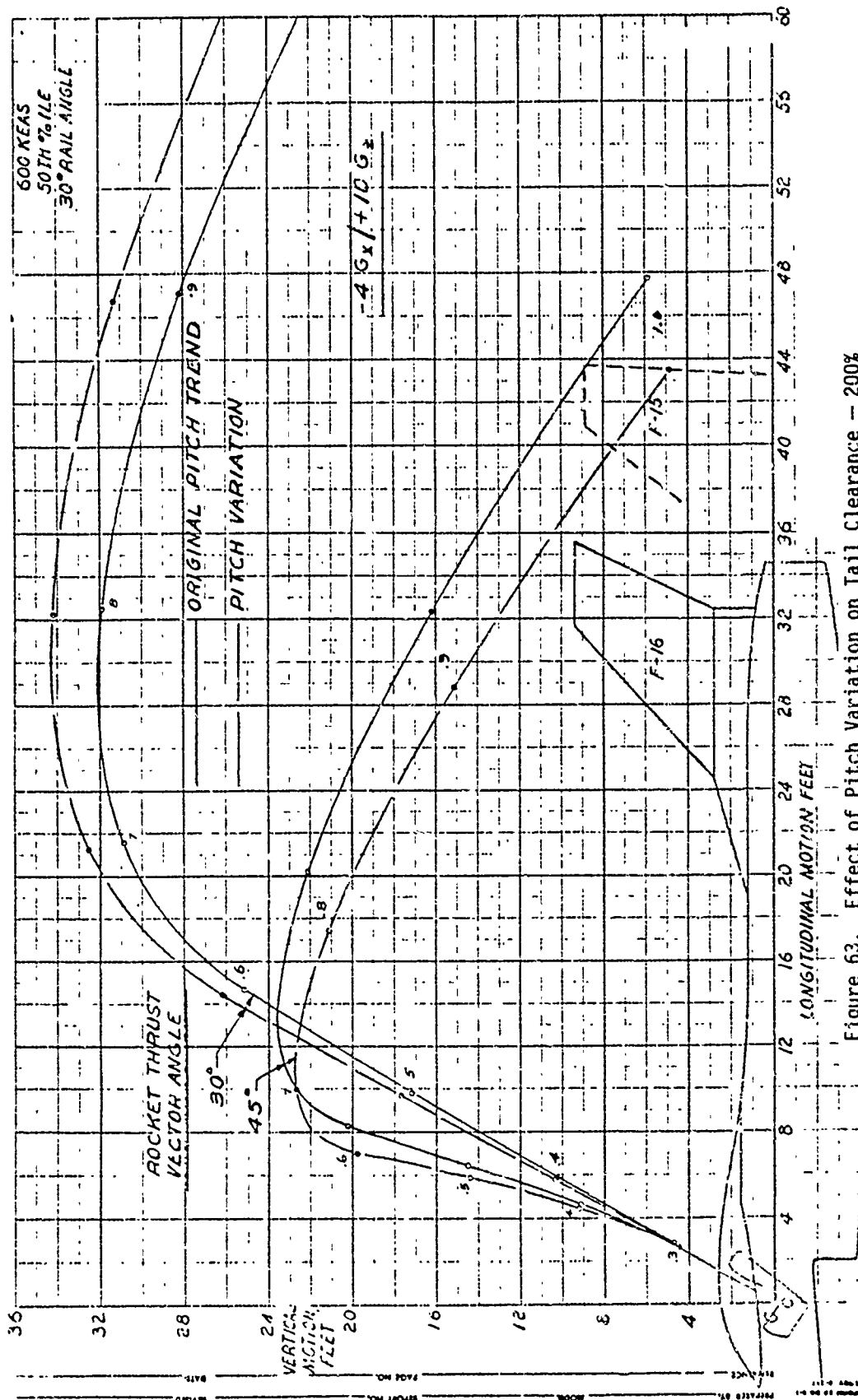


Figure 63. Effect of Pitch Variation on Tail Clearance - 200% Rocket Thrust

### 3.9 AIRCRAFT $G_x$ EFFECT

Tail Clearance trajectories for the 200 percent rocket thrust level are shown in Figure 64 for thrust vectors of 30 and 45 degrees. Trajectories for the zero  $G_x$  condition are with a catapult thrust level of 17.8 G. The trends of 0 and +2  $G_x$  are similar. The -4  $G_x$  case remains critical for tail clearance, while the +2  $G_x$  case with maximum aero forces is critical for spinal loads.

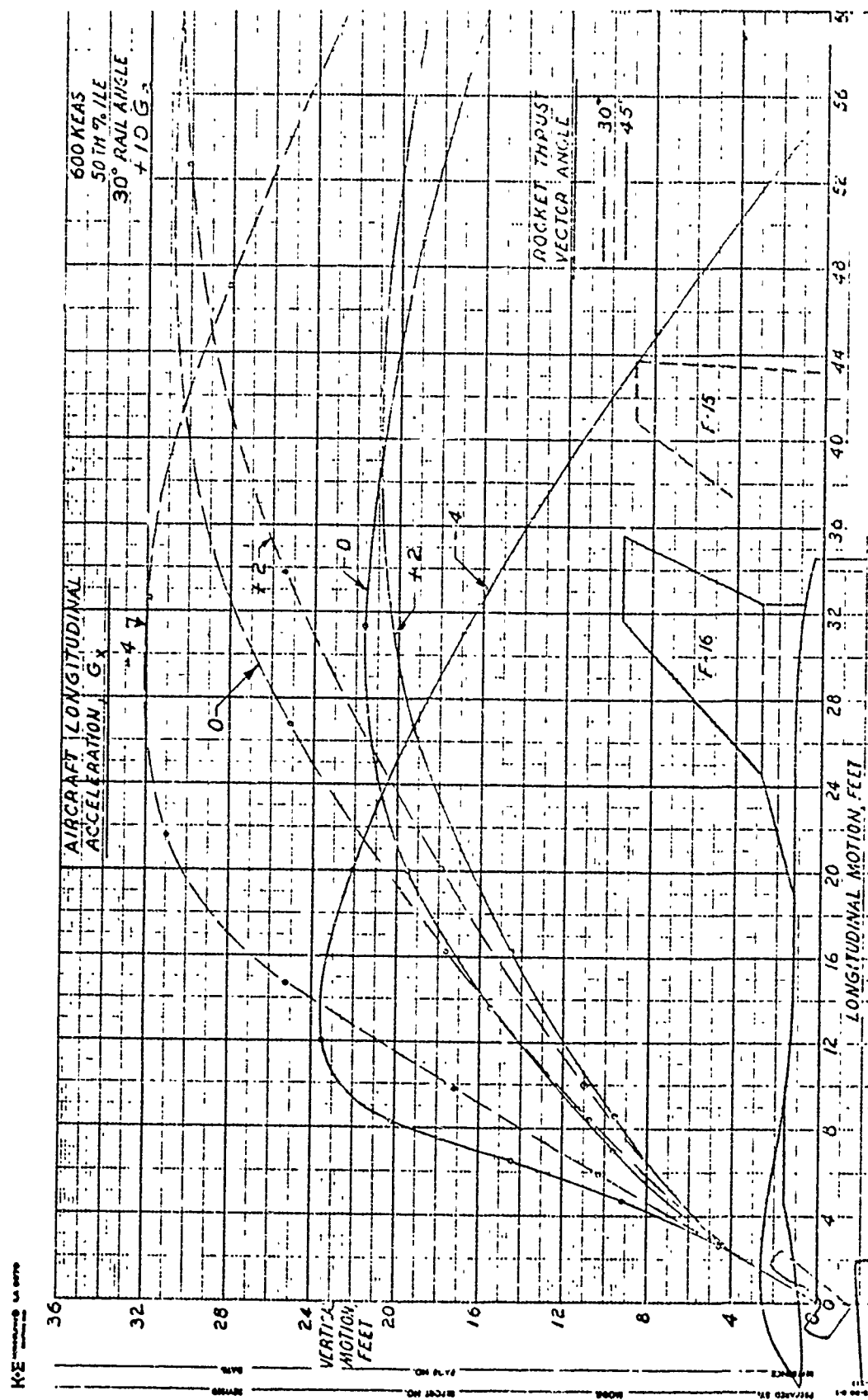


Figure 64. Parametric Trajectories, 30° Rail Angle, 200% Rocket Thrust, Effect of Aircraft  $G_x$

SECTION IV  
FIFTEEN DEGREE RAIL ANGLE

4.1 TRAJECTORIES

Figures 65-A and -B show trajectories for a rail angle of 15 degrees with 200 percent rocket thrust. Tail clearance is adequate except for a rocket thrust vector angle of 45 degrees under  $-4 G_x$  conditions.

This trajectory is a typical example of the effect of excessive forward thrust vector inclination. The increased forward thrust component more effectively opposes drag while the aircraft is decelerating at  $-4 G_x$ . Vertical acceleration of the seat due to rocket force is low compared with the upward  $+10 G_z$  aircraft acceleration. As a result the rocket phase of the trajectory is steep and low. Rocket thrust begins to fall off at about 0.54 seconds and rocket burn-out occurs at 0.65 seconds. The seat is then driven aft by aerodynamic forces and the  $+10 G_z$  vertical aircraft acceleration causes the aircraft to move rapidly towards the seat resulting in seat/tail interference.



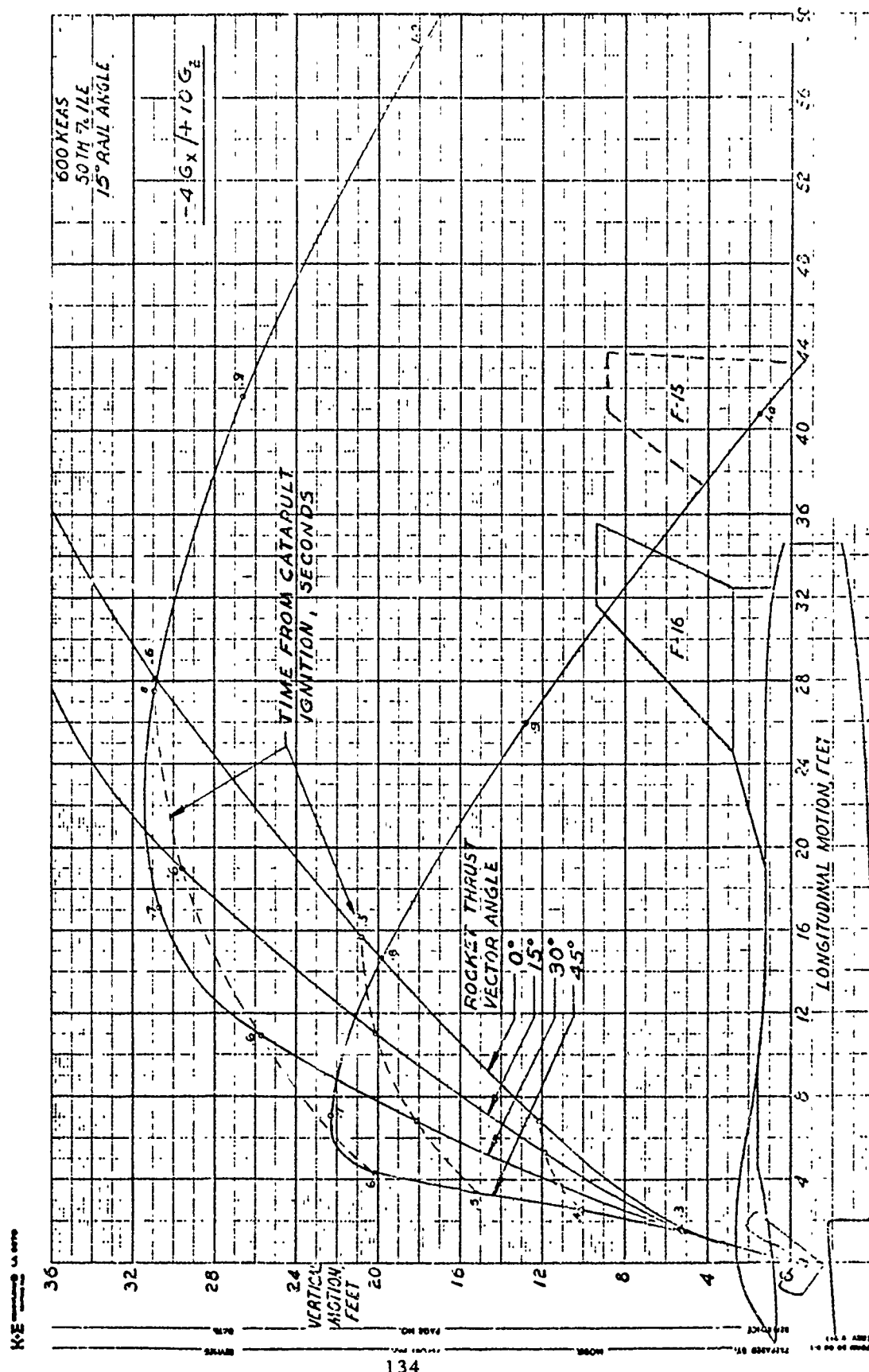


Figure 65-A. Parametric Trajectories, 15° Rail Angle, 200% Rocket Thrust



## SECTION V

### THIRTY DEGREE RAIL ANGLE

#### 5.1 ACCELERATION VECTORS

Figure 66 shows thrust and aerodynamic acceleration vectors for 30 degree rail angle at 150 percent rocket thrust at the time of seat/aircraft separation. STAPAC thrust and gravity vectors are eliminated to simplify the presentation. The STAPAC thrust equivalent of 2.1 G is nearly vertical at this point and the resultant vector is not significantly affected. The  $+2 G_x$  condition results in the highest spinal force, with the 17.1 g value at or near maximum for a DRI of 18. Higher drag results from increased speed at seat/aircraft separation. This condition exists for all rail angles. Positive lift increases, and negative lift decreases, spinal loads at a ratio of about 0.6 G of load per G of lift.

Figure 67 shows acceleration vectors for the 30 degree rail angle with 200 percent rocket thrust. Vectors are plotted in the aircraft coordinate system. Thrust vector angles below 30 degrees result in components along the spinal axis greater than the 17.0 G maximum for a DRI limit of 18. Thrust vector angles forward of the perpendicular to the spine reduce spinal loads. The aircraft acceleration condition of  $+2 G_x$ , produces maximum speed at seat/aircraft separation and determine the lower limit of usable thrust vector angles.

#### 5.2 TRAJECTORIES

Figures 68-A and -B show tail clearance trajectories for the 150 percent thrust level. At  $-4 G_x$ , the 30 degree thrust vector trajectory is marginal and the 45 degree trajectory is unacceptable. For  $+2 G_x$ , the 45 degree trajectory is marginal. All other cases provide adequate tail clearances.

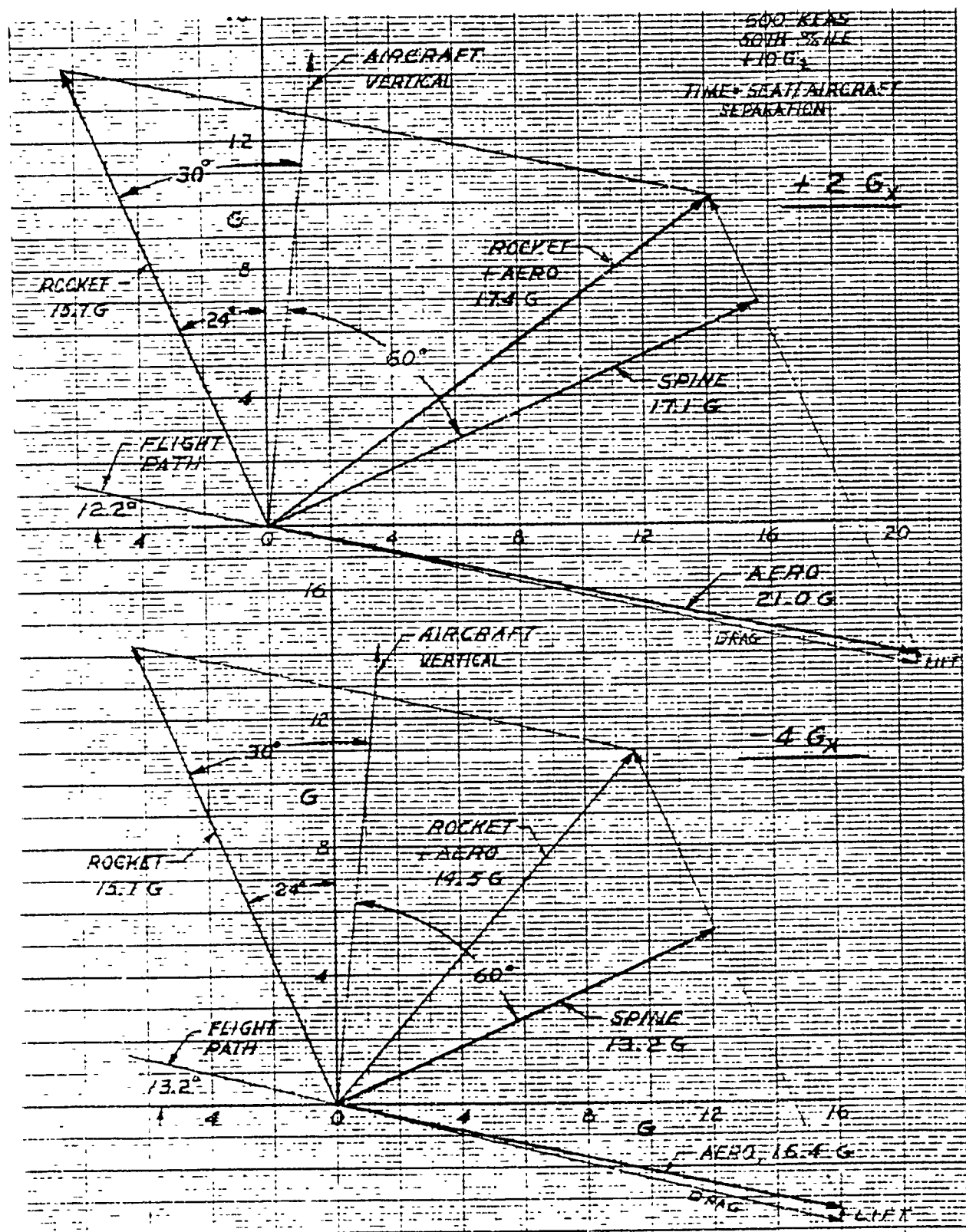


Figure 66. Acceleration Vectors, 30° Rail Angle, 150% Rocket Thrust

600 KEAS  
50TH 7.1LE  
30° RAIL ANGLE

$\pm 2 G_x / +10 G_z$

TIME = SEAT/AIRCRAFT SEPARATION

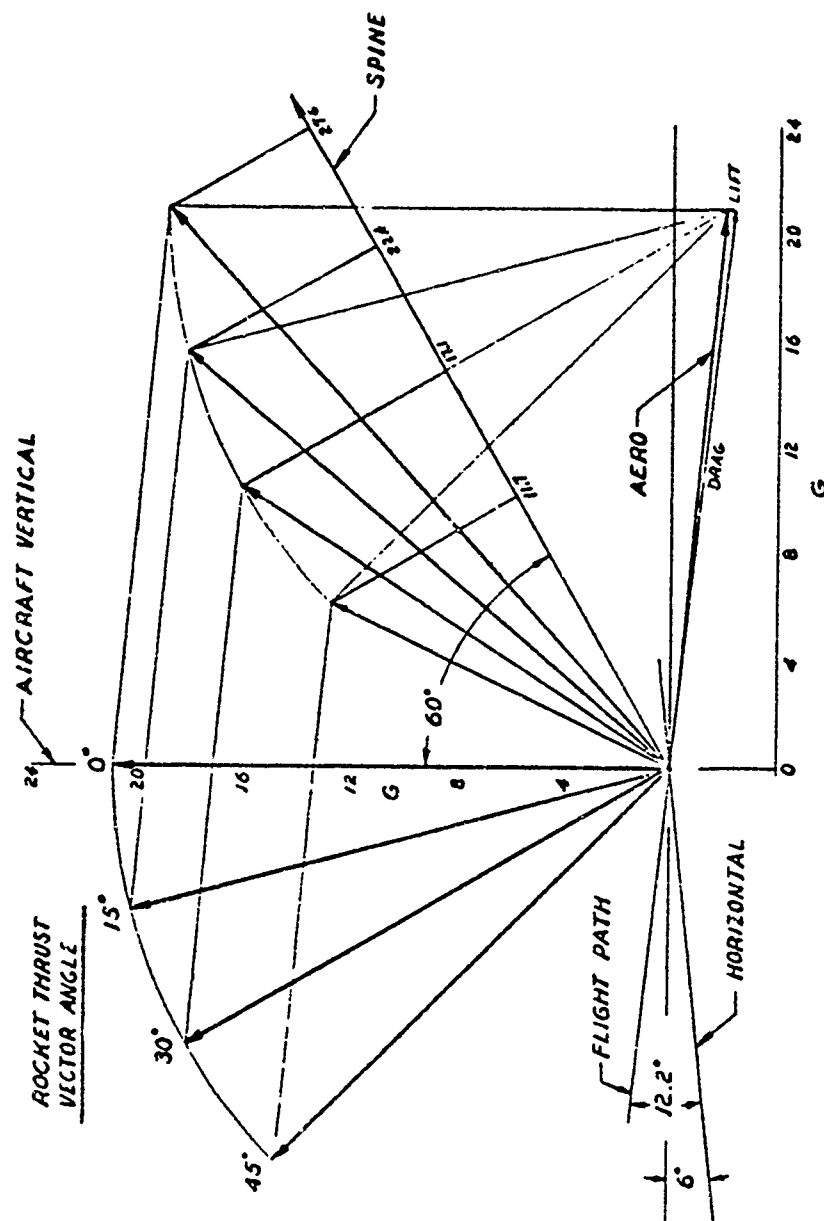


Figure 67. Acceleration Vectors, 30° Rail Angle, 200% Rocket Thrust

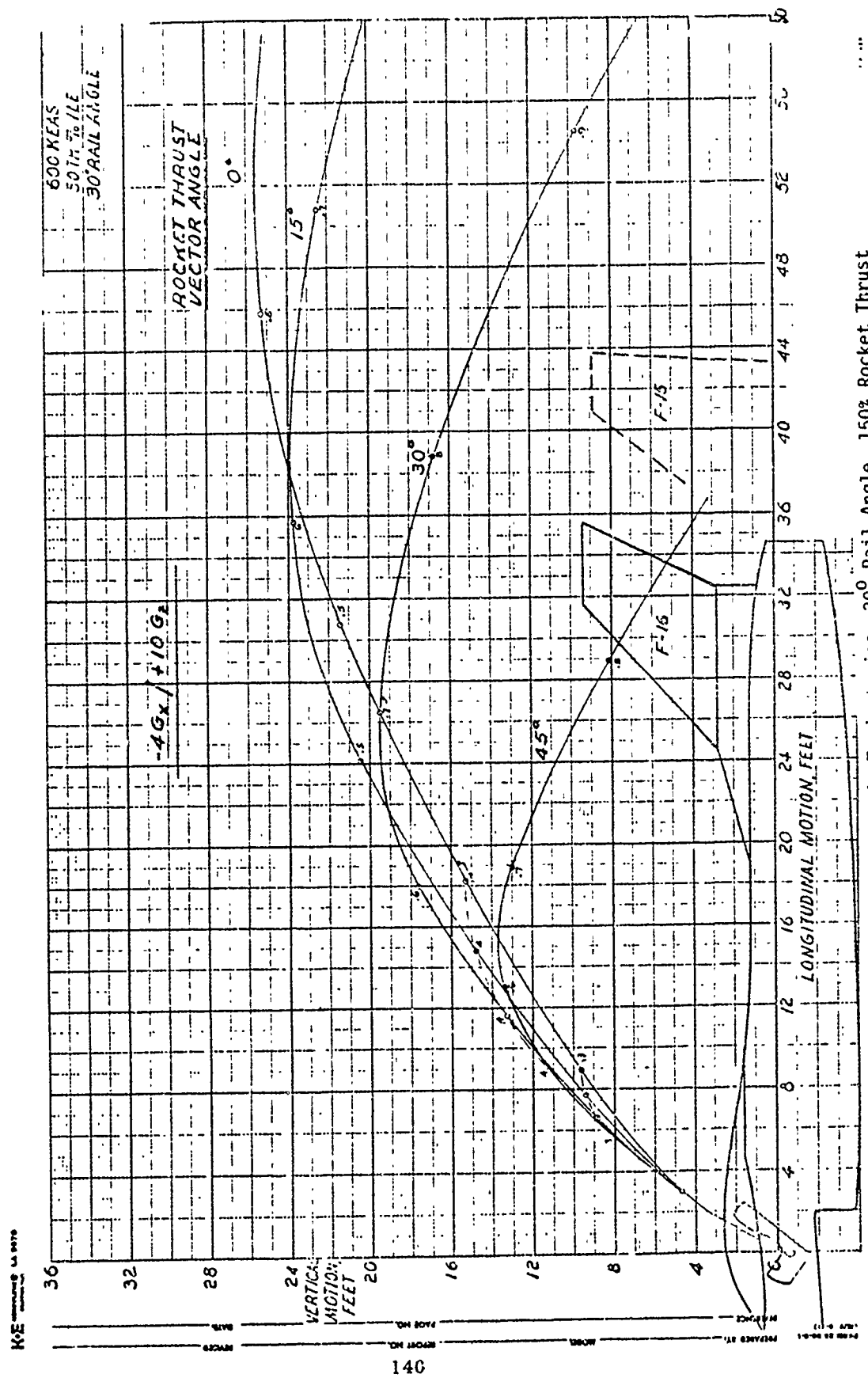


Figure 68-A. Parametric Trajectories, 30° Rail Angle, 150% Rocket Thrust



Figures 69-A and -B show trajectories for the 200 percent rocket thrust level. Tail clearance trends are similar to those shown for the 15 degree rail angle, with some improvement evident for the 30 degree rail angle. The  $-4 G_x$  trajectories are characterized by considerable sensitivity to rocket thrust vector angle while the  $+2 G_x$  trajectories remain relatively insensitive. The 45 degree thrust vector condition is critical for both acceleration conditions.

### 5.3 THRUST VECTOR ANGLES

Figure 70 shows the effects of rocket thrust vector angle on spinal force and tail clearance for the 150 percent rocket thrust level at a 30 degree rail angle and 60 degree spinal angle.

A longitudinal distance of 32 feet is used for the critical position of the upper leading edge of the F-16 vertical tail and 44 feet for the upper trailing edge of the F-15 vertical tail. A trajectory height of 14 feet is selected as a minimum for tail clearance at these two positions.

Spinal forces are maximum for the  $+2 G_x$  condition at seat/aircraft separation for the limited range of angle-of-attack experienced by the seat configuration. Maximum dynamic pressure and initial peak of the rocket thrust curve of Figure 56 are both encountered at this time. Approximately 80 milliseconds later rocket thrust has decreased to the constant level of Figure 56 and dynamic pressure has decreased, resulting in the lower spinal forces shown.

The limiting values of 17 G for spinal forces and 14 feet for tail clearance result in a narrow usable range of rocket thrust vector angles, at approximately 30 degrees, which will not accommodate normal thrust vector variations.



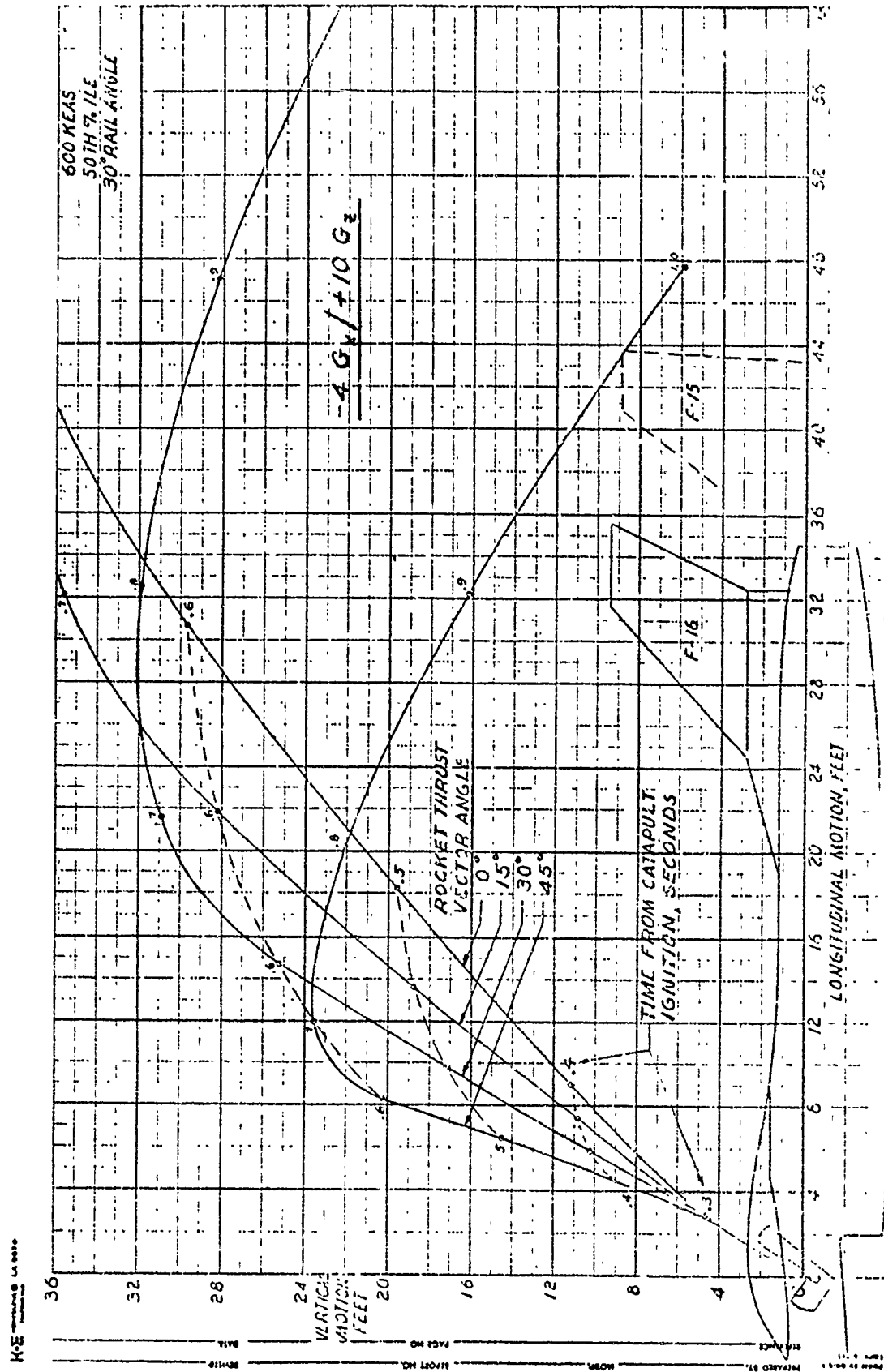


Figure 69-A. Parametric Trajectories, 30° Rail Angle, 200% Rocket Thrust

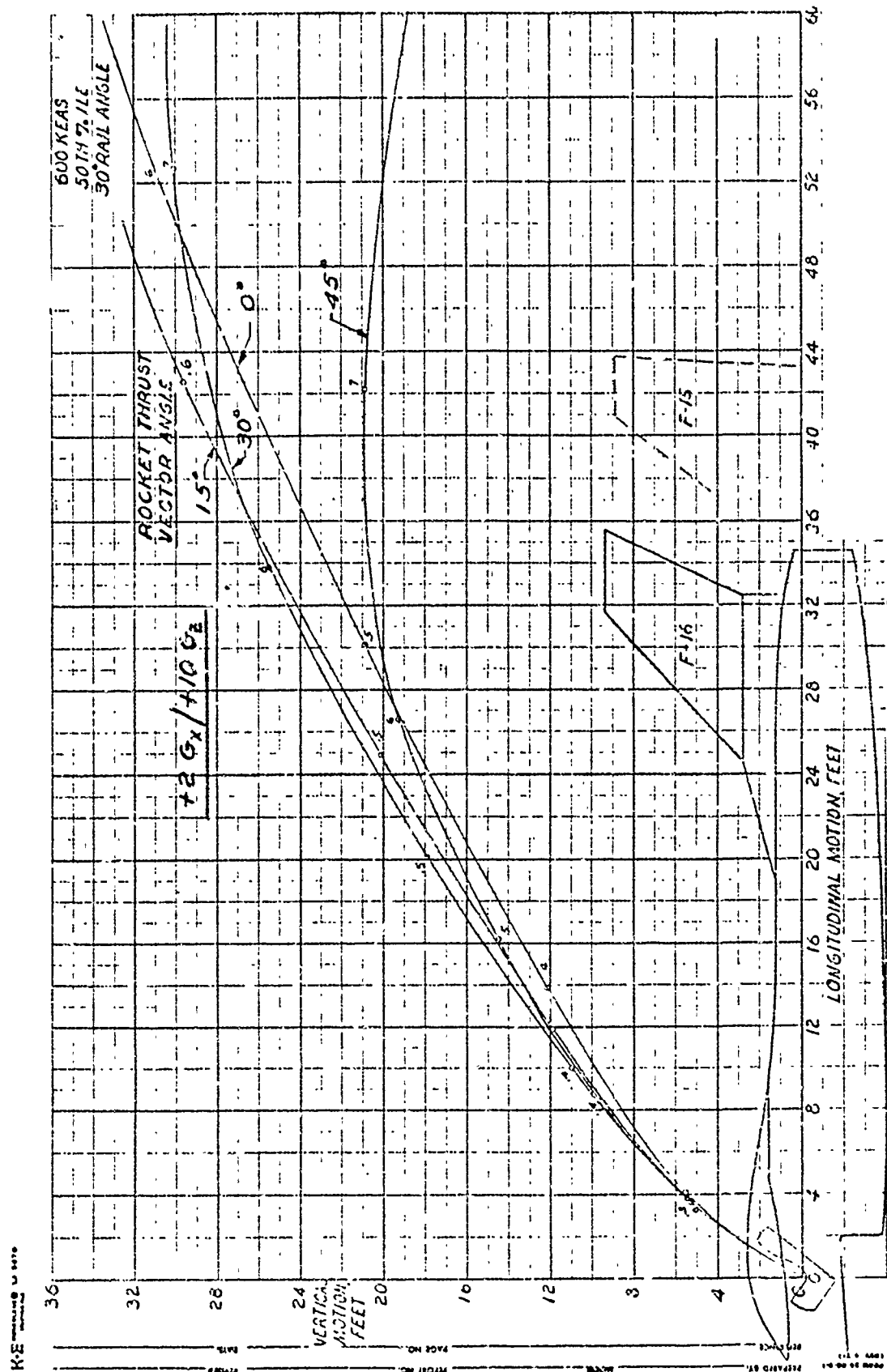


Figure 69-B. Parametric Trajectories, 30° Rail Angle, 200% Rocket Thrust

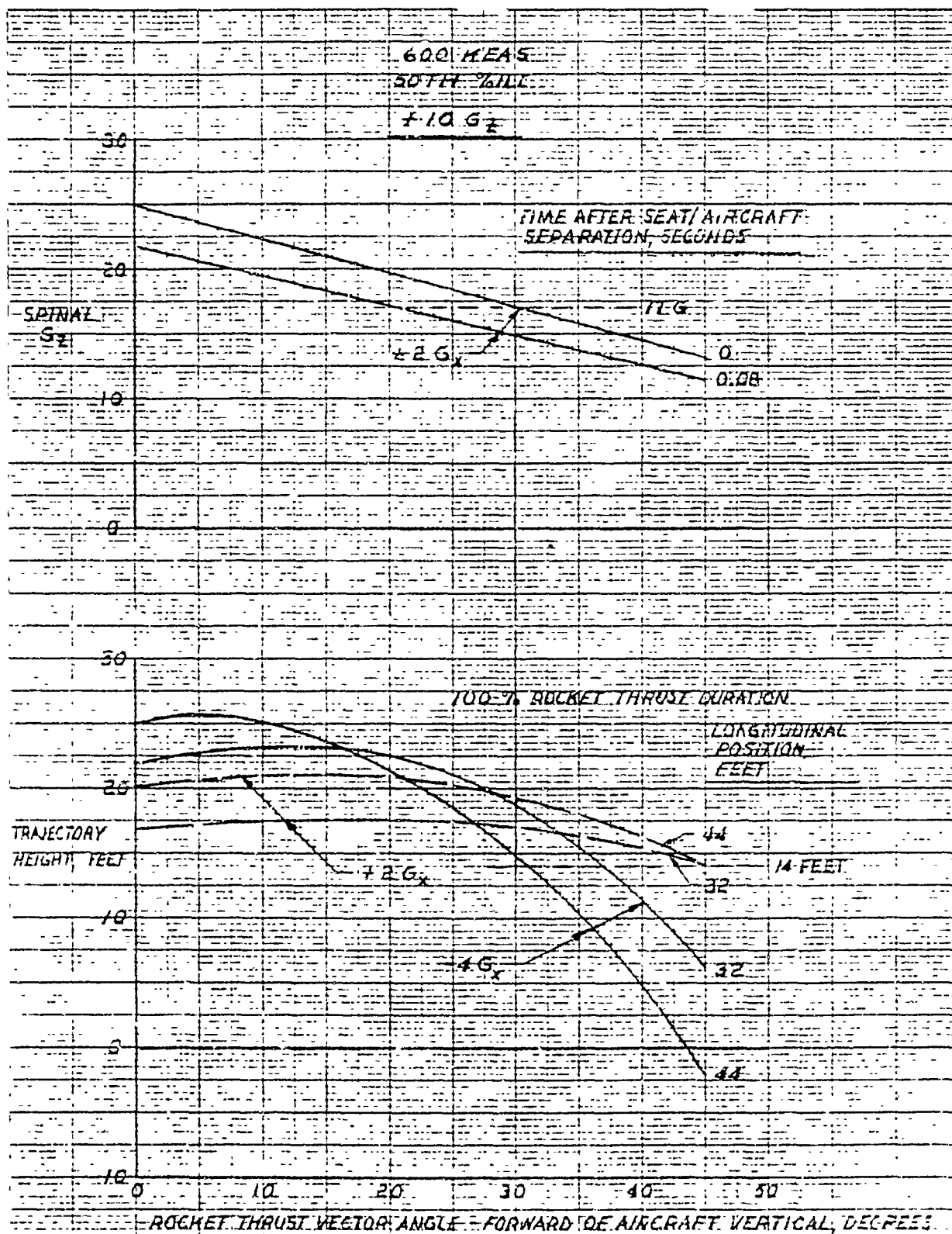


Figure 70. Tail Clearance and Spinal G<sub>z</sub>, 30° Rail Angle, 150% Rocket Thrust

Figure 71 shows similar trends for 200 percent rocket thrust. A theoretical band of about 12 degrees in thrust vector angle is available. The steep slope of the trajectory height curves in the 30 - 45 degree region indicate that the upper thrust vector angle limit remains critical.

#### 5.4 INCREASED SPINAL ANGLE

Increased spinal angles reduce spinal loads and increase the usable range of thrust vector orientation. Investigation of trajectory effects for a 90 degree spinal angle requires articulation of the seat 60 degrees aft of the rail axis. A 34.0 G catapult with original burn duration results in a spinal component of 17.0 G. The 29.4 G component normal to the spine remains within the MIL-S-9479 limit of 30.0 G for spinal  $G_x$ . Peak acceleration is 16.6 G in 1-G level flight.

Rocket thrust at the 150 percent level is used due to the increase in catapult performance. Figure 72 shows the resulting trajectories for the  $-4 G_x/+10 G_z$  load condition. The trade off between rocket and catapult performance improves tail clearances only for the 45 degree thrust vector angles when compared to the trajectories shown in Figure 69-A. The resulting increase in usable thrust vector orientation range is from 10 to 42 degrees.

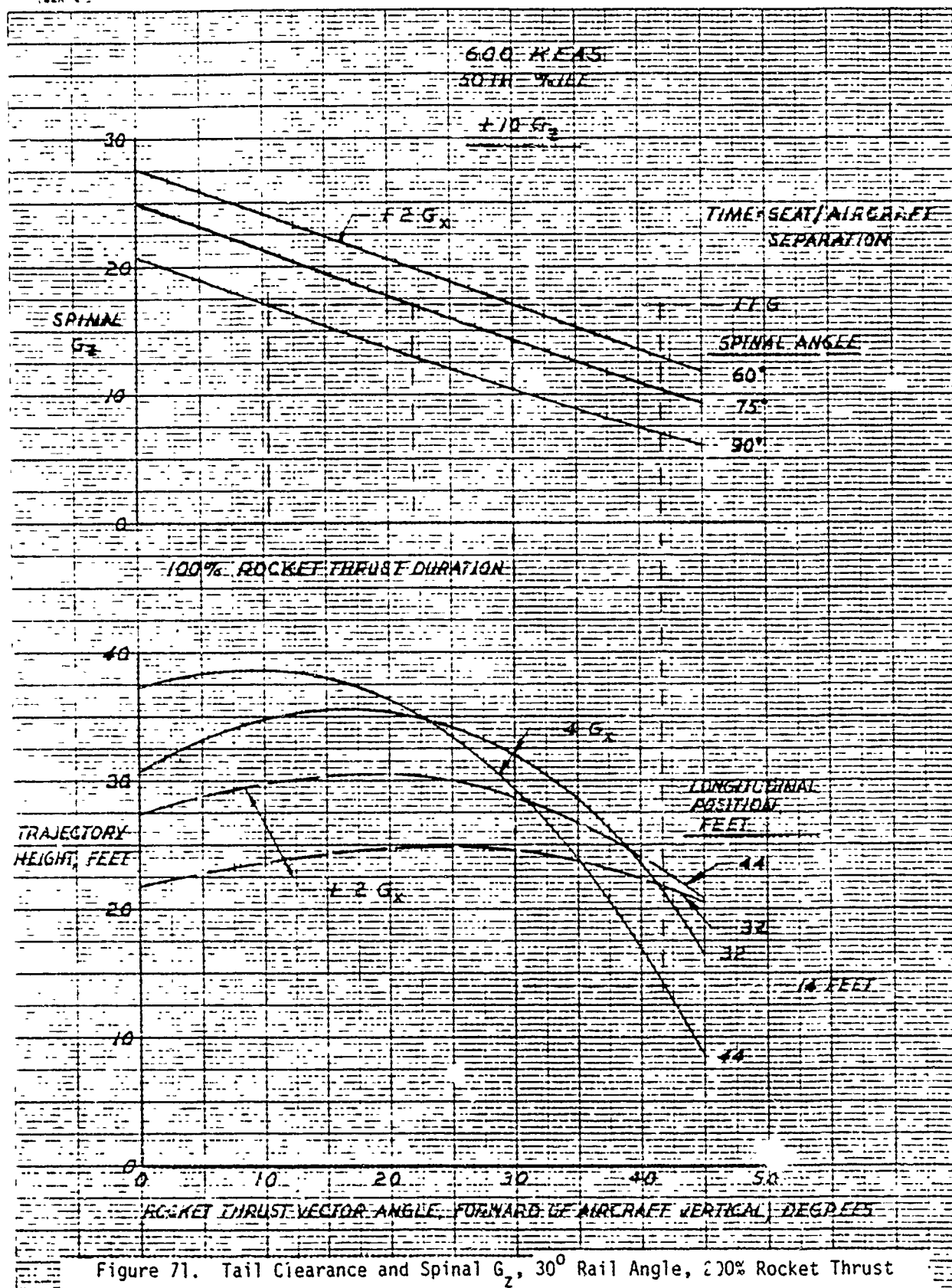


Figure 71. Tail Clearance and Spinal  $G_z$ , 30° Rail Angle, 100% Rocket Thrust

REPORT NO. 148

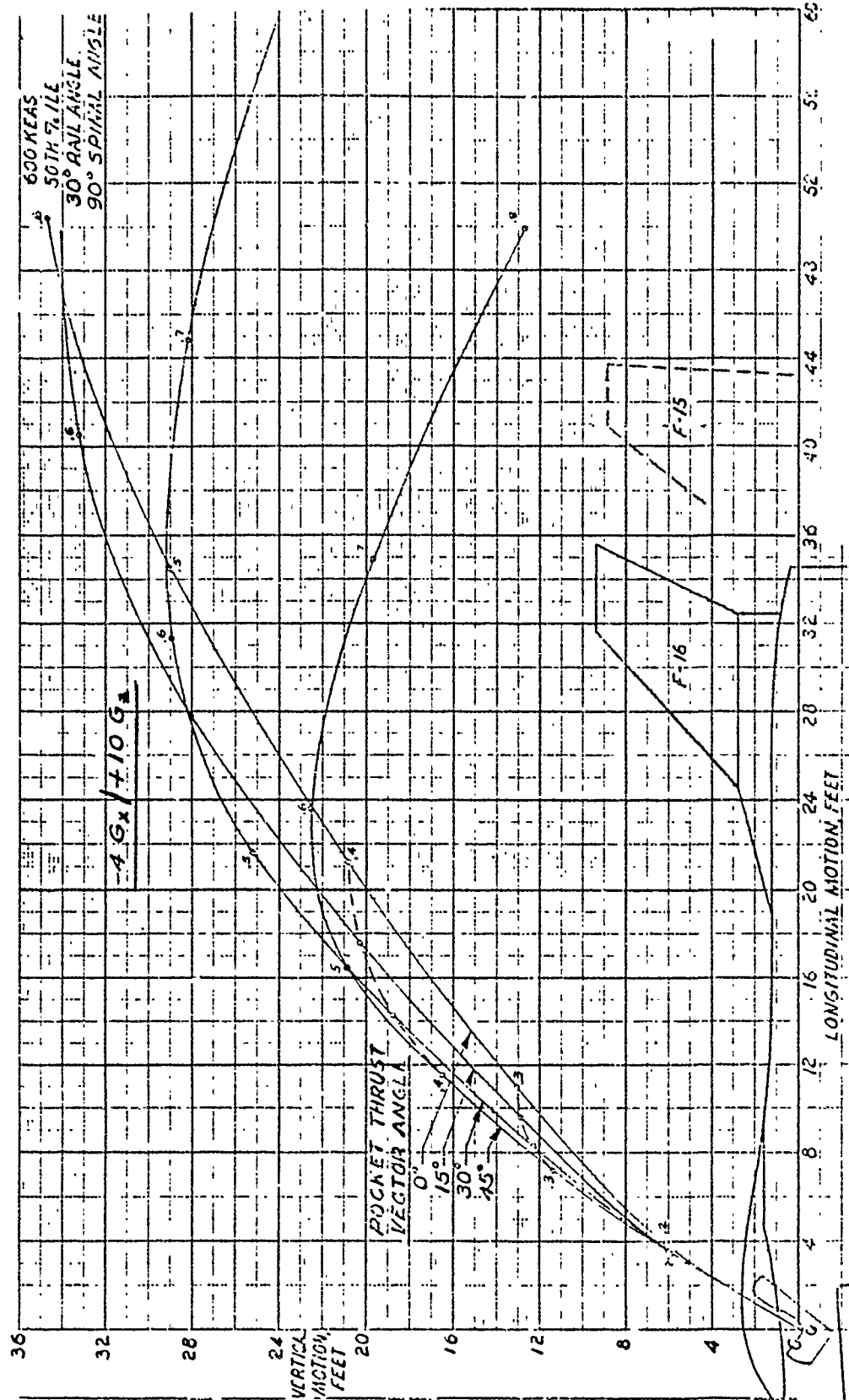


Figure 72. Parametric Trajectories, 30° Rail Angle, 150% Rocket Thrust, 34.0 G Catapult

## SECTION VI

### FORTY FIVE DEGREE RAIL ANGLE

#### 6.1 ACCELERATION VECTORS

Figure 73 shows acceleration vectors for the 45 degree rail angle, 75 degree spinal angle, with 200 percent rocket thrust.

#### 6.2 TRAJECTORIES

Figures 74-A and -B show trajectories for 200 percent rocket thrust. Under the  $-4 G_x$  conditions of Figure 74-A, tail clearance heights are adequate for all thrust vector angles except the 45 degree vector. Tail clearance height with a 30 degree thrust vector angle is lower than that shown in Figure 69-A for a 30 degree rail angle.

Tail clearance for all  $+2 G_x$  conditions is slightly improved for the 45 degree rail angle over that of the 30 degree rail.

#### 6.3 THRUST VECTOR ANGLES

Figure 75 shows the variation of tail clearance height and spinal  $G_z$  with rocket thrust vector angle. The range of potentially usable thrust vector angles is from 22 to 40 degrees with the 75 degree spinal angle or 30 degrees aft of the rail. An increase of 15 degrees in spinal angle to 90 degrees, provides a range of  $\pm 15$  degrees in usable thrust vector angles.

600 KEAS  
50 TH 9.1LE  
45° RAIL ANGLE

$+2G_x / +10G_z$

TIME = SEAT/AIRCRAFT SEPARATION

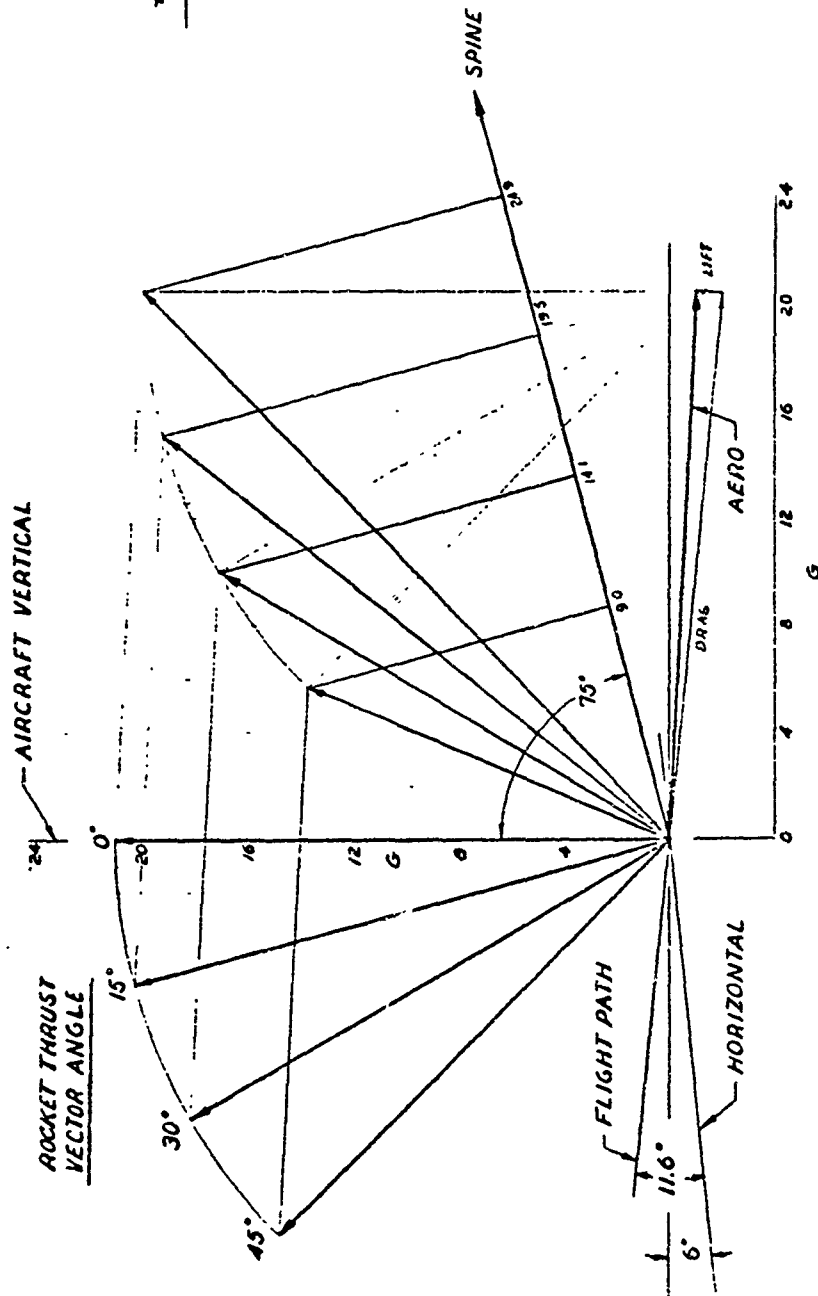
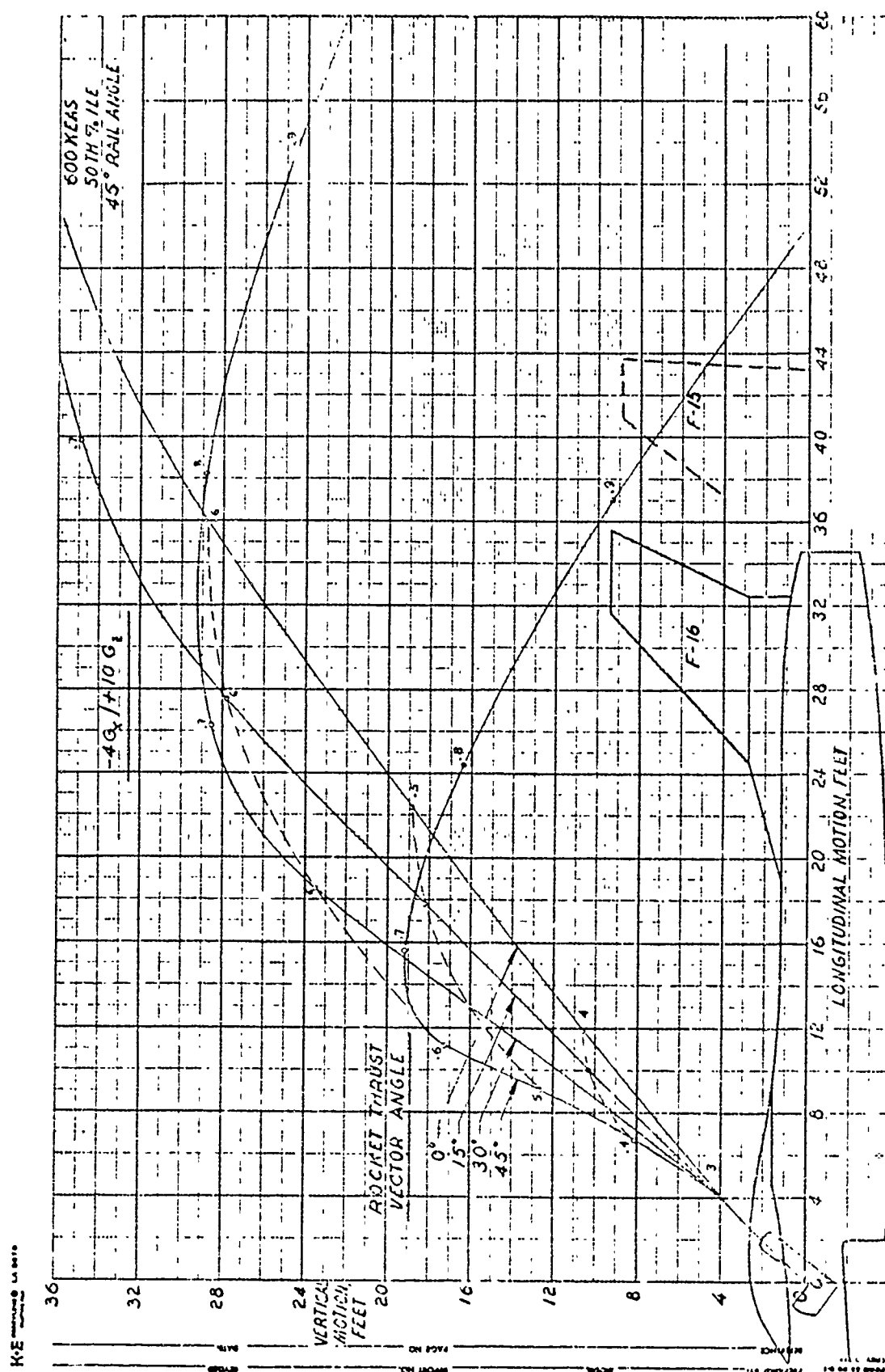


Figure 73. Acceleration Vectors, 45° Rail Angle, 200% Rocket Thrust





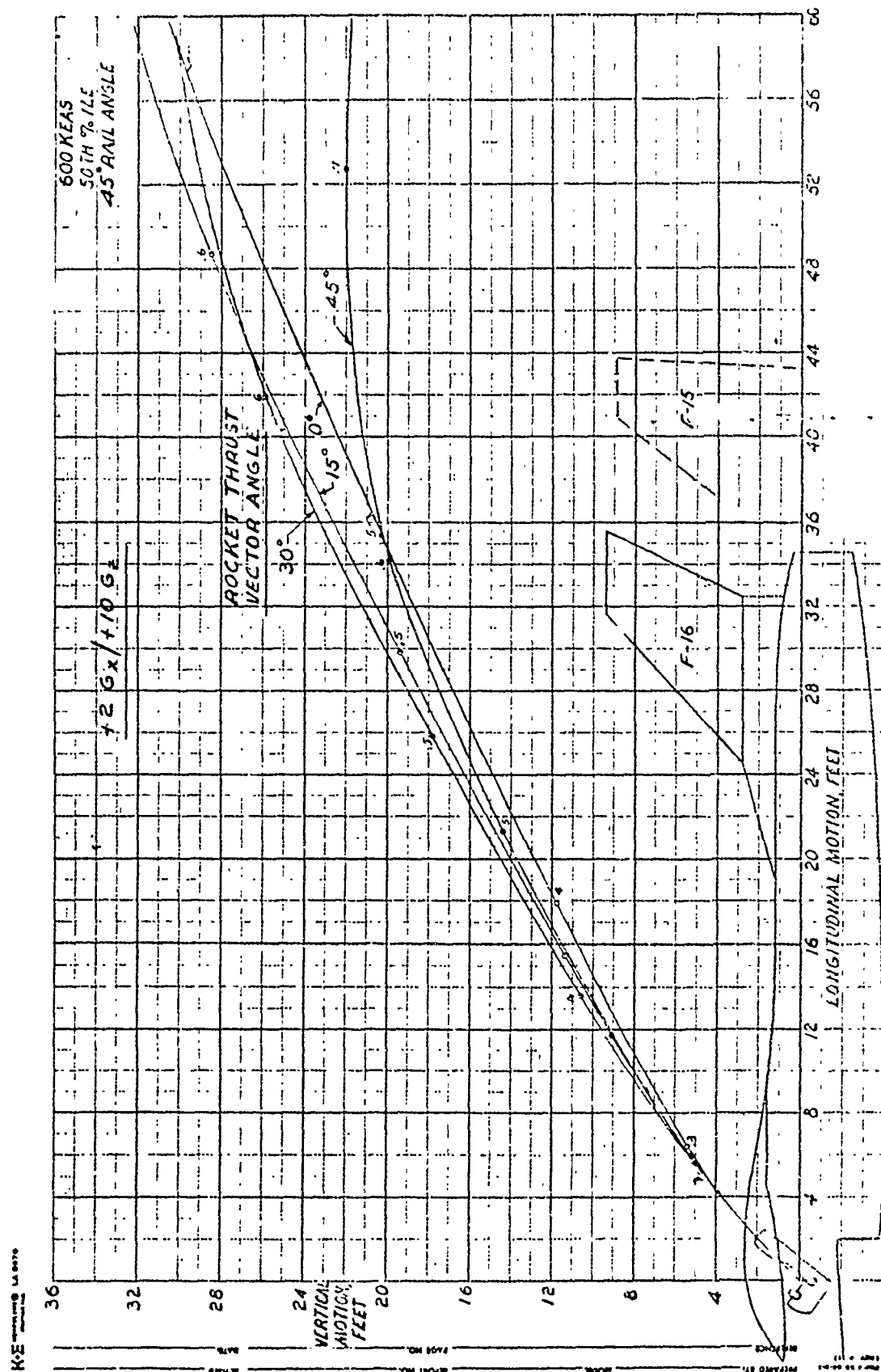


Figure 74-B. Parametric Trajectories, 45° Rail Angle, 200% Rocket Thrust

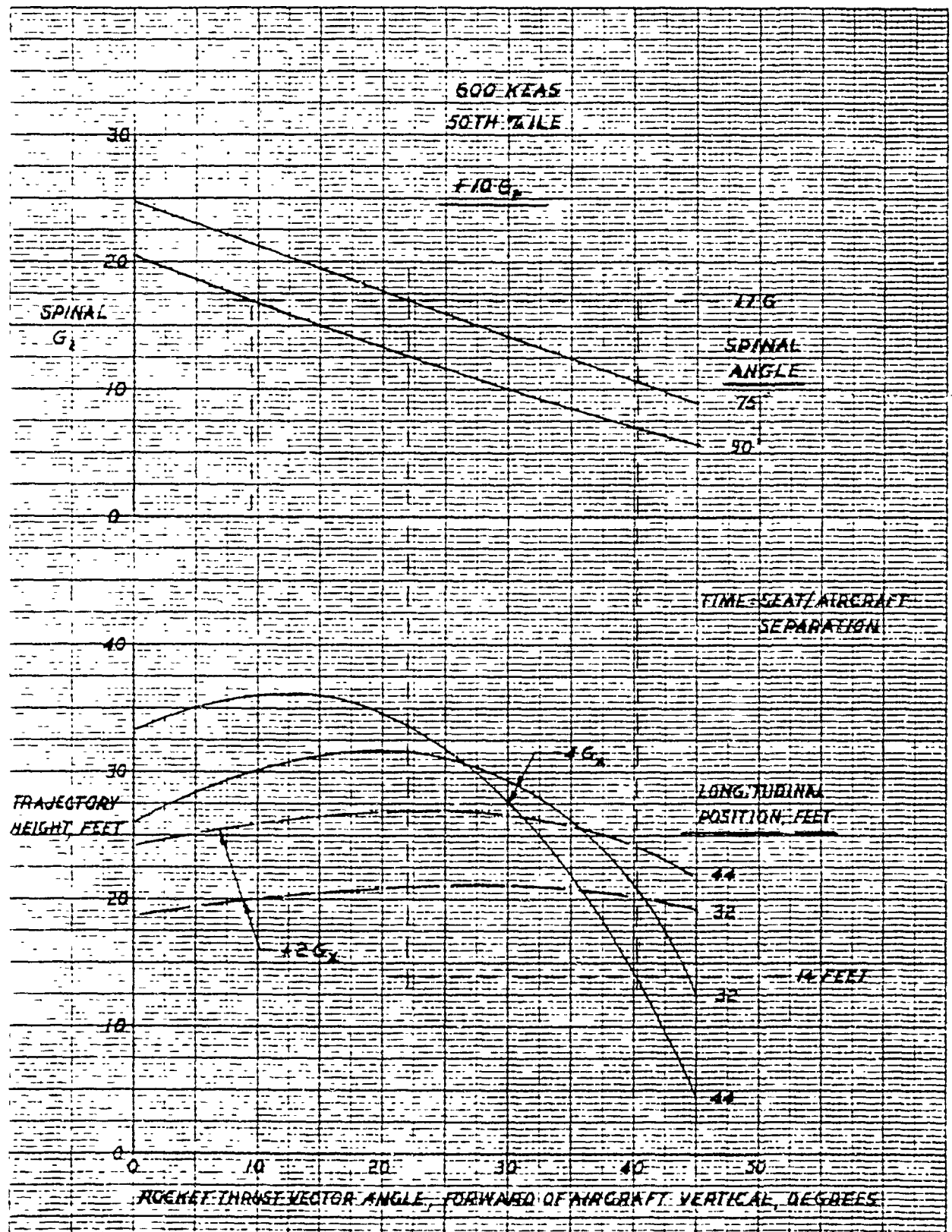


Figure 75. Tail Clearance and Spinal  $G_z$ ,  $45^\circ$  Rail Angle, 200% Rocket Thrust

## SECTION VII

### SIXTY DEGREE RAIL ANGLE

#### 7.1 ACCELERATION VECTORS

Figure 76 shows thrust and aerodynamic acceleration vectors for 200 percent rocket thrust. The spine is horizontal in the aircraft for this case and all thrust vector angles above 0 degrees reduce spinal force components. As the thrust and drag vector relationships do not change significantly with the rail angle, this diagram is used for the spinal angle previously discussed in Section 5.4.

#### 7.2 TRAJECTORIES

Figures 77-A and -B show trajectories for 200 percent rocket thrust. Tail clearance heights are generally lower than for the 30 and 45-degree rail angle.

The clearance heights at the forward upper corner of the F-16 tail are marginal for the +2  $G_x$  case and are unacceptable for the -4  $G_x$  case.

#### 7.3 USABLE THRUST VECTOR ANGLES

Figure 78 shows tail clearance height and spinal  $G_z$  as a function of rocket thrust vector angle. Although a wide range of 32 degrees in thrust vector angle is available, the +2  $G_x$  trajectories at the 32-foot position are low compared to those of other rail angles.

TIME-SEAT/AIRCRAFT SEPARATION

600 KEAS  
50 TH % ILE  
60° RAIL ANG-E  
 $+2G_x / +10G_z$

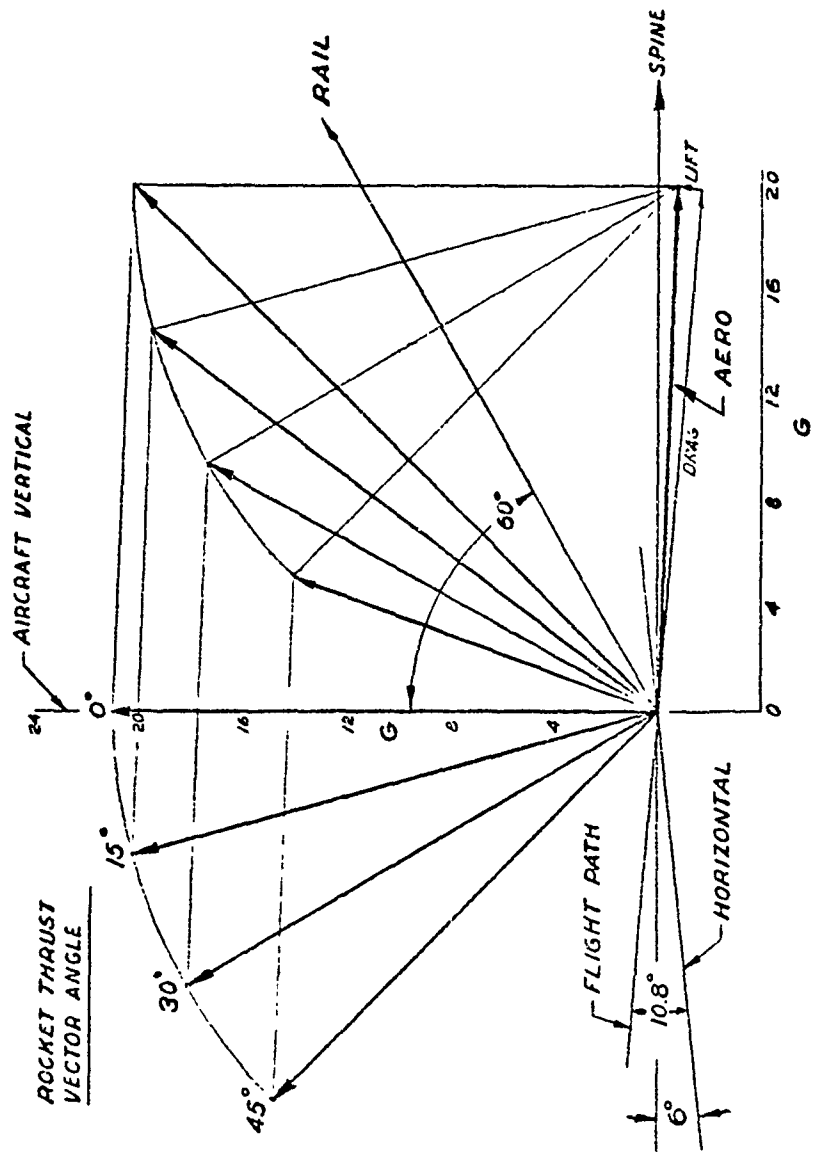


Figure 76. Acceleration Vectors, 60° Rail Angle, 200% Rocket Thrust

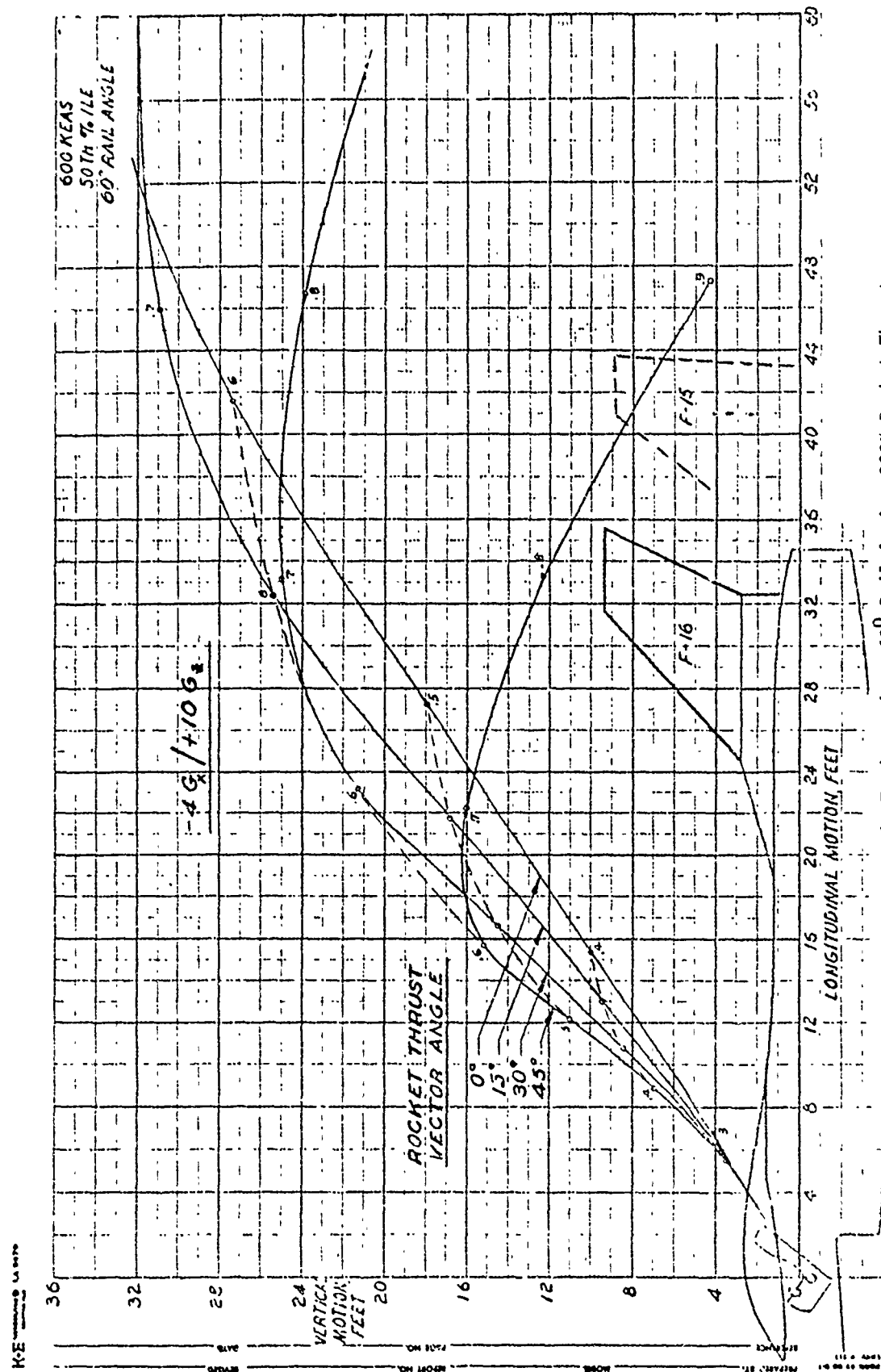
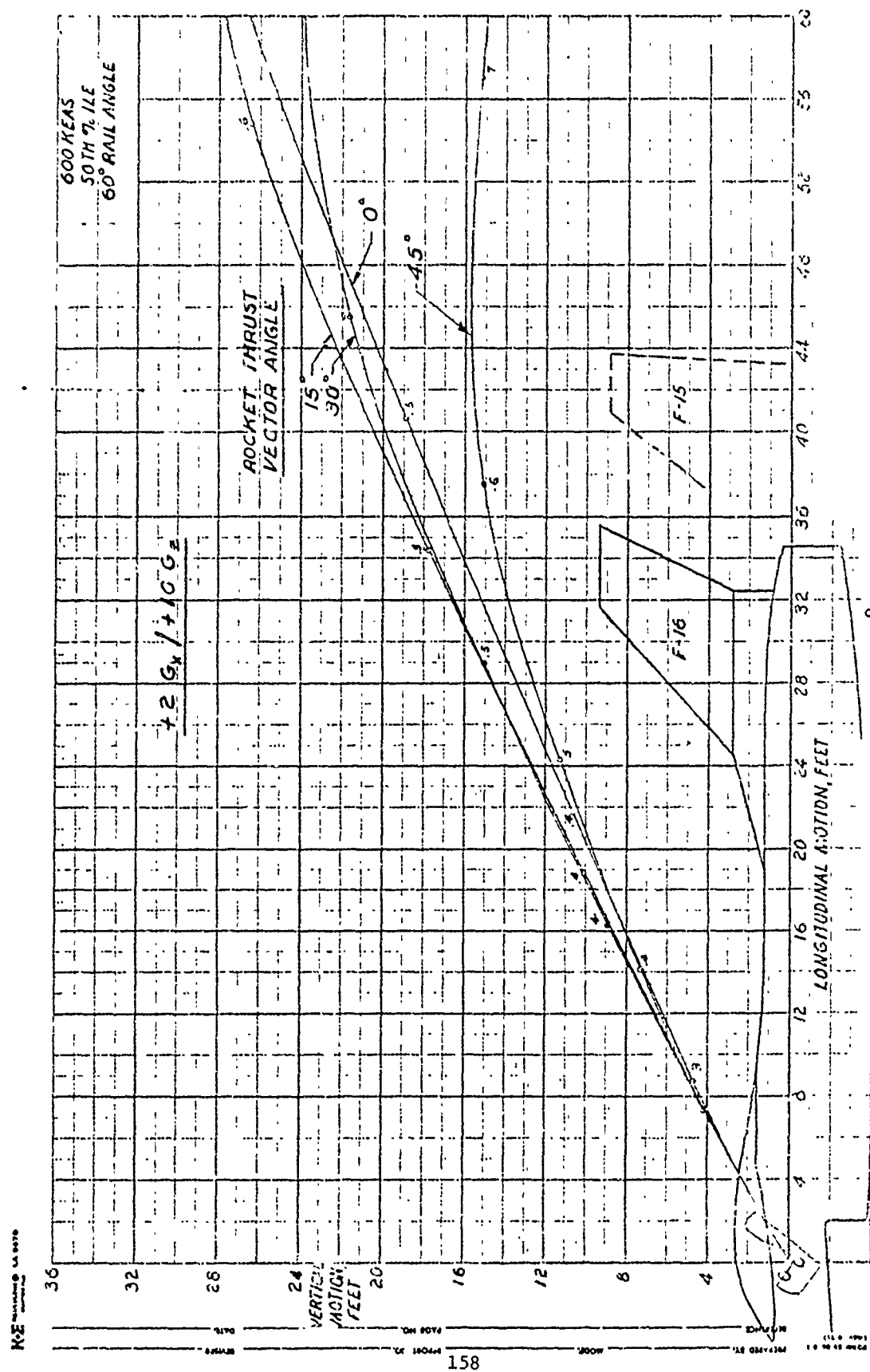


Figure 77-A. Parametric Trajectories, 60° Rail Angle, 200% Rocket Thrust



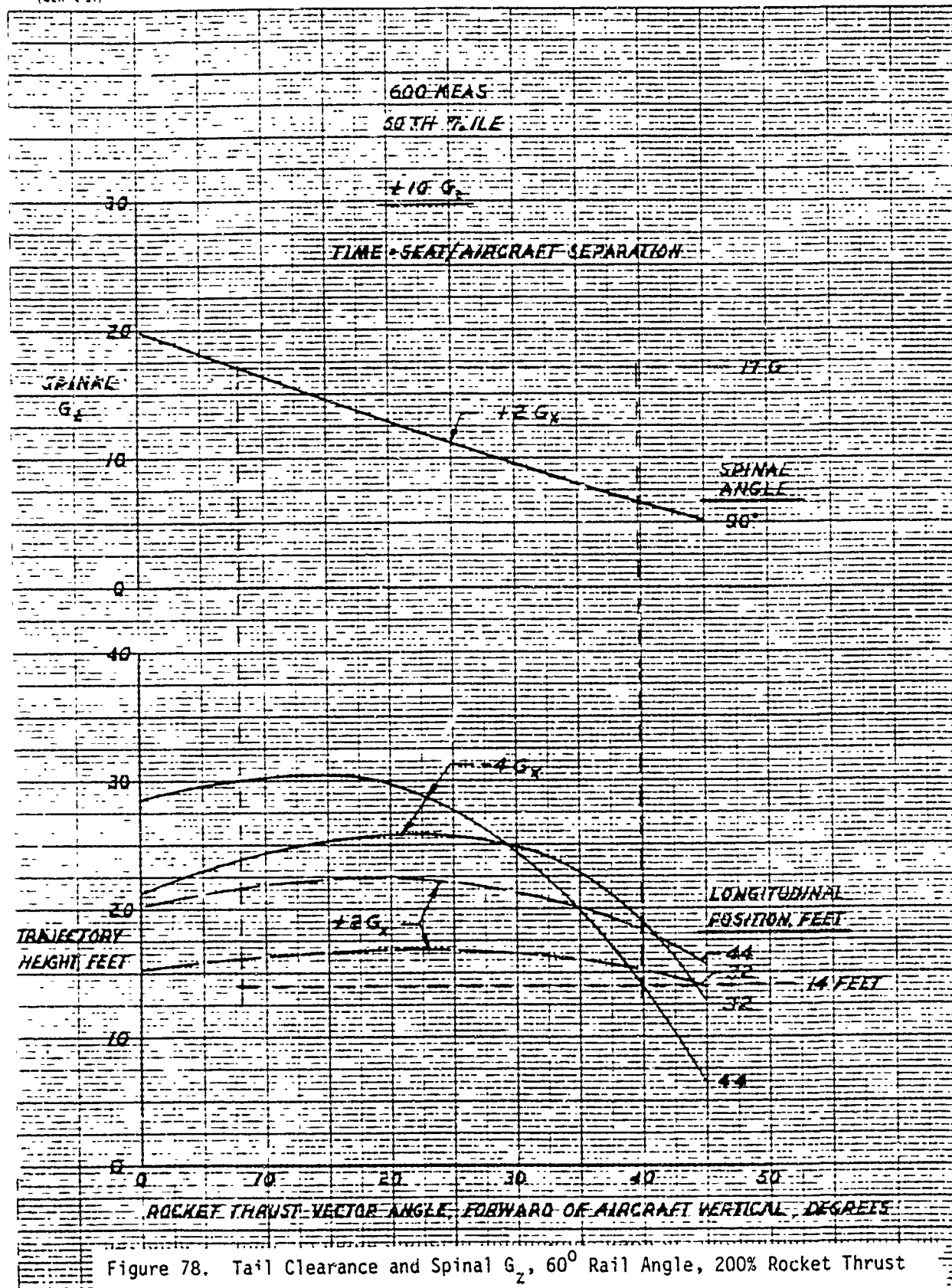


Figure 78. Tail Clearance and Spinal  $G_z$ ,  $60^\circ$  Rail Angle, 200% Rocket Thrust



## SECTION VIII

### RAIL ANGLE EFFECTS

Figure 79 shows the effects of rail angle variation on tail clearance heights for  $-4 G_x/+10 G_z$  aircraft acceleration. In most cases of varying rocket thrust vector angles, tail clearance decreases with increasing rail angle. This variation is much smaller than the loss of height between rocket thrust vector angles of 30 and 45 degrees, illustrating the adverse effects of excessive forward orientation of rocket thrust. The loss of clearance height with increasing rail angle is significant, however, and results in a bias toward the lower angles.

Scatter in the data for the 45-degree thrust vector cases does not permit drawing smooth curves through these points. This condition is attributed to pitch sensitivity effects associated with trajectories which peak forward of the tail and drop down through, or just aft of, the tail region.

Figure 80 shows rail angle effects for the  $+2 G_x/+10 G_z$  condition. Tail clearance height is again decreased with increasing rail angle for angles between 15 and 60 degrees. The decreased sensitivity, with variation in rocket thrust vector angle, is evident for this acceleration condition. Tail clearance heights are lowest for the longitudinal position of 32 feet. Some scatter is again evidenced in the 45-degree thrust vector angle curve.

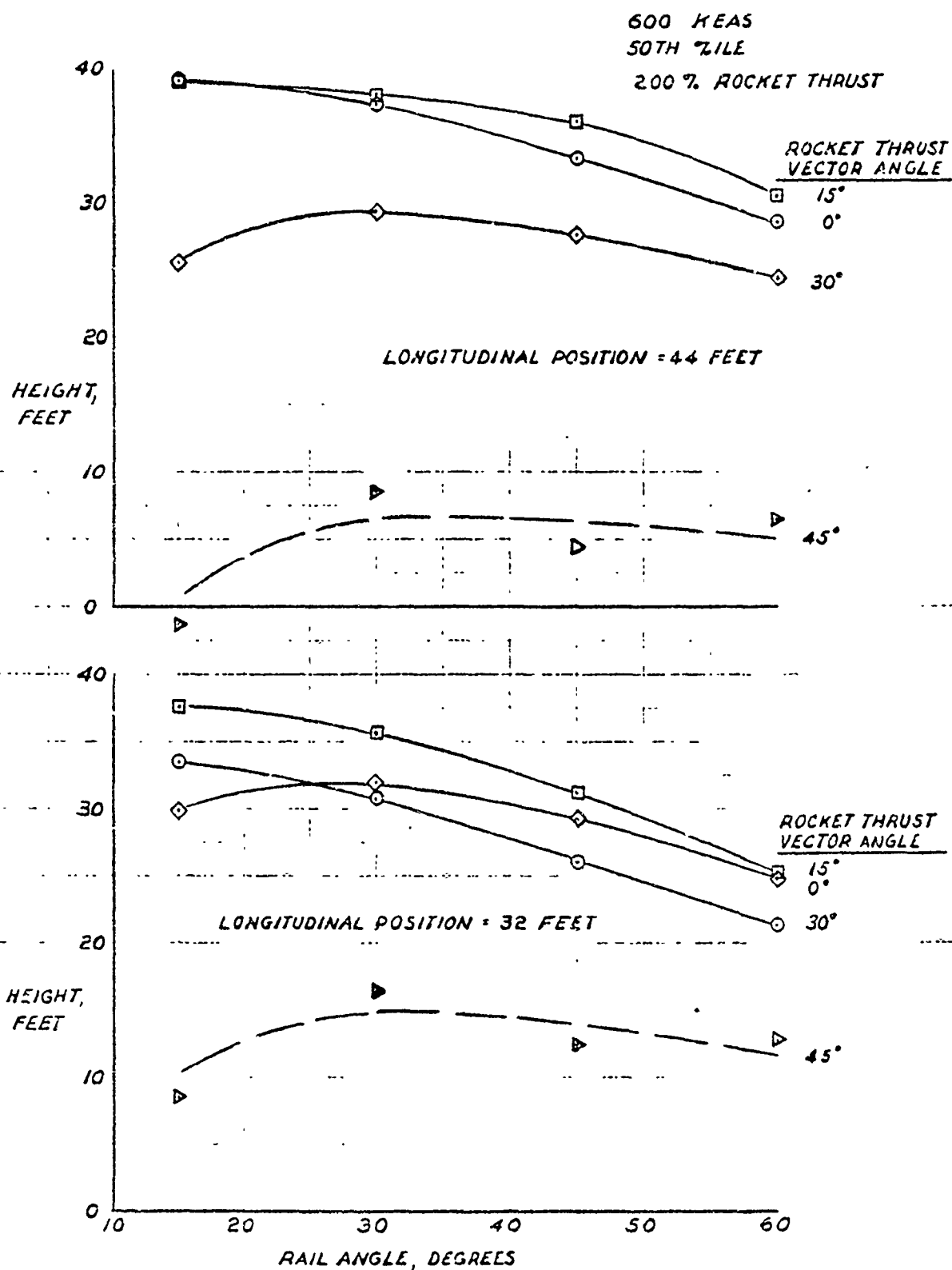


Figure 79. Tail Clearance Height Versus Rail Angle,  $-4G_x/+10 G_z$

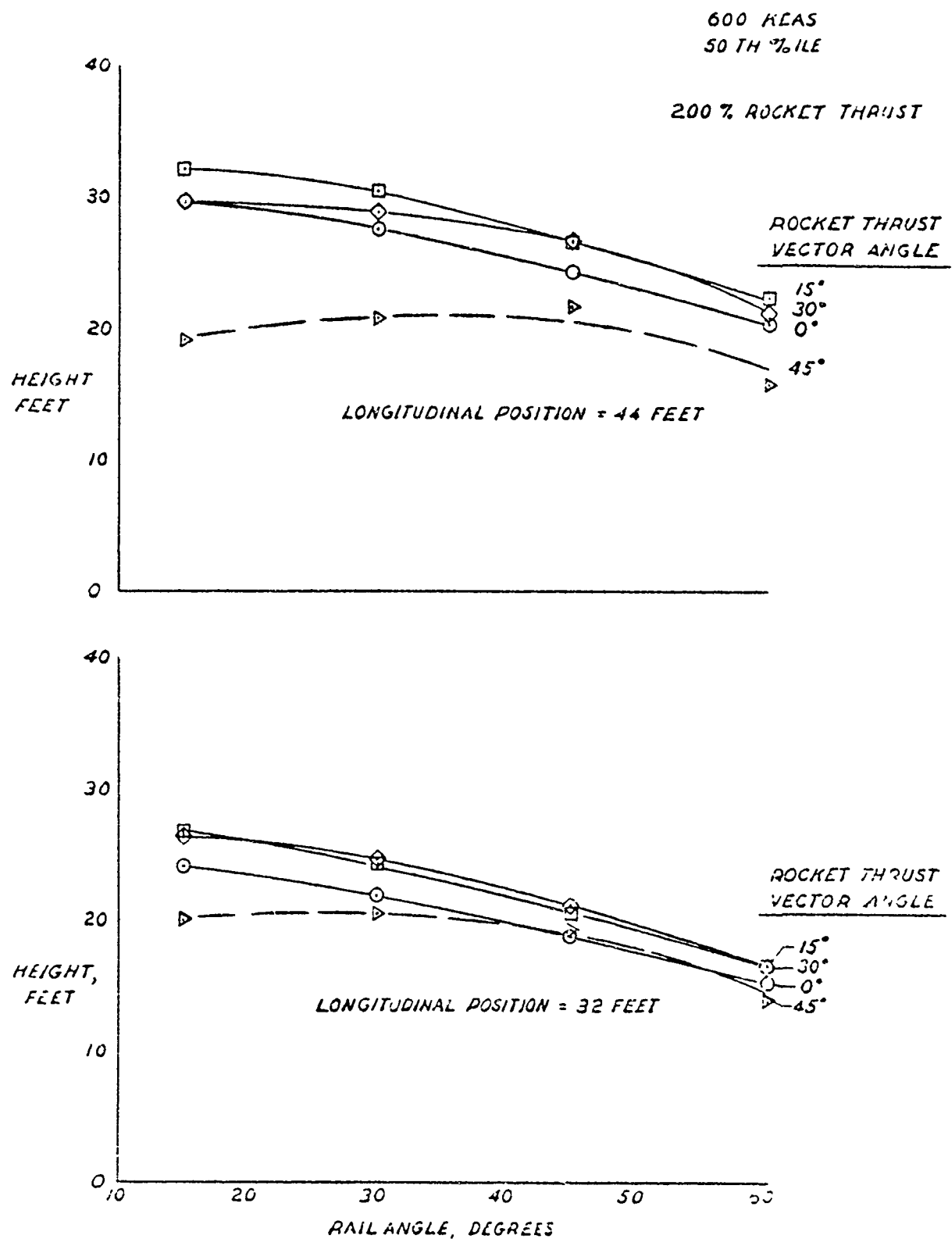


Figure 80. Tail Clearance Height Versus Rail Angle, +2G<sub>x</sub>/+10G<sub>z</sub>

## SECTION IX

### EJECTION SPEED EFFECTS

Propulsion and aerodynamic characteristics are the same as those used for the 600 KEAS trajectories. A spinal angle of 30 degrees aft of the rail is used for all cases. Rocket thrust is 200 percent of the CKU-5/A rocket.

#### 9.1 450 KEAS, 30-DEGREE RAIL ANGLE

Figure 81 shows trajectories for the  $-4G_x$  and  $+2 G_x$  longitudinal acceleration in combination with the  $+10 G_z$  load factor. The reduced drag at 450 KEAS causes all trajectories to be steeper than trajectories at 600 KEAS. Increased sensitivity to rocket thrust vector angle is also due to the reduced drag. Spinal load is about  $18 G_z$  at a thrust vector angle of 0 degrees but decreases rapidly as this angle is increased.

#### 9.2 450 KEAS, 45 DEGREE RAIL ANGLE

Figure 82 shows trajectories for the 45 degree rail angle case. Adequate tail clearance is provided under  $+2 G_x$  and  $-4 G_x$  conditions except for a 30 degree thrust vector angle in the  $-4 G_x$  case. Some improvement over the 30 degree rail angle for the 15 degree thrust vector angle at  $-4 G_x$  is evident. The 0 to 15 degree thrust vector angle range provides acceptable clearance for both 30 and 45 degree rail angles. This range, however, is below the thrust vector spinal G limit for either rail angle at 600 KEAS. A fixed thrust vector angle cannot be selected for both speeds cases under  $-4 G_x/+10 G_z$  conditions.

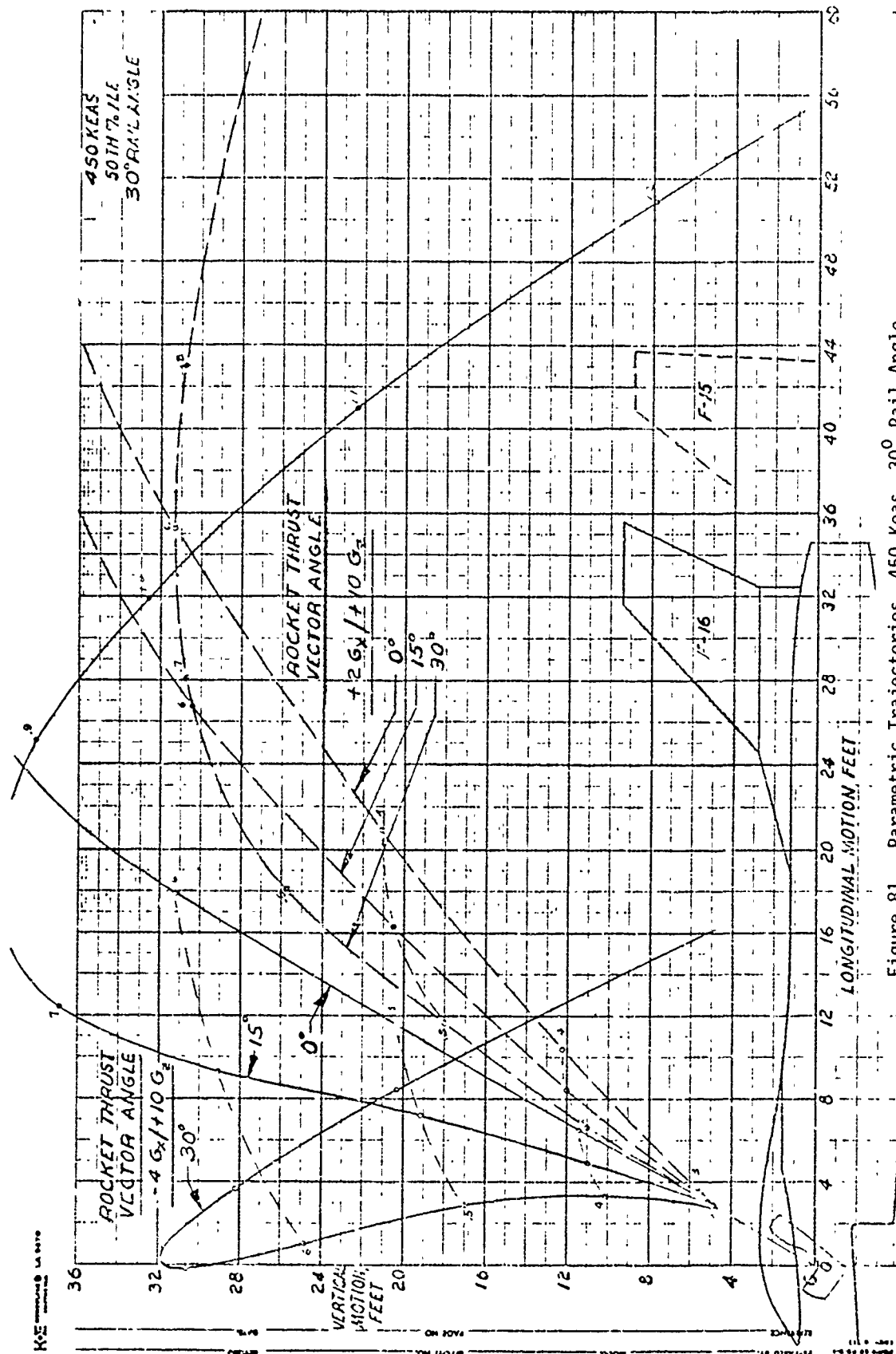


Figure 81. Parametric Trajectories, 450 Keas, 30° Rail Angle, 200% Rocket Thrust

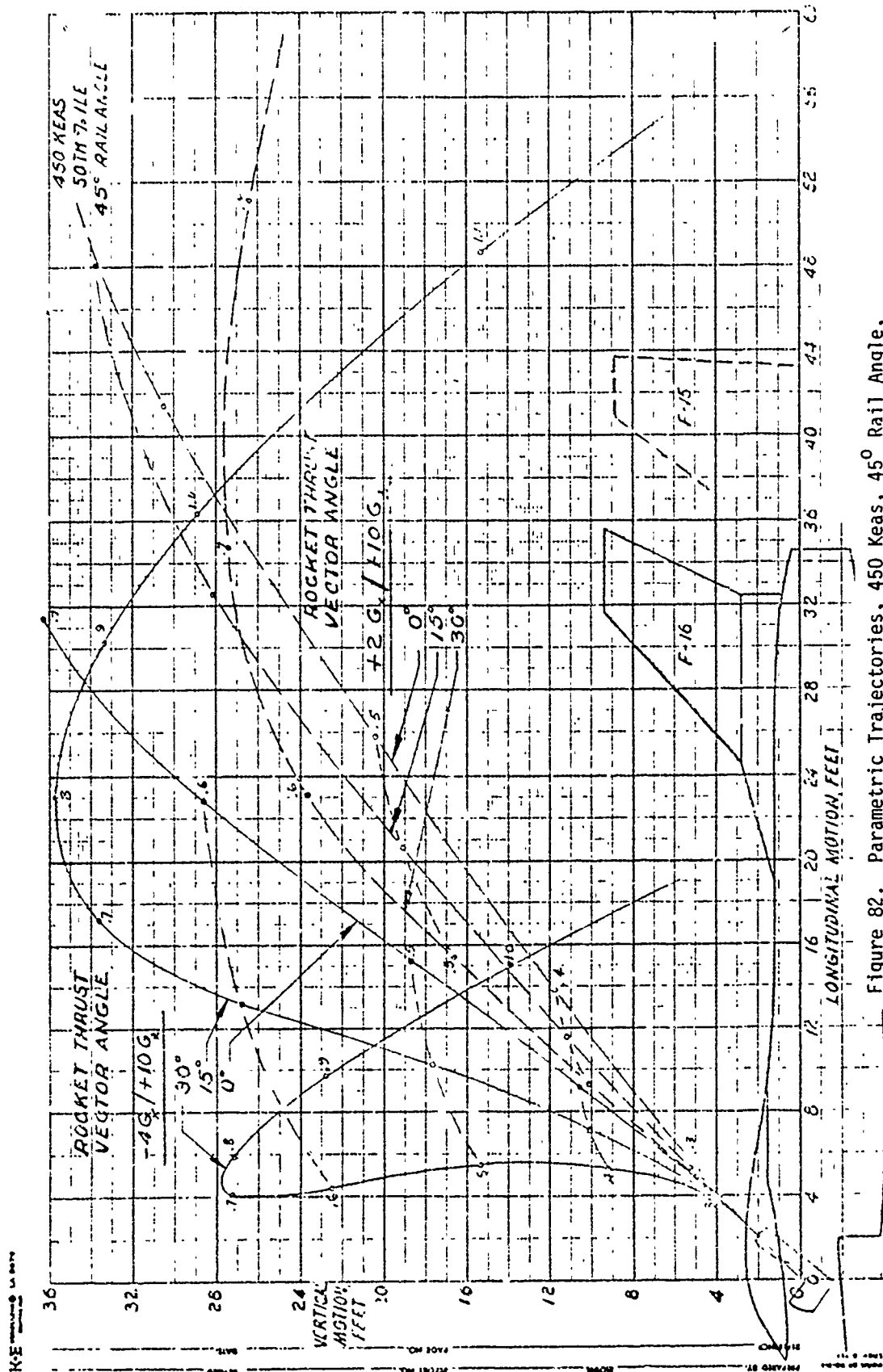


Figure 82. Parametric Trajectories, 450 Keas, 45° Rail Angle, 200% Rocket Thrust

To improve the usable thrust vector angle range trajectory runs at the 150 percent rocket thrust level are shown. The trajectories of Figure 83 are for a rail angle of 45 degrees and  $-4G_x/+10 G_z$ . The 15 degree thrust vector angle trajectory is moved aft, but the peak is lower than for 200 percent thrust. The  $10 G_z$  has a greater effect than the increased drag/thrust differential and requires a near-vertical orientation of the 150 percent thrust vector to provide aircraft clearances.

Ejection at a 45 degree rail angle at the 200 percent thrust level requires the seat to pitch aft after separation from the aircraft to produce a more vertical thrust vector orientation. With a 30 degree thrust vector angle at 600 KEAS, aft seat pitch of 15 to 30 degrees will achieve the usable range of thrust vector angles shown in Figure 82. This aft pitch can be accomplished by biasing the pitch control system as a function of ejection speed.

### 9.3 450 KEAS, 60 DEGREE RAIL ANGLE

Tail clearance trajectories for the 60 degree rail angle are shown in Figure 84. Tail clearances are adequate for all cases except the 30 degree thrust vector under  $-4 G_x$  conditions and are marginal for a 15 degree thrust vector angle at  $-4 G_x$ . The usable thrust vector range of 0 to 15 degrees to provide acceptable clearances in the  $-4 G_x$  condition includes the lower limit of 8 degrees for the 600 KEAS speed and provides a range of 7 degrees between the two speed cases.

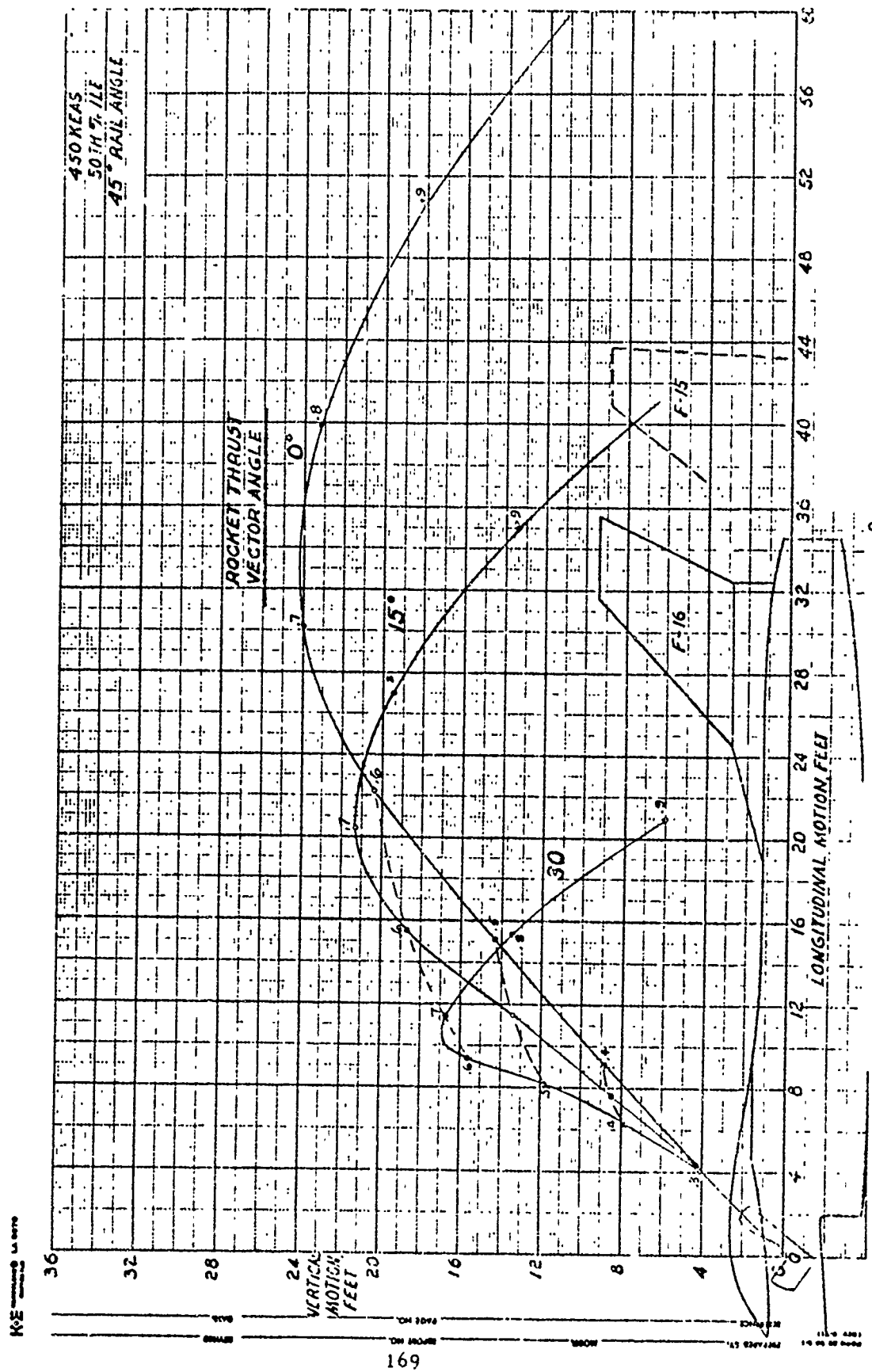


Figure 83. Parametric Trajectories, 450 Keas, 45° Rail, 150% Rocket Thrust



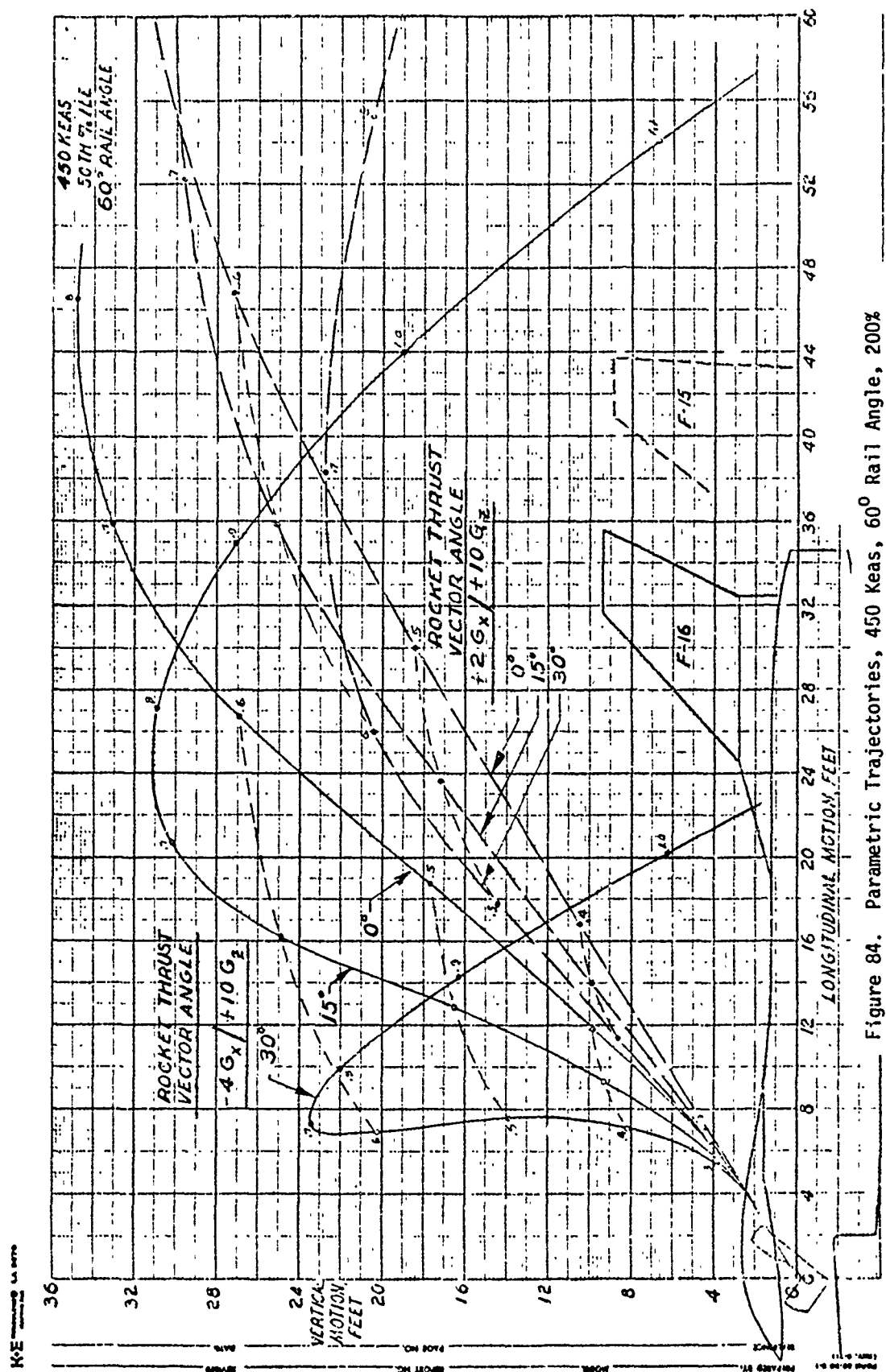


Figure 84. Parametric Trajectories, 450 Keas, 60° Rail Angle, 200% Rocket Thrust

#### 9.4 300 KEAS TRAJECTORIES

Trajectory clearances in the aircraft speed region between 450 and 300 KEAS involve considerations of aircraft capability in achieving the critical acceleration conditions of  $+10 G_z/-4 G_x$ . At 300 KEAS the F-15 aircraft requires an angle-of-attack of 26.5 degrees at sea level to generate these maximum accelerations and has reached an essentially unflyable condition. At all altitudes above sea level angle-of-attack will be excessive and in some cases will not be capable of generating the specified accelerations. The determination of low aircraft speeds at which maximum G conditions can be achieved is beyond the scope of the present study.

For the parametric study a 6 degree aircraft angle-of-attack at 300 KEAS is used for comparison with other speed ranges. Under  $-4 G_x$  conditions with 200 percent rocket thrust and 30 degrees thrust vector angle all trajectories in the rail angle range of 15 to 60 degrees are forward rather than aft of the aircraft. At speeds between 300 and 450 KEAS thrust, drag and longitudinal accelerations are balanced and steep, vertical trajectories result.

This parametric comparison is useful only in the determination of ejection speed effects. Aircraft tail clearances are adequate under other than maximum adverse  $+10 G_z/-4 G_x$  conditions.

## SECTION X

### SUMMARY

#### 10.1 AERODYNAMIC FORCES

Aerodynamic lift is eliminated as an uncontrolled variable in the parametric study. Lift coefficients are reduced on the basis of previous trajectory simulations and lift is limited to  $\pm 1$  G for the angle-of-attack range of interest. Increased positive lift aids tail clearance but increases spinal loads. Negative lift decreases spinal loads but reduces tail clearance.

Drag coefficients vary from 0.65 to 0.75 producing a drag force of 20 to 21 G at seat/aircraft separation. This is near maximum for spinal loading at thrust levels of 200 percent of the CKU-5/A rocket.

Further studies of tail clearance trajectories at high aircraft angle of attack require additional data on aerodynamic coefficients in the vicinity of the fuselage to account for flow field effects.

#### 10.2 SPINAL ANGLE

A spinal angle of 30 degrees aft of the rail is used in the parametric study. This angle permits potentially usable ranges of rocket thrust vector angles in the rail angle region of 15 to 60 degrees.

Inclination of the spinal axis to 90 degrees from the aircraft vertical results in lower spinal force components with a range of usable thrust vector angles from 8 to 39 degrees. Trajectories at a 30 degree rail angle and a spinal angle 60 degrees aft permit increased catapult thrust and reduced rocket thrust. Tail clearance is improved and spinal loading

reduced over the corresponding case of the parametric study. Increased spinal angles are a desirable design objective.

### 10.3 CATAPULT PERFORMANCE

Maximum allowable catapult peak G is determined by the  $-4 G_x/+10 G_z$  aircraft acceleration condition and the spinal angle and is independent of rail angle. A spinal angle of 30 degrees aft of the rail permits a maximum value of 19.6 G. This catapult has a peak G of 9.6 in 1.0 G level flight conditions.

In the reduced G fields of  $+2 G_x/+10 G_z$ , peak G decreases with increasing rail angle, but the differential between impressed and peak G remains essentially constant. Catapult performance is not significantly affected by rail angle.

### 10.4 ROCKET THRUST MAGNITUDE AND DURATION

A rocket thrust level of 200 percent of the CKU-5/A rocket permits a usable range of rocket thrust vector angles at rail angles of 15 to 60 degrees for ejection speeds of 600 KEAS. At 450 KEAS the 200 percent thrust level is satisfactory when seat attitude and thrust vector orientation is controlled. A thrust duration of 100 percent of the CKU-5/A rocket is satisfactory for all conditions.

A rocket thrust level of 150 percent requires vertical orientation of the thrust vector angle to achieve acceptable tail clearance with the catapult performance associated with the 30 degree rail angle and spinal angle 30 degrees aft of the rail. At 600 KEAS, this orientation produces excessive spinal G for rail angles of 30 and 45 degrees and inadequate tail clearance for the  $+2 G_x/+10 G_z$  condition at a 60 degree rail angle.

#### 10.5 RAIL AND ROCKET THRUST VECTOR ANGLES

The data shown in Figures 71, 75, and 78 provide selection criteria for rail and thrust vector angles for the High-G escape system.

At 600 KEAS, the lower limit of rocket thrust vector angle is determined by the  $+2 G_x/+10 G_z$  aircraft load condition because of spinal load limitations. Tail clearance is critical for the same G load condition at these lower vector angles.

The upper limit of potentially usable rocket thrust vector angles is determined by tail clearance height for the  $-4 G_x/+10 G_z$  aircraft load condition. Clearance height is sensitive to thrust vector/seat attitude at the higher thrust vector angles. The practical limit is that vector angle at which minimum tail clearance height is equal for both the  $+2 G_x$  and  $-4 G_x$  load conditions. The  $+2 G_x$  condition is then critical for all tail clearance heights in the usable thrust vector angle range. Application of the above limits produces thrust vector angle ranges and tail clearance heights shown in Table 1 for each rail angle. This comparison illustrates the compromise between tail clearance and spinal  $G_z$  required for concept selection.

TABLE I

## RAIL AND ROCKET THRUST VECTOR ANGLES-VS-TAIL CLEARANCE HEIGHT

RAIL ANGLE DEGREES	SPINAL ANGLE DEGREES	ROCKET THRUST VECTOR ANGLE DEGREES		TAIL CLEARANCE HEIGHT, FEET		SPINAL G, INCREMENT BELOW 17G AT MIDRANGE ANGLE
		MIN.	MAX.	MIN.	MAX.	
15°	45°	35°	35°	8.0	14.0	0
30°	60°	30°	35°	23.5	24.5	1.0
45°	75°	21°	36°	20.5	21.0	3.0
60°	90°	8°	39°	15.5	17.0	5.0

600 KEAS

200% ROCKET THRUST LEVEL

The 30 degree rail angle has more than adequate tail clearance height. Thrust vector angle range is acceptable but indicates a lower range of permissible angles for pitch control effectivity. Spinal  $G_z$  margin is the lowest for application of aerodynamic stabilizing devices.

The 60 degree rail angle, with a 90 degree spinal angle, shows the best spinal  $G_z$  characteristics and provides the greatest range for aerodynamic devices. Trajectories for the +2  $G_x$  condition, however, are marginal. The 60 degree rail angle represents an upper limit for selection of rail angle.

Design concepts with spinal angles parallel to rail angles of 60 or 65 degrees will exhibit the same spinal  $G$  characteristics as that shown for the 30 degree rail angle.

For a 45 degree rail angle a rocket thrust vector angle of 30 degrees results in a range of 14 degrees and an increment of 3.0 spinal  $G_z$  below the 17  $G$  spinal limit. As the corresponding values for the 15 degree rail angle are zero, the 45 degree rail angle offers the greatest potential of the rail angles considered. The 45 degree rail angle is the best compromise from a flight dynamics standpoint for the High- $G$  escape systems.

Rail angle effect plots are not as useful as rocket thrust vector angles in the selection of these variables for the High- $G$  escape system. Refining thrust vector effect plots to account for pitch-effect scatter will not significantly affect the conclusions of this study.

#### LIST OF REFERENCES

1. Man at High Sustained +Gz Acceleration: A Review., Aerospace Medicine 45 (10): 1115-1136, Burton, R. R., et al, October 1974.
2. High Acceleration Cockpit - The Maneuvering Countermeasure., AD-770-287, Aerospace Medical Research Laboratory, Wright-Patterson AFB, Ohio, Kulwicki, Philip V., et al, September 1973.
3. Effect of Modified Seat Angle on Air Weapons System Performance Under High Acceleration., AMRL-TR-73-5, Aerospace Medical Research Laboratory, Wright-Patterson AFB, Ohio, Rogers, Dana B. et al, July 1973.
4. Reevaluation of a Tilt-Back Seat as a Means of Increasing Acceleration Tolerance, Extract from Aviation, Space and Environmental Medicine 46 (1): 55-63, Burns, John W., January 1975.
5. Pilot Tracking Performance as a Function of G Stress and Seat Back Angle, AMRL-TR-76-107, Aerospace Medical Research Laboratory, Wright-Patterson AFB, Ohio, McElreath, Kenneth W. and Clader, Michael D., May 1977.
6. Centrifuge Assessment of a Reclining Seat., AGARD-CP-189, AGARD Conference Proceedings No. 189 on the Pathology of Maneuvering and the Use of Centrifuge in Performance Training., Glaister, David H. and Lisher, Brian J., April 1976.
7. Pilot Supination in High Performance Aircraft is both Essential and Achievable, NADC-74204-40, Naval Air Development Center, Warminster, Pennsylvania, Horan, John J., September 1974.
8. G Protective Aircraft Seats, with Special Consideration Given to Pelvis and Legs Elevating (Pale) Seats., AD-756 630, Naval Development Center, Warminster, Pennsylvania, von Beckh, Harald J., October 1972.
9. The Physiologic Effects of Seat Back Angles  $<45^{\circ}$  (from the vertical) Relative to G., Biodynamics Branch, USAF School of Aerospace Medicine, Brooks AFB, Texas, Burton, R. R., Iampietro, P. F., and Leverett, Jr., S. D.



LIST OF REFERENCES (CONT'D)

10. Positioning of Aircrews - Ultima Ratio of G Protection., Aerospace Medicine 43 (7): 743-754, von Beckh, Harald J., July 1972.
11. Catapult Dynamics in an Environment of High Acceleration., Extract from Proceedings of the Thirteenth Annual Conference of the SAFE Association, San Antonio, Texas, Higgins, A. M., September 1975.
12. Rocket Catapult Negative G Simulation Program., IHTR 342, Naval Ordnance Station, Indian Head, Maryland, Frankle, Edward A., July 1971.
13. Ejection Under Deceleration., NADC-77209-40, Naval Air Development Center, Warminster, Pennsylvania, Sanford, Russell L. and Miller, Kenneth L., August 1977.
14. Computer Analysis of Ejection Under Deceleration., NADC-75078-40., Naval Air Development Center, Warminster, Pennsylvania, Cantor, Alan E. and Miller, Kenneth L., June 1975.
15. Fluidic Thrust Vector Control for the Stabilization of Man/Ejection Seat Systems., AFFDL-TR-75-105, Honeywell, Inc., September 1975.
16. Two Axis, Fluidically Controlled Thrust Vector Control System for an Ejection Seat., Report 77SRC40, Honeywell, Inc., March 1977.
17. Aeromechanical Properties of Ejection Seat Escape Systems., AFFDL-TR-74-57, White, B. J., April 1974.
18. High Acceleration Cockpits for Advanced Fighter Aircraft, Crew Station Design/Integration., AFFDL-TR-74-48, Volume II, Air Force Flight Dynamics Laboratory, Wright-Patterson AFB, Ohio, Mattes, Robert E. et al, McDonnell Aircraft Company, May 1974.
19. High Acceleration Cockpit Applications Study, Crew Station Design/Integration., AFFDL-TR-75-139, Volume II. Air Force Flight Dynamics Laboratory, Wright-Patterson AFB, Ohio, Mattes, Robert E. and Roberts, J. W., November 1975.

LIST OF REFERENCES (CONT'D)

20. Advanced Fighter Technology Integration (AFTI), Near Term Demonstrator - Phase I, Task II Definition Refinement Studies., AFFDL-TR-75-86, Part 4, Volume V., Guenther, L. H. et al, McDonnell Aircraft Company, September 1975.
21. AFTI-5 HAD Design Criteria Document., MDC IR0080, McDonnell Aircraft Company, St. Louis, Missouri, April 1978.
22. AFTI-15 Predesign and Preliminary Development of DFCS and HAC, Phase I, Supplement III, Preliminary Development of HAC., AFFDL-TR-78-XX, McDonnell Aircraft Company, St. Louis, Missouri, Pope, I., April 1978.
23. Advanced Fighter Aircraft Crew Stations and High Acceleration Cockpit Designs, AFFDL-TR-72-118, Air Force Flight Dynamics Laboratory, Wright-Patterson AFB, Ohio, Schroll, Dennis W., October 1972.
24. AFTI-15 Predesign and Preliminary Development of DFCS and HAC, Volume III, Technical Proposal., MDC A4697, Volume III, McDonnell Aircraft Company, St. Louis, Missouri, Pope, I., March 1977.
25. Advanced Fighter Technology Integration (Phase I)., AFFDL-TR-75-88, Air Force Flight Dynamics Laboratory, Wright-Patterson AFB, Ohio, Rockwell International, September 1975.
26. Escape Problems and Maneuvers in Combat Aircraft., AGARD-CP-134, AGARD Conference Proceedings No. 134 at Soesterberg, Netherlands., AGARD, September 1973.
27. Aeronautical Systems Technology Needs: Escape, Rescue and Survival., ASD-TR-77-2, Aeronautical Systems Division, Air Force Systems Command, Wright-Patterson AFB, Ohio, January 1977.
28. Crewman's Retention System for Protection Against High Speed Ejection up to 600 Knots., NADC-76119-40, Naval Air Development Center, Warminster, Pennsylvania, Grumman Aerospace Corporation, October 1976.
29. Restraint for High Acceleration Cockpits., Extract from Proceedings of the Thirteenth Annual Conference of the SAFE Association, San Antonio, Texas, Drsata, Frank E., September 1975.

LIST OF REFERENCES (CONT'D)

30. An Investigation of Automatic Restraint and Body Positioning Techniques., AMRL-TR-71-101, Aerospace Medical Research Laboratory, Wright-Patterson AFB, Ohio, Phillips, Norman S., et al, Beta Industries, Inc., December 1973.
31. Biodynamic Response to Windblast., AGARD-CP-170, AGARD Conference Proceedings No. 170 at Toronto, Canada, Glaister, D. H., May 1975.
32. Aerodynamic Forces Exerted on an Articulated Human Body Subjected to Windblast., Extract from Aviation, Space and Environmental Medicine 49 (1): 183-190, Schneck, Daniel J., January 1978.
33. Inflatable Body and Head Restraint., NADC-77176-40, Naval Air Development Center, Warminster, Pennsylvania, Schulman, Marvin and McElhenney, James., September 1977.
34. Restraint Harness - A Review., Tech. Note Mech. Eng. 375, Royal Aircraft Establishment, Ministry of Aviation, London, Chisman, S. W., April 1963.
35. Stability and Limb Dislodgement Force Measurements with the F-105 and ACES II Ejection Seats., AMRL-TR-75-8, Aerospace Medical Research Laboratory, Wright-Patterson AFB, Ohio, Payne, Inc., July 1975.
36. Principles of Biodynamics Applicable to Manned Aerospace Flight - Prolonged Linear and Radial Acceleration., AGARDograph No. 150, AGARD, March 1971
37. Spatial Disorientation in Flight, A Handbook for Aircrew., AGARD-AG-170, Advisory Group for Aerospace Research and Development, Benson, A. J. and Burchard, E., September 1973
38. Thresholds for the Perception of Angular Acceleration as Indicated by the Oculogyral Illusion., AD-769 268, Naval Aerospace Medical Research Laboratory, Pensacola, Florida, Miller, Earl F. et al, June 1973.
39. Acceleration and Vision., WADC TR 58-333, AD 208 147, Aero Medical Laboratory, Wright-Patterson AFB, Ohio, White, William J., November 1958.
40. Biophysical Evaluation of the Human Vestibular System., NASA CR-140063, N74 32535, Massachusetts Institute of Technology, Cambridge, Massachusetts, Young, L. R. August 1974.

LIST OF REFERENCES (CONCLUDED)

41. Reichenau, David E. A., "Aerodynamic Characteristics of an Ejection Seat Escape System with Cold Flow Rocket Plume Simulation at Mach Numbers from 0.6 through 1.5", AEDC-TR-69-218, October 1969.
42. White, B. J., "Aeromechanical Properties of Ejection Seat Escape Systems", AFFDL-TR-74, April 1974.